

**DOKUZ EYLÜL UNIVERSITY**  
**GRADUATE SCHOOL OF NATURAL AND APPLIED SCIENCES**

**DETERMINATION OF ACOUSTIC  
PERFORMANCE PARAMETERS OF  
INSULATION MATERIALS IN CONDITIONED  
MEDIUM**

by  
**Yusuf İHTİYAROĞLU**

**June, 2018**  
**İZMİR**

**DETERMINATION OF ACOUSTIC  
PERFORMANCE PARAMETERS OF  
INSULATION MATERIALS IN CONDITIONED  
MEDIUM**

**A Thesis Submitted to the  
Graduate School of Natural and Applied Sciences of Dokuz Eylül University  
In Partial Fulfillment of the Requirements for the Degree of Master of Science  
in Mechanical Engineering, Machine Theory and Dynamics Program**

**by  
Yusuf İHTİYAROĞLU**

**June, 2018  
İZMİR**

**M.Sc. THESIS EXAMINATION RESULT FORM**

We have read the thesis entitled “**DETERMINATION OF ACOUSTIC PERFORMANCE PARAMETERS OF INSULATION MATERIALS IN CONDITIONED MEDIUM**” completed by **YUSUF İHTİYAROĞLU** under supervision of **ASSOC. PROF. DR. ABDULLAH SEÇGİN** and we certify that in our opinion it is fully adequate, in scope and in quality, as a thesis for the degree of Master of Science.



Assoc. Prof. Dr. Abdullah SEÇGİN

Supervisor



Dr. Öğr. Üy. Mehmet SARIKANAT

(Jury Member)



Prof. Dr. Ayşe Saide SARIĞÜL

(Jury Member)



Prof. Dr. Latif SALUM

Director

Graduate School of Natural and Applied Sciences

## ACKNOWLEDGMENTS

This thesis with the title “Determination of acoustic performance parameters of insulation materials in conditioned medium” is one of the outcomes of 114M753 numbered project supported by The Scientific and Technological Research Council of Turkey, TÜBİTAK.

I would like to express my sincere appreciation to my thesis advisor Assoc. Prof. Dr. Abdullah SEÇGİN for all his patience, time and efforts in my entire master education. His guidance and countless critical suggestions helped me to finish this project.

I would also like thanks to Prof. Dr. A. Saide SARIGÜL, Asst. Prof. Dr. Mehmet Akif Ezan, my friends Murat KARA, Altay OZANKAN and Cihan Mete BAHADIR for their supports to this studies.

Finally, thanks to my family and my fiancée Özgün ÇILDIR for their support in my entire education.

Yusuf İHTİYAROĞLU

# **DETERMINATION OF ACOUSTIC PERFORMANCE PARAMETERS OF INSULATION MATERIALS**

## **ABSTRACT**

Acoustic performance parameter tests are required to be performed in order to select suitable method or material to provide sound insulation in many sectors and applications like construction, heating, ventilating, white goods, automotive, aeronautical. These performance parameters are sound absorption coefficient, surface impedance, insertion loss, noise reduction and transmission loss. Generally, special acoustic rooms or special measurement systems are required for determining the performance parameters. Impedance tube system is the most commonly used apparatus that was also standardized in ISO and ASTM measurement standards. This system enables to determine the performance parameters via processing the sound pressures based on standing wave principle in a tube. Today, determination of acoustic performances of insulation materials under operating conditions is requested especially from automotive and aeronautical industries. Standard impedance tube systems are not able to simulate operating conditions such as the humidity and the temperature of the medium. Specially-conditioned acoustic rooms as an alternative can be quite expensive.

In this study, an impedance tube apparatus that meet with related standards and with conditioned medium is designed and produced for insulation materials. Designed apparatus has a sandwich composite construction; therefore, it is lighter than existing ones, quite stiff and it has less sound leakage. Moreover, with this new system having a conditioner unit, it is available to make tests for the insulation materials under different humidity and temperatures of the medium and specimen. In addition to that, the new apparatus has a design and measurement capability to measure random incidence acoustic parameters with a rotating specimen apparatus. By this apparatus, acoustic performance parameters of several insulation materials are determined in the cases of random incidence angles and under varied air conditioned. In this regard, incident and random absorption coefficients of several

samples of isolation materials are measured under conditioned medium and presented to the literature as a benchmark study.

**Keywords:** Impedance tube, insulation materials, conditioned medium, silencers, acoustic performance parameters, transmission loss, sound absorption coefficient, random incidence



# ŞARTLANDIRILMIŞ ORTAMDA YALITIM MALZEMELERİNİN AKUSTİK PERFORMANS PARAMETRELERİNİN BELİRLENMESİ

## ÖZ

İnşaat, ısıtma, havalandırma, beyaz eşya, otomotiv, havacılık gibi pek çok sektör ve uygulamada ses yalıtımını sağlamak üzere en uygun malzeme ve yöntemin seçilebilmesi için akustik performans testlerinin yapılması gereklidir. Bu performans parametreleri ses yutma katsayısı, yüzey empedansı, eklenti kaybı, gürültü azaltımı ve iletim kaybı olarak sınıflandırılmaktadır.

Performans parametrelerinin tespiti için genellikle özel akustik odalar veya özel ölçüm sistemleri gereklidir. Empedans tüp sistemi bu sistemler arasında en yaygın olanıdır. Ayrıca ISO ve ASTM standartlarında da bu sistemlere yer verilmiştir. Bu sistem ile bir tüp içerisinde durağan dalga prensibine dayalı olarak yayılmakta olan sesin, ses basınç değerleri işlenerek akustik performans parametreleri hesaplanır. Günümüzde, özellikle havacılık ve otomotiv endüstrilerinde, susturucuların ve yalıtım malzemelerinin akustik performanslarının çalışma koşulları altında belirlenmesi yönünde bir talep olduğu bilinmektedir. Ancak bu sistemler ortamın nemliliği ve sıcaklığı gibi çalışma şartlarını tümüyle simüle edememektedir. Alternatif olarak şartlandırılmış özel akustik odalar ise oldukça maliyetlidir.

Bu çalışmada yalıtım malzemeleri için standartlara uygun bir empedans tüp düzeneği tasarlanmış ve üretilmiştir. Tasarlanan empedans tüp sistemi sandviç kompozit yapıya sahiptir ve mevcut sistemlerden daha hafiftir. Buna karşın rijitlik ve ses geçirgenliği konusunda ise oldukça başarılıdır. Ayrıca bir şartlandırma ünitesine sahip bu yeni sistem ile yalıtım malzemelerinin farklı nem ve sıcaklıklar altındaki akustik performansları ölçülebilmektedir. Bununla birlikte malzemelerin rastgele geliş açılara ait akustik özelliklerini belirleyebilmek için numune döndürme aparatı geliştirilmiştir. Bu bağlamda pek çok yalıtım malzemesinin direk ve rastgele geliş açılara bağlı ses yutma katsayıları şartlandırılmış ortam içerisinde ölçülmüş ve bir temel çalışma olarak literatüre sunulmuştur.

**Anahtar kelimeler:** Empedans t p , yalıtım malzemeleri, ŐartlandırılmıŐ ortam, susturucular, akustik performans parametreleri, iletim kaybı, ses yutma katsayısı, rastgele geliŐ





## CONTENTS

	<b>Page</b>
M.Sc THESIS EXAMINATION RESULT FORM.....	ii
ACKNOWLEDGEMENTS .....	iii
ABSTRACT .....	iv
ÖZ .....	vi
LIST OF FIGURES .....	xii
LIST OF TABLES .....	xix
<b>CHAPTER ONE - THEORY .....</b>	<b>1</b>
<b>CHAPTER TWO - INTRODUCTION .....</b>	<b>8</b>
2.1 Vibro-Acoustic Modal Analysis.....	8
2.1.1 Structural Modal Analysis .....	8
2.1.1.1 Single Degree of Freedom Approach.....	9
2.1.1.1.1 Peak Selection Method.....	10
2.1.2 Acoustical Modal Analysis .....	11
2.2 Acoustical Performance Parameters.....	13
2.2.1 Sound Absorption Coefficient .....	14
2.2.2 Surface Impedance .....	15
2.2.3 Insertion Loss .....	16
2.2.4 Noise Reduction.....	17
2.2.5 Transmission Loss.....	17
2.3 Analytical Methods for Acoustic Performance Parameters .....	18
2.3.1 Analytical Transfer Matrix Method .....	18
2.4 Experimental Methods for Acoustic Performance Parameters .....	22

2.4.1 ASTM E 1050-98 - Standard Test Method for Impedance and Absorption of Acoustical Materials Using a Tube, Two Microphones, and a Digital Frequency Analysis System .....	22
2.4.2 ASTM E 2611-09 - Standard Test Method for Measurement of Normal Incidence Sound Transmission of Acoustical Materials Based on Transfer Matrix Method.....	25
2.4.2.1 Two Load Method.....	25
2.4.2.1.1 Four Pole Parameters Signal Processing Method. The transfer matrix elements of muffler or material between 2-3 microphones can be determined with the following equations: .....	26
2.4.2.1.2 Wave Decomposition Signal Processing Method. The transfer matrix elements of muffler or material between 2-3 microphones can also be determined via wave decomposition method with the following equations.....	27
<b>CHAPTER THREE - DEVELOPMENT OF THE IMPEDANCE TUBE APPARATUS AND SOFTWARE .....</b>	<b>32</b>
3.1 Designing and Manufacturing of an Insulated Cabin.....	33
3.2 Designing, Manufacturing and Analyzing of the “First Prototype Tube Kit”	34
3.2.1 Vibro-Acoustic Properties of the “First Prototype Tube” .....	34
3.2.1.1 Cavity Frequencies of the “First Prototype Tube” .....	35
3.2.1.2 Acoustical Mode Shapes of the “First Prototype Tube” .....	37
3.2.1.3 Inner Surface Impedances of the “First Prototype Tube Set” .....	38
3.2.2 Vibro-Acoustic Performance of the “First Prototype Tube” .....	39
3.2.2.1 In Situ Structural Modal Analysis of the “First Prototype Tube” .....	40
3.2.2.2 Outer Surface Impedances of the “First Prototype Tube” .....	42

3.3 Designing, Manufacturing and Analyzing of the “Second Prototype Tube Kit” .....	47
3.3.1 Vibro-Acoustic Properties of the “Second Prototype Tube Kit” .....	48
3.3.1.1 Cavity Frequencies of the “Second Prototype Tube” .....	49
3.3.1.2 Inner Surface Impedances of the “Second Prototype Tube” .....	50
3.3.2 Vibro-Acoustic Performance of the “Second Prototype Tube” .....	51
3.3.2.1 In Situ Structural Modal Analysis of the “Second Prototype Tube” ..	51
3.3.2.2 Outer Surface Impedances of the “Second Prototype Tube” .....	53
3.4 Sound Absorption Coefficient Measurements via “First and Second Prototype Tubes” .....	56
3.5 Designing, Manufacturing and Analyzing of “New Impedance Tube Set” ....	59
3.6 Development of Software.....	65
3.6.1 Measurement and Calculation Programs .....	65
3.6.1.1 Sound Absorption Coefficient Measurement Program .....	66
3.6.1.2 Transmission Loss Measurement Program .....	66
3.6.1.3 Sound Absorption Calculation Program .....	67
3.6.1.4 Transmission Loss Calculation Program .....	68
3.6.1.5 Verification of Measurement Programs .....	69
3.6.1.6 Verification of Calculation Programs .....	70
3.7 Design and Manufacturing of Conditioning System.....	71
3.8 Design and Manufacturing of Specimen Rotation Apparatus.....	72
<b>CHAPTER FOUR - EXPERIMENTAL RESULTS .....</b>	<b>75</b>
4.1 Measurement Results of Normal Incidence Sound Absorption Coefficient, Impedance and Reflection Coefficient of Materials .....	75

4.1.1 Normal Incidence Sound Absorption Coefficient Results of Materials....	76
4.1.2 Normal Incidence Reflection Coefficient Results.....	78
4.1.3 Normal Incidence Specific Impedance Results.....	81
4.2 Measurement Results of Normal Incidence Sound Absorption Coefficient of Materials Under Different Temperature Conditions .....	84
4.2.1 Sound absorption coefficients of materials at different ambient temperatures and relative humidity.....	84
4.2.2 Sound absorption coefficients of materials at different specimen temperatures .....	86
4.3 Measurement Results of Varied Angle Incidence Sound Absorption Coefficient of Materials .....	87
4.3.1 Random incidence sound absorption coefficients of fiberglass material..	88
4.3.2 Random incidence sound absorption coefficients of petroleum based insulant material .....	89
4.3.3 Random incidence sound absorption coefficients of pyramid shaped sponge material .....	91
4.3.4 Evaluation of results.....	93
4.4 Transmission Loss Measurement Results of Materials.....	94
<b>CHAPTER FIVE - CONCLUSION .....</b>	<b>96</b>
<b>REFERENCES.....</b>	<b>98</b>

## LIST OF FIGURES

	<b>Page</b>
Figure 2.1 Quality factor.....	11
Figure 2.2 Acoustical modal analysis experimental setup.....	13
Figure 2.3 Impedance tube kit a) for sound absorption measurements b) for transmission loss measurements.....	14
Figure 2.4 Standing wave and its maximum and minimum sound pressures.....	15
Figure 2.5 Insertion loss in-situ measurement system.....	16
Figure 2.6 Setup for noise reduction system. ....	17
Figure 2.7 Setup for transmission loss system.....	18
Figure 2.8 Sub-systems of a silencer .....	18
Figure 2.9 Four pole parameter of an acoustical element.....	19
Figure 2.10 Different acoustic elements of a muffler.....	21
Figure 2.11 Measurement setup of two microphone method .....	23
Figure 2.12 Measurement setup of two load method .....	26
Figure 2.13 Random incidences and reflected a sound wave.....	31
Figure 3.1 Insulated acoustic cabin .....	33
Figure 3.2 3-D design of first prototype tube .....	34
Figure 3.3 The first prototype tube.....	34
Figure 3.4 Experimental setup of acoustical modal analysis.....	35
Figure 3.5 Acoustical mode shapes of the “first prototype tube set” for closed-closed condition (‘—’: absolute of analytical results, ‘--’: analytical result, ‘o’: experimental results) .....	37
Figure 3.6 Acoustical mode shapes of brass tube set for closed-closed condition (‘— ’: absolute of analytical results, ‘--’: analytical result, ‘o’: experimental results) .....	38
Figure 3.7 Experimental setup of in-situ structural modal analysis of the “first prototype tube” .....	40
Figure 3.8 Experimental setup of in-situ structural modal analysis of brass tube ...	40
Figure 3.9 Frequency response matrix of the “first prototype tube” for in-situ condition .....	41

Figure 3.10 Frequency response matrix of brass tube for in-situ condition.....	41
Figure 3.11 Laser vibrometer and surface sound pressure microphone.....	42
Figure 3.12 Experimental setup of outer surface impedance measurements .....	43
Figure 3.13 Surface vibration velocities of the “first prototype” and brass tubes (red line: brass tube, blue line: “first prototype tube”; a) under first structural natural frequencies b) under second structural natural frequencies).....	43
Figure 3.14 Surface sound pressures of the “first prototype” and brass tubes (red line: brass tube, blue line: the “first prototype tube”; a) under first structural natural frequencies b) under second structural natural frequencies).....	44
Figure 3.15 Outer surface acoustic impedances of the “first prototype” and brass tubes (red line: brass tube, blue line: the “first prototype tube”; a) under first structural natural frequencies b) under second structural natural frequencies) .....	44
Figure 3.16 Surface vibration velocities of the “first prototype” and brass tubes (red pluses: brass tube, blue pluses: the “first prototype tube”; a) under first cavity frequencies, b) under second cavity frequencies, c) under third cavity frequencies, d) under fourth cavity frequencies).....	45
Figure 3.17 Surface sound pressure levels of the “first prototype” and brass tubes (red pluses: brass tube, blue pluses: the “first prototype tube”; a) under first cavity frequencies, b) under second cavity frequencies, c) under third cavity frequencies, d) under fourth cavity frequencies) .....	46
Figure 3.18 Outer surface impedances of the “first prototype” and brass tubes (red pluses: brass tube, blue pluses: the “first prototype tube”; a) under first cavity frequencies, b) under second cavity frequencies, c) under third cavity frequencies, d) under fourth cavity frequencies).....	46
Figure 3.19 Low frequency sound absorption coefficient measurement tube kit of the “second prototype tube” .....	48
Figure 3.20 All parts of the “second prototype tube” .....	48
Figure 3.21 Acoustical mode shapes of the “second prototype tube” set for closed-closed condition (‘—’: absolute of analytical results, ‘-’: analytical result, ‘o’: experimental results).....	50
Figure 3.22 In situ modal test setup of the “second prototype tube”.....	52

Figure 3.23 3x3 frequency response matrix of the “second prototype tube” for in-situ condition .....	52
Figure 3.24 Outer surface impedance measurements setup .....	53
Figure 3.25 Outer surface vibration velocities and surface sound pressures of tubes, a) at first structural natural frequencies b) at second structural natural frequencies (red line: brass tube, blue line: the “first prototype tube”, green line: the “second prototype tube”).....	54
Figure 3.26 Outer surface impedance values of tubes, a) at first structural natural frequencies b) at second structural natural frequencies (red line: brass tube, blue line: the “first prototype tube”, green line: the “second prototype tube”) .....	54
Figure 3.27 Surface vibration velocity values of tubes. a) at first structural natural frequency, b) at second cavity frequency, c) at third cavity frequency, d) at fourth cavity frequency (red plus: brass tube Hz, blue plus: the “first prototype tube”, green plus: the “second prototype tube”).....	55
Figure 3.28 Surface sound pressures of tubes. a) at first structural natural frequency, b) at second cavity frequency, c) at third cavity frequency, d) at fourth cavity frequency (red plus: brass tube Hz, blue plus: the “first prototype tube”, green plus: the “second prototype tube”) .....	55
Figure 3.29 Outer surface impedance values of tubes. a) at first structural natural frequency, b) at second cavity frequency, c) at third cavity frequency, d) at fourth cavity frequency (red plus: brass tube Hz, blue plus: the “first prototype tube”, green plus: the “second prototype tube”).....	56
Figure 3.30 Sound absorption coefficient of the “first prototype tube” for rigid end condition .....	57
Figure 3.31 Sound absorption coefficient of the “second prototype tube” for rigid end condition .....	57
Figure 3.32 Sound absorption coefficient of brass tube for rigid end condition.....	57
Figure 3.33 Attenuation coefficients of the “first and second prototype tubes” (blue line: the “first prototype tube”, green line: the “second prototype tube”) .....	58

Figure 3.34 Sound absorption coefficient measurement results of a felt material (red circles: brass tube, blue line: the “first prototype tube”, green line: the “second prototype tube”).....	59
Figure 3.35 Low frequency sound absorption coefficient measurement set (a: 3-D design model, b: manufactured system, c: painted system).....	60
Figure 3.36 High frequency sound absorption coefficient measurement set (a: 3-D design model, b: manufactured system, c: painted system).....	61
Figure 3.37 Low frequency transmission loss measurement set (a: 3-D design model, b: manufactured system, c: painted system).....	61
Figure 3.38 High frequency transmission loss measurement set (a: 3-D design model, b: manufactured system, c: painted system).....	62
Figure 3.39 Imaginary part of wave number that has been determined for tube attenuation of the “new impedance tube set” (100 Hz – 1000 Hz) .....	62
Figure 3.40 Imaginary part of wave number that has been determined for tube attenuation of the “new impedance tube set” (1 kHz- 5 kHz).....	63
Figure 3.41 Sound absorption coefficient of the “new impedance tube set” for rigid end condition (100 Hz- 1000 Hz).....	63
Figure 3.42 Sound absorption coefficient of the “new impedance tube set” for rigid end condition (1 kHz- 5 kHz).....	64
Figure 3.43 Sound absorption coefficient measurement results of a felt material (Red circles: brass tube, blue line: the “first prototype tube”, green line: the “second prototype tube”, black line: the “new impedance tube set”).....	64
Figure 3.44 Algorithm of measurement programs.....	65
Figure 3.45 Sound Absorption Coefficient Set Measurement Program main pages ..	66
Figure 3.46 Transmission Loss Set Measurement Program main pages.....	67
Figure 3.47 Sound Absorption Coefficient Set Calculation Program .....	68
Figure 3.48 Transmission Loss Set Calculation Program.....	68
Figure 3.49 Compared results of Signal Express and Sound Absorption Coefficient Set Measurement Program measurements for low frequency bandwidth; 100 Hz – 1000 Hz (red line: Signal Express FRF result; blue line: Alfa Measurement Program FRF result).....	69



Figure 3.50 Compared results of Signal Express and Sound Absorption Coefficient Set Measurement Program measurements for low frequency bandwidth; 1000 Hz - 5000 Hz (red line: Signal Express FRF result; blue line: Alfa Measurement Program FRF result).....	69
Figure 3.51 Expansion chamber.....	70
Figure 3.52 Compared results of transmission loss of expansion chamber (red line: analytical result; blue line: calculated result via Transmission Loss Set Calculation Program).....	70
Figure 3.53 Scheme of conditioning system .....	71
Figure 3.54 Conditioning test system.....	72
Figure 3.55 Rotation apparatus with low frequency sound absorption coefficient measurement set (a: design drawing b: manufactured system c: painted system).....	73
Figure 3.56 Constant angled specimen holders (a: 15° b: 30° c: 40°).....	73
Figure 4.1 Sound absorption coefficient measurement results of Ax (blue line: two-microphone method via the “new impedance tube set”, black line: standing wave ratio method via brass tube).....	76
Figure 4.2 Sound absorption coefficient measurement results of Bx (blue line: two-microphone method via the “new impedance tube set”, black line: standing wave ratio method via brass tube).....	77
Figure 4.3 Sound absorption coefficient measurement results of Cx (blue line: two-microphone method via the “new impedance tube set”, black line: standing wave ratio method via brass tube).....	77
Figure 4.4 Sound absorption coefficient measurement results of pyramid shaped sponge material.....	78
Figure 4.5 Sound absorption coefficient measurement results of petroleum based insulant material .....	78
Figure 4.6 Reflection coefficient of Ax .....	79
Figure 4.7 Reflection coefficient of Bx .....	79
Figure 4.8 Reflection coefficient of Cx .....	80
Figure 4.9 Reflection coefficient of pyramid shaped sponge material .....	80
Figure 4.10 Reflection coefficient of petroleum based insulant material .....	81

Figure 4.11 Resistance and reactance ratios of Ax.....	82
Figure 4.12 Resistance and reactance ratios of Bx .....	82
Figure 4.13 Resistance and reactance ratios of Cx .....	83
Figure 4.14 Resistance and reactance ratios of pyramid shaped sponge material .....	83
Figure 4.15 Resistance and reactance ratios of petroleum based insulant material .....	84
Figure 4.16 Sound absorption coefficient measurement result of pyramid shaped sponge material at different ambient temperatures (black line: temperature of tube inside is 32°C and relative humidity is %36, red line: temperature of tube inside is 42°C and relative humidity is %51, blue line: temperature of tube inside is 19°C and relative humidity is %20) .....	85
Figure 4.17 Sound absorption coefficient measurement result of petroleum based insulant material at different ambient temperatures (black line: temperature of tube inside is 25°C and relative humidity is %31, red line: temperature of tube inside is 43°C and relative humidity is %48, blue line: temperature of tube inside is 16°C and relative humidity is %17).....	85
Figure 4.18 Sound absorption coefficient measurement result of pyramid shaped sponge material at different specimen temperatures (red line: temperature of tube inside is 50°C, green line: temperature of tube inside is 25°C, black line: temperature of tube inside is 10°C, blue line: temperature of tube inside is -9°C) .....	86
Figure 4.19 Sound absorption coefficient measurement result of petroleum based insulant material at different specimen temperatures (red line: temperature of tube inside is 50°C, green line: temperature of tube inside is 25°C, black line: temperature of tube inside is 10°C, blue line: temperature of tube inside is -9°C) .....	87
Figure 4.20 Random incidence sound absorption coefficient measurement result of fiberglass material (red lines: results of constant angled specimen holders, green lines: results of rotation apparatus, blue lines: results empirical formula; a) for 0° b) for 15° c) for 30° d) for 40°).....	88

Figure 4.21 Random incidence sound absorption coefficient measurement result of fiberglass material (green lines: for 0°, red lines: for 15°, blue lines: for 30°, black lines: for 40°; a) results of rotation apparatus b) results of constant angled specimen holders) .....	89
Figure 4.22 Random incidence sound absorption coefficient measurement result of petroleum based insulant material (red lines: results of constant angled specimen holders, green lines: results of rotation apparatus, blue lines: results empirical formula; a) for 0° b) for 15° c) for 30° d) for 40°) .....	90
Figure 4.23 Random incidence sound absorption coefficient measurement result of petroleum based insulant material (green lines: for 0°, red lines: for 15°, blue lines: for 30°, black lines: for 40°; a) results of rotation apparatus b) results of constant angled specimen holders).....	91
Figure 4.24 Random incidence sound absorption coefficient measurement result pyramid shaped sponge material (red lines: results of constant angled specimen holders, green lines: results of rotation apparatus, blue lines: results empirical formula; a) for 0° b) for 15° c) for 30° d) for 40°) .....	92
Figure 4.25 Random incidence sound absorption coefficient measurement result of pyramid shaped sponge material (green lines: for 0°, red lines: for 15°, blue lines: for 30°, black lines: for 40°; a) results of rotation apparatus b) results of constant angled specimen holders).....	93
Figure 4.26 Transmission loss measurement result of pyramid shaped sponge material .....	94
Figure 4.27 Transmission loss measurement result of foam material.....	95
Figure 4.28 Transmission loss measurement result of petroleum based insulant material .....	95

## LIST OF TABLES

	<b>Page</b>
Table 2.1 Acoustical natural frequencies and mode shapes of tubes for different end conditions .....	13
Table 3.1 Cavity frequencies of the “first prototype tube” set for closed-closed boundary condition.....	35
Table 3.2 Cavity frequencies of the “first prototype tube” set for closed-open boundary condition.....	36
Table 3.3 Cavity frequencies of the brass tube set for closed-closed boundary condition.....	36
Table 3.4 Cavity frequencies of brass tube set for closed-open boundary condition.. ..	36
Table 3.5 Measured phase shifts and computed surface impedances of first prototype and brass tubes .....	39
Table 3.6 Natural frequencies tubes for in-situ condition.....	42
Table 3.7 Cavity frequencies of the “second prototype tube” for closed-closed boundary condition.....	49
Table 3.8 Measured phase shifts and computed surface impedances of the “second prototype tube” .....	51
Table 3.9 Natural frequencies of the “second prototype tube” for in-situ condition .. ..	52

## **CHAPTER ONE**

### **INTRODUCTION**

Acoustic performance parameters of insulation materials or mufflers are generally determined via impedance tube apparatus. These apparatus generally have hollow tubes made of brass since it is too rigid for vibration and too hard for acoustic transmission. However, it is too heavy and expensive. Composite materials are preferred in many areas such as aerospace, automotive industries because of their high strength-weight ratio. Therefore, it can also be used as a main tube in impedance measurement kits. For this purpose, vibro-acoustic performance parameters of composite structures have been determined in this thesis. Vibration and acoustic modal analysis have been performed. For the determination of frequency modal responses, modal analysis can be used. Modal analysis gives information about dynamic characteristics of structures, for instance natural frequencies, mode shapes etc.

Experimental structural modal analysis technique is a very well-known method and used for many years to define dynamic characteristics of structures;

Kennedy & Pancu (1948) recommended the first and important technique of experimental modal analysis before FFT was well accepted. This method has been discarded after FFT using in experimental modal analysis technique.

Cooley & Tukey (1965) have invented fast Fourier transform algorithm. Frequency response of a structure can be calculated from the measurement of given inputs and resultant responses by FFT.

Allemang (1984) has described bibliography of experimental modal analysis technique.

Ahn & Mote (1998) have performed modal testing of a rotating testing.

Gaul et al. (1999) determined material properties of plates from modal measurements.

Structural modal analysis applications were used comprehensively not only in mechanical engineering but also in different areas of engineering branches such as, civil, aeronautical, electronic, etc.

For example, experimental modal analysis technique has been used to determine modal parameters of a cable-stayed bridge by Clemente et al. (1998).

Couteau et al. (1998) investigated and compared modal behavior of normal and implanted human femur via experimental modal analysis.

Also, experimental and numerical modal analysis techniques have been used in order to determine modal behavior of hard disk drive (Xu & Guo, 2003).

Dynamic characteristics of different kind of structures are determined still via modal analysis techniques with recent technological developments;

Stochastic dynamic responses of one-stage pump have been identified with experimental modal data. (Batou, Soize, & Audebert, 2015).

Modal behaviors of li-on cells which are widely used in hybrid vehicles have been investigated (Hooper, & Marco, 2016).

Modal testing of a hydraulic pipeline system has been performed. (Mikota, Manhartgruber, Kogler & Hammerle, 2017).

Acoustical modal analysis technique has been used for dynamic characterization of cavities. Experimental, numerical and analytical methods exist in literature.

An acoustical modal analysis experiment has been performed. Acoustic system has been excited by a vibrating piston and it has been driven by a shaker with random noise signal (Nieter & Singh, 1982).

Whear & Morrey (1995) have developed a new technique for experimental acoustic modal analysis. This method uses a finite difference calculation for determination of spatial variations in sound pressure.

Ver & Beranek (2005) described analytical formulas of acoustic modal parameters of cavities.

Determining acoustic performance parameters is significant to select suitable insulation material or mufflers in noisy systems or environments. These materials and mufflers are used in many sectors and applications such as construction, heating and ventilating systems, air conditioning plants, electronic, white good, automotive, aeronautical (aircraft, rocket, missile). Sound absorption coefficient, surface impedance, insertion loss (IL), noise reduction (NR) and transmission loss (TL) are the main acoustic performance parameters. Although some parameters are related to each other, each one presents different information about sound insulation characteristics (Munjaj, 1987). In general, special acoustic rooms and special measurement apparatus and systems are required for determining the performance parameters.

Impedance tube system is the most commonly used apparatus, since it is much simpler and faster, easy to produce its samples with short test time. However, it only gives parameters in normal direction. There is a lot of varied technique for measurement of sound absorption coefficients.

Seybert & Ross (1977) have produced two-microphone random excitation technique for determination of acoustic properties of materials.

Mason et al. (1983) have investigated and compared different techniques for impedance measurements.

Dunlop (1985) has developed a new technique; the method is based on the measurements of radiation impedance at the end of an open flanged pipe placed against a specimen.

Also, most accurate and current method for determination of sound absorption coefficients of materials is the transfer function method;

Seybert & Soenarko (1980) have investigated differences of pure tone and random excitations on the determination of acoustic properties using transfer function method.

On the other hand, impedance tubes are used for determination of transmission loss of materials and mufflers and there is a lot of study for that in the literature.

To & Doige (1979a, 1979b) has investigated a transient technique for determination of matrix parameters. However, their results were not good at low frequency region.

Lung & Doige (1983) used similar method for measuring the four pole parameters of tubes and expansion chambers. They use two loads, four-microphone method. However, the method is unstable and unreliable when loads are not enough different.

The major disadvantage of this method is that an anechoic end is required for measurements but fully anechoic termination is so difficult to provide especially at low frequency region. Whereas acoustical elements can be modeled by its four-pole parameters (Munjaj, 1987).

The transmission loss can be measured via the decomposition method. Decomposition theory was used to measure acoustic parameters in duct like



absorption coefficient and impedance of materials. Sound pressure may be decomposed into its incident and reflected waves via using two microphone and random excitation technique. The sound power of input wave can be calculated after decomposition (Seybert, 1988).

Well accepted method is developed by Munjal and Doige (1990). Two-source method has been used for measuring the four pole parameters.

Tao & Seybert (2003) have reviewed and compared current techniques for measuring muffler transmission loss.

Acoustical performance parameters are affected from temperature and humidity conditions. There are a few studies in the literature.

Harris (1966) has measured absorption of sound in air as a function of humidity at six temperatures.

Ando & Kosaka (1970) have experimentally investigated effect of humidity on sound absorption coefficients of porous materials.

Wong (1986) has investigated effects of humidity on the characteristic impedance of air and all results are listed for different temperatures and atmospheric pressures with relative humidity levels.

Hamilton et al. (2003) has investigated thermal effects on acoustic streaming.

Sound absorption coefficients of materials can be determined via reverberation room or impedance tube measurements. Reverberation rooms can simulate nature, so it gives accurate and reliable results. Also, random incidence sound absorption coefficients can be determined via reverberation room measurements. (ASTM C-423-09, 2009).

Impedance tube measurements can determine only normal incidence sound absorption coefficients (ASTM C-384-04, 2004).

Also, random incidence sound absorption coefficients can be determined analytically from normal incidence sound absorption coefficient data (Fahy, 2001).

In this thesis a sandwich composite impedance tube was designed and manufactured as a part of a nationally funded project. Various experimental works were performed for determination of structural and acoustical performance of the tube. An air conditioning system was developed for investigation of humidity and temperature effect of the medium on sound absorption coefficients of porous materials. Also materials themselves are conditioned by different temperatures, and tests have been repeated. Beside this, a rotation apparatus and constant-angled specimen holders are designed and manufactured for the determination of random incidence sound absorption coefficients of materials via impedance tube which is not available in literature. In addition to those, effects of the thermal condition of materials on the sound absorption coefficient were submitted for the first time in literature.

The thesis is organized as five main chapters;

First chapter begins with an introduction section.

In Chapter 2, one can find the theoretical bases of various analytical, numerical and experimental methods.

Chapter 3 presents designing and manufacturing of sandwich composite impedance tube kit, measurement and calculation software, air conditioning system and rotation apparatus. Various experimental works have been performed for investigation and verification of tube performance in the chapter.

Chapter 4 present experimental results with verification studies.

Finally, Chapter 5 ends up with a conclusion of the thesis.

This study is sponsored by the Scientific and Technological Research Council of Turkey (TÜBİTAK) with the project number 114M753.

Symbol list:

$k_s$ : stiffness constant	
$c_d$ : damping constant	$Z_s$ : source impedance
$m$ : mass	$Z_T$ : radiation impedance
$f$ : frequency	$k$ : wavenumber
$t$ : time	$k''$ : tube attenuation
$\omega$ : angular frequency of excitation	$k'$ : complex wavenumber
$\alpha_r$ : receptance	$\Delta_{ij}$ : determinant of transfer matrix between i and j microphones
$\xi$ : damping ratio	$T_{ij}^{ij}$ : transfer matrix element
$\omega_0$ : natural frequency	$t$ : transmission coefficient
$j$ : $\sqrt{-1}$	$r$ : reflection coefficient
$A_n$ : modal constant	$k_m$ : propagation wave number in material
$f_l$ : lower frequency	$Z_m$ : characteristic impedance
$f_u$ : upper frequency	$n$ : minimum peak number
$c$ : speed of sound	$\delta_n$ : shift of the nth peak
$x$ : distance from reference point	$\theta$ : phase shift
$\alpha$ : sound absorption coefficient	$\phi$ : incidence sound wave angle
$I$ : incidence sound pressure level	$L$ : length
$T$ : transmitted sound pressure level	$s_{ij}$ : distance between i. and j. microphones
$R$ : reflected sound pressure level	$d$ : diameter of tube
$T^s$ : transfer matrix	
$v$ : particle velocity amplitude	
$k$ : complex wave number	

## **CHAPTER TWO**

### **THEORY**

In this section, methods used in this thesis, are briefly explained. In this regard, vibro-acoustic modal analysis and determination of acoustic performance parameters of materials are given.

#### **2.1 Vibro-Acoustic Modal Analysis**

Impedance tubes are a kind of experimental setup for determination of acoustic performance parameters of insulation materials or mufflers. Sound energy is absorbed, reflected and transmitted in every material. The coefficients of absorption, transmission and reflection are computable via standing wave method in impedance tubes. After, using these coefficients, acoustic performance parameters of insulation materials or mufflers can be calculated. Impedance tubes should be smooth and have constant cross section and its walls should be rigid and non-porous for determination of the parameters in accordance with standards. Also surface vibration velocity and surface sound pressure values of the tube should be in neglected levels for reliable analyses.

Rigidity of tube walls is evaluated by the information of surface impedance. Acoustical and structural modal tests have been performed for determination of surface impedance. The impedance tubes shouldn't operate at their acoustical and structural natural frequencies. Therefore modal tests are important for determination of critical frequencies of the tubes. The surface vibration and sound pressures of tubes are determined via experimental methods.

##### ***2.1.1 Structural Modal Analysis***

Modal analysis gives information about characteristics of structures, such as natural frequencies, mode shapes or damping ratio etc. Structural modal analysis,

especially experimental one, is well known and applied method in literature for determination of dynamic characteristics of structures (He & Fu, 2001).

In vibration theory, the model of the mechanical systems can be created as single degree of freedom (SDOF) or multi degree of freedom (MDOF) systems. Also multi degree of freedom systems can be modeled as summation of single degree of freedom systems by linear vibration theory. Methods of peak selection and circle fit are used for SDOF systems and curve fitting method is the common for MDOF systems. In this thesis, SDOF Peak Selection Method was used. This method is also known as half power method. Here, the peak selection method and SDOF system approach are explained briefly.

#### *2.1.1.1 Single Degree of Freedom Approach*

SDOF systems are modeled as a spring with a stiffness constant  $k_s$ , an element with a mass  $m$  and a damper with a damping constant  $c_d$ . For harmonic force excitation at frequency  $\omega$ ;

$$f(t) = F(\omega)e^{j\omega t}, \quad (2.1)$$

the response of the system can be written as;

$$x(t) = X(\omega)e^{j\omega t}. \quad (2.2)$$

Receptance response of the system can be represented for viscous damping as follows:

$$\alpha_r = \frac{X(\omega)}{F(\omega)} = \frac{1}{k_s - \omega^2 m + j\omega c_d}. \quad (2.3)$$

Receptance ( $\alpha_r$ ) is the ratio of displacement over force applied to the system. Equation (2.3) can be rewritten with modal parameters for viscous damping as;

$$\alpha_r(\omega) = \frac{1/m}{\omega_0^2 - \omega^2 + 2j\omega\omega_0\xi} \quad (2.4)$$

In these formulas,  $\omega_0$  is the natural frequency,  $\omega$  is the excitation frequency and  $\xi$  is the viscous damping ratio of the SDOF system.

*2.1.1.1.1 Peak Selection Method.* Frequency response function of a system having N number of modes can be written as follows (He & Fu, 2001);

$$\alpha(\omega) = \sum_{n=1}^N \frac{A_n}{\omega_n^2 - \omega^2 + 2j\omega\omega_n\xi_n} \quad (2.5)$$

For small damped systems, damping ratio can be neglected;

$$\alpha(\omega) = \sum_{n=1}^N \frac{A_n}{\omega_n^2 - \omega^2} \quad (2.6)$$

$A_n$  is the modal constant and it can be described as (He & Fu, 2001);

$$A_n = 2 \cdot \alpha_{\max} \cdot \xi_n \cdot \omega_n^2 \quad (2.7)$$

Viscous damping ratio can be derived from quality factor. Quality factor known as modal bandwidth is a dimensionless parameter of the bandwidth frequency values, which is 3 dB less than the peak value (Figure 2.1).

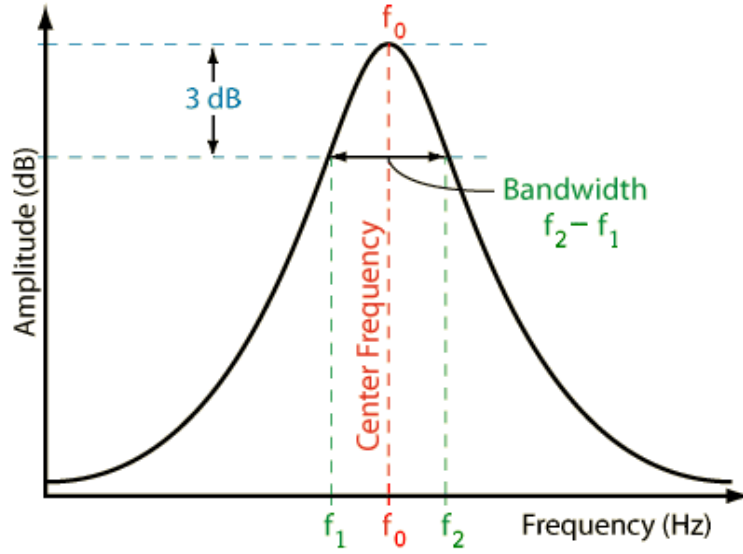


Figure 2.1 Quality factor

Viscous damping ratio and peak value is also derived respectively as follows:

$$\xi_n = \frac{f_2 - f_1}{2f_0}, \quad (2.8)$$

$$\alpha_{\max} = |\alpha_n(\omega_n)_{\max}|. \quad (2.9)$$

Here,  $f_1$  and  $f_2$  are lower and higher frequency of modal bandwidth respectively where  $f_0$  is the center frequency of the band.

### 2.1.2 Acoustical Modal Analysis

Standing wave method is the commonly used approach for determination of acoustic characteristics of materials. In this method, maximum and minimum sound pressures and their locations in the tube are determined with a movable microphone. Sound absorption coefficient, reflection coefficient and transmission coefficient of materials could be specified with this information. However, acoustical natural frequencies and modes are also determined by another method; Nieter and Singh are developed a direct acoustical modal analysis method and measurement setup. The method is similar to structural modal analysis technique (Nieter & Singh, 1982).

Before performing experiments for acoustical modal analysis, operating frequency range of the tube should be defined so that the plane wave approach could be applied for. The operating frequency of tube,  $f$ , should be;

$$f_l < f < f_u . \quad (2.10)$$

Here,  $f_l$  lower frequency limit and  $f_u$  is the upper frequency limit of tube. The lower frequency limit  $f_l$  is determined by wavelength of sound waves. The length of tube should be greater than quarter wavelength of the lowest frequency of interest. On the other hand, in order to maintain the plane wave approach, the upper frequency limit  $f_u$  should meet the following equality (ASTM E2611, 2009);

$$f_u < \frac{0.586c}{d} , \quad (2.11)$$

where,  $c$  : speed of sound (m/s),  $d$  :diameter of tube (m). After that, the propagation of sound wave is measured via a movable microphone as shown in Figure 2.2.; excitation frequency is changed step by step and acoustical natural frequency corresponding to the maximum sound pressure level in the tube is determined. After, that the tube is acoustically excited by its natural frequency, then the sound pressure levels in the tube are determined via movable microphone, and thus acoustic mode at that natural frequency is obtained. Sound pressure values are normalized between “1” to “-1”.



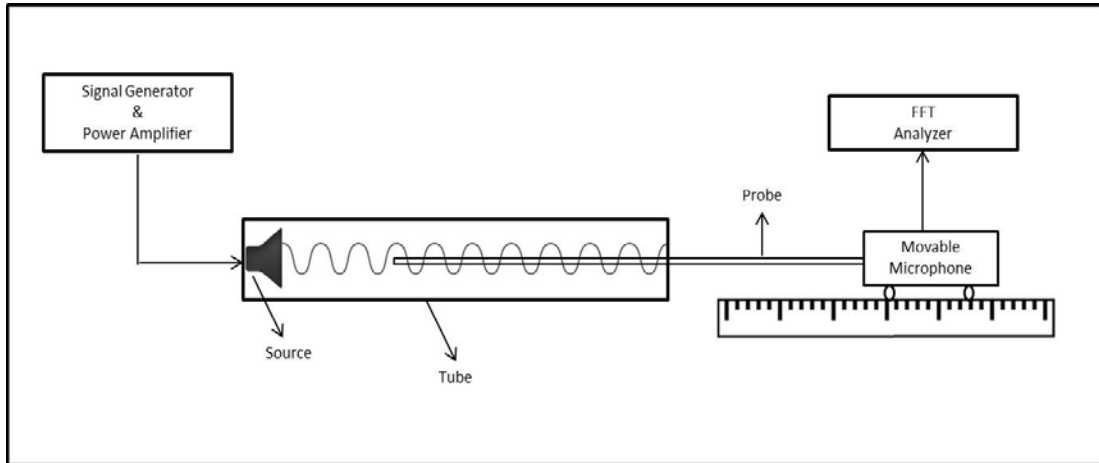





Figure 2.2 Acoustical modal analysis experimental setup

Table 2.1 Acoustical natural frequencies and mode shapes of tubes for different end conditions

End Condition	Natural Frequency	Mode Shape
Closed Closed $D \ll L$ 	$\frac{ic}{2L}$	$\frac{\cos(i\pi x)}{L}$ $i=0,1,2,\dots$
Closed Open $D \ll L$ 	$\frac{ic}{4L}$	$\frac{\cos(i\pi x)}{2L}$ $i=0,1,3,5,\dots$
Open Open $D \ll L$ 	$\frac{ic}{2L}$	$\frac{\sin(i\pi x)}{L}$ $i=1,2,3,\dots$

Here in the Table 2.1,  $L$  is length of tube,  $m$ ,  $x$  is the distance from reference point,  $m$ .

Acoustical natural frequencies and corresponding mode shapes of tubes with different boundary conditions are given in Table 2.1 (Ver & Benarek, 2005).

## 2.2 Acoustical Performance Parameters

Impedance tube kits (Figure 2.3) are experimental kits for determination of acoustical performance parameters of insulation materials or mufflers. They are also called as standing wave apparatus.



Figure 2.3 Impedance tube kit a) for sound absorption measurements b) for transmission loss measurements

There are five important acoustic performance parameters;

1. Sound absorption coefficient,  $\alpha$
2. Surface impedance,  $Z_s$
3. Insertion loss, IL
4. Noise reduction, NR
5. Transmission loss, TL

### ***2.2.1 Sound Absorption Coefficient***

Conservation energy law remarks that the energy cannot be created or destroyed. However, it can be changed from one type to another. Therefore, the sound energy is not destroyed but it is dissipated in the form of heat energy. Materials reflect, transmit and absorb the sound energy. Sound absorption is a function of material and it depends on physical and chemical properties of material. Porous and soft materials absorb the sound more than rigid ones. In addition, porous materials are more effective at high frequencies while volume absorbers and panels are more effective at lower frequencies (Everest & Pohlmann, 2009). The sound absorption coefficient could be measured via impedance tube kits or reverberation chambers. In this thesis, impedance tube method is used.

Figure 2.4 shows standing wave model of sound waves. Here A is the amplitude

of incidence sound wave from source. B is the amplitude of the reflected sound energy. The sound wave propagates along the tube and strikes specimen at the end of the tube. Some amount of energy is absorbed by the material and the rest of it reflects and transmits. The incidence and reflected waves are interfered in the tube, and a sound pressure pattern called as standing wave is observed. Sound absorption coefficient can be calculated from this standing wave by measuring the wave's maximum and minimum amplitudes at each frequency, generally for octave band frequencies.

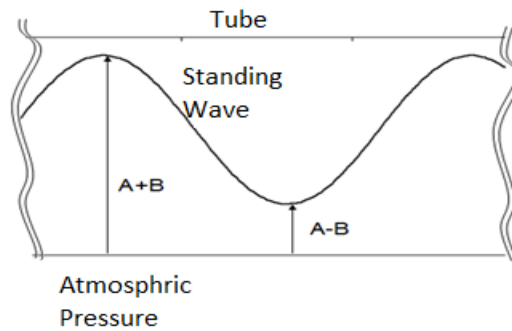


Figure 2.4 Standing wave and its maximum and minimum sound pressures

In this regard, sound absorption coefficient ( $\alpha$ ) is written as;

$$\alpha = 1 - \frac{B^2}{A^2} = 1 - \left( \frac{n-1}{n+1} \right)^2, \quad (2.12)$$

where  $n$  is the standing wave ratio and defined as;

$$n = \left( \frac{A+B}{A-B} \right) = \frac{SPL_{\max}}{SPL_{\min}}. \quad (2.13)$$

### 2.2.2 Surface Impedance

Acoustic surface impedance is the resistance of materials and mufflers against to the propagation of sound. It depends on the physical properties of materials and surrounding fluids. It is defined as;

$$Z / \rho_0 c = \frac{1+R}{1-R}. \quad (2.14)$$

Here, R is reflection coefficient and it can be described as;

$$R = \frac{B}{A}. \quad (2.15)$$

### 2.2.3 Insertion Loss

Insertion loss (IL) is the sound pressure level difference at a reference point, generally outside of the system, with and without muffler or material (Tao & Seybert, 2003). Figure 2.5 shows experimentally IL measurement system.

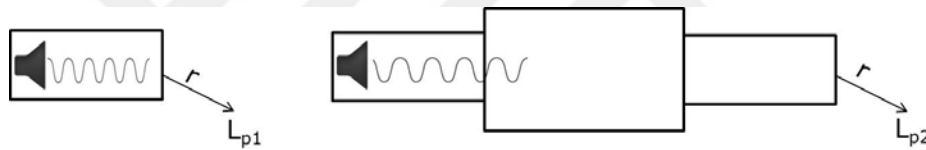


Figure 2.5 Insertion loss in-situ measurement system

Insertion loss can be described as in dB;

$$IL = L_{p1} - L_{p2}. \quad (2.16)$$

IL is the easiest acoustic performance parameters that can be determined experimentally so it is commonly used in industry. Moreover, IL does not give information about only muffler performance, since it depends not only on muffler but also on radiation impedance and source impedance. Therefore, it is not so easy to calculate it via analytically or numerically. Laser vibro-meter and surface microphones should be used for determination of source impedance. Radiation impedance can be calculated analytically (Ver & Benarek, 2005).

### 2.2.4 Noise Reduction

Noise reduction (NR) is the sound pressure level difference between input and output ducts. Although, NR can be measured easily, it isn't the best method for muffler design. It depends on muffler and radiation impedance. If the radiation impedance is known, NR can be calculated analytically for mufflers (Munjal, 1987). Figure 2.6 shows schematic noise reduction measurement.



Figure 2.6 Setup for noise reduction system

Noise reduction can be described as in dB;

$$NR = L_{p,in} - L_{p,out} = 20 \log \left( \frac{P_{in}}{P_{out}} \right). \quad (2.17)$$

### 2.2.5 Transmission Loss

Transmission loss (TL) is the sound power level ratio between input and output ducts. In transmission loss measurements, the end of the tube should be anechoic. In other words, transmitted sound wave should not be reflected from the end of the tube. Therefore, output duct should be long enough or a high absorber material should be placed at the end as shown in Figure 2.7. Since transmission loss depends on only muffler or material properties, no need for calculation of radiation and source impedances;

$$TL = 20 \log \left( \frac{I}{T} \right) + 10 \log \left( \frac{S_i}{S_o} \right). \quad (2.18)$$

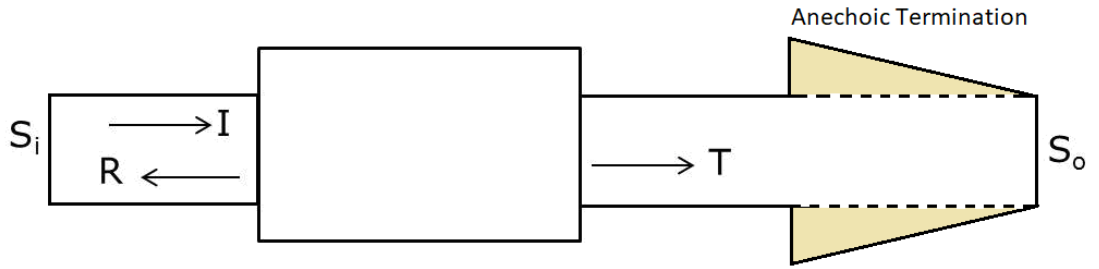


Figure 2.7 Setup for transmission loss system

Here;  $S_i$  is inlet pipe cross section area,  $S_o$  is output pipe cross section area,  $I$  is incidence sound pressure level,  $T$  is transmitted sound pressure level.

### 2.3 Analytical Methods for Acoustic Performance Parameters

Insertion loss, noise reduction and transmission loss parameters can be determined by writing mass and pressure continuities at discontinuity points or transfer matrix method for simple silencers. In this thesis, experimental transfer matrix method is used. Therefore, the transfer matrix method is explained briefly in next sections.

#### 2.3.1 Analytical Transfer Matrix Method

In the transfer matrix method, acoustical structures are modelled by sub-systems created as continues pieces of acoustic cavities, as shown in Figure 2.8.

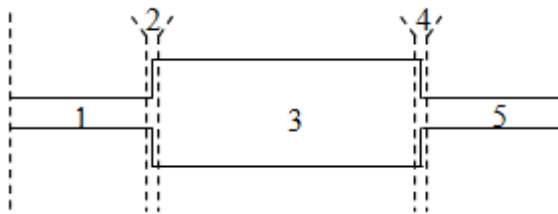


Figure 2.8 Sub-systems of a silencer

Transfer matrix of the entire system  $T^{(s)}$  shown in Figure 2.8 can be calculated as;

$$T^{(s)} = T^{(1)}T^{(2)}T^{(3)}T^{(4)}T^{(5)} . \quad (2.19)$$

where  $T^{(i)}$  is the transfer matrix of each  $i$ th sub-system and can be determined by four pole parameters, as given in Figure 2.9.

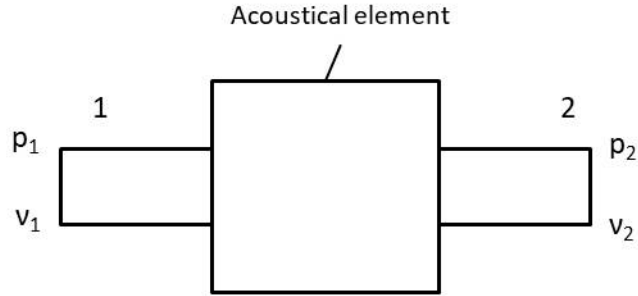


Figure 2.9 Four pole parameter of an acoustical element

The transfer matrix of each substructure can be written as (Tao & Seybert, 2003).

$$\begin{bmatrix} p_1 \\ v_1 \end{bmatrix} = \begin{bmatrix} A & B \\ C & D \end{bmatrix} \begin{bmatrix} p_2 \\ v_2 \end{bmatrix}. \quad (2.20)$$

Here  $p_1$  and  $p_2$  are the sound pressure amplitudes and  $v_1$  and  $v_2$  are the particle velocity amplitudes at the inlet and outlet respectively.  $A$ ,  $B$ ,  $C$  and  $D$  are four pole parameters of the element.

Analytical transfer matrix of a straight tube (elements 1, 3 and 5 in Figure 2.8) can be found as (Munjal, 1987).

$$\mathbf{T}_{\text{pipe}} = \begin{bmatrix} T_{11} & T_{12} \\ T_{21} & T_{22} \end{bmatrix}_{\text{pipe}} = e^{-jMk_0 l} \begin{bmatrix} \cos k_0 l & jY_0 \sin k_0 l \\ \frac{j}{Y_0} \sin k_0 l & \cos k_0 l \end{bmatrix}. \quad (2.21)$$

Here,  $M = V/c$  is Mach number ( $V$ : Flow velocity) and  $Y_0$  is the characteristic impedance of the pipe and is written as;

$$Y_0 = \frac{c}{S} . \quad (2.22)$$

Analytical transfer matrix of discontinuities, i.e. expansion area (element 2) and reduction area (element 4) can be written as

$$T_{discontinuity} = \begin{bmatrix} 1 & KM_{out} Y_{out} \\ 0 & 1 \end{bmatrix} . \quad (2.23)$$

Here,  $Y_{out}$  is the characteristic impedance of discontinuity and  $K$  can be written for expansion area (element 2) as;

$$K = \left( \frac{S_3}{S_1} - 1 \right)^2 , \quad (2.24)$$

and for reduction area (element 4) as;

$$K = \left( 1 - \frac{S_5}{S_3} \right) / 2 . \quad (2.25)$$

Transmission loss (TL) can be calculated when input and output pipe diameters are equal:

$$TL = 20 \log \left| \frac{T_{11} + \frac{S}{c} T_{12} + \frac{c}{S} T_{21} + T_{22}}{2} \right| , \quad (2.26)$$

where  $S$  is the diameter of inlet and outlet.

Insertion loss (IL) can be written as;



$$\mathbf{IL} = 20 \log \left| \frac{\tilde{T}_{11}Z_T + \tilde{T}_{12} + \tilde{T}_{21}Z_S Z_T + \tilde{T}_{22}Z_S}{D'_{11}Z_T + D'_{12} + D'_{21}Z_S Z_T + D'_{22}Z_S} \right| . \quad (2.27)$$

Here;  $\tilde{T}$  is the transfer matrix of muffler and it can be computed with multiplying  $T$  and  $D$  as given in Figure 2.10.  $D'$  is the transfer matrix of pipe without silencer or material.  $Z_s$  is source impedance and  $Z_T$  is radiation impedance.

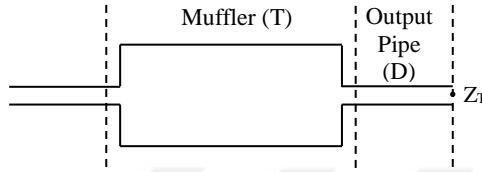


Figure 2.10 Different acoustic elements of a muffler

Radiation impedance of open-end system can be written as (Munjaj, 1987);

$$Z_T = Y_0 \frac{1+R}{1-R} , \quad (2.28)$$

where,  $R$  is radiation coefficient and it can be written as;

$$R = |R| e^{j(\pi - 2k_0\delta)} \quad (2.28)$$

$\delta$  and  $|R|$  are given empirically as (Munjaj, 1987);

$$\begin{aligned} \delta / r_0 &= 0.6133 - 0.1168(kr_0)^2 , & k_0r_0 < 0.5 \\ \delta / r_0 &= 0.6393 - 0.1104kr_0 , & 0.5 < kr_0 < 2 \end{aligned} \quad (2.29)$$

$$\begin{aligned} |R| &= 1 + 0.01336kr_0 - 0.59079(kr_0)^2 \\ &+ 0.33576(kr_0)^3 - 0.06432(kr_0)^4 , & kr_0 < 1.5 \end{aligned} \quad (2.30)$$

Here;  $k$  is wave number,  $r_0$  is the radius of output pipe (outlet). Noise reduction (NR) can be computed by the same method as;

$$NR = 20 \log \left| \frac{\tilde{T}_{11} Z_T + \tilde{T}_{12}}{D_{11} Z_T + D_{12}} \right| . \quad (2.31)$$

## 2.4 Experimental Methods for Acoustic Performance Parameters

Acoustic performance parameters could be determined by several experimental methods; two-microphone method (transfer function method), two-load or two-source methods (transfer matrix method) are mostly preferred methods for this purpose. ISO and ASTM standardize these methods. ASTM E 1050 – 98 is used for sound absorption coefficient and ASTM E2611 – 09 is used for transmission loss measurements. These standards are examined in the following sections.

### *2.4.1 ASTM E 1050-98 - Standard Test Method for Impedance and Absorption of Acoustical Materials Using a Tube, Two Microphones, and a Digital Frequency Analysis System*

ASTM E 1050-98 is a standard which covers impedance tube design criteria and test method for measurement of normal incidence sound absorption coefficient and specific acoustic impedance ratios of materials. Two-microphones are used in this measurement method and so the method is called two-microphone method. Position of microphones in tube, measurement frequency range, diameter and length of tubes and formulas are stated in standard.

Measurement frequency range depends on the diameter and the length of the tube and the distance between two microphones. The upper frequency limit is determined with standing wave condition (Equation 2.11) and it depends on the distance between the microphones. The lower frequency limit depends on the length of the tube. Quarter wavelength of the lower frequency should be smaller than the length of the tube. The measurement setup of two-microphone method is shown in Figure 2.11.

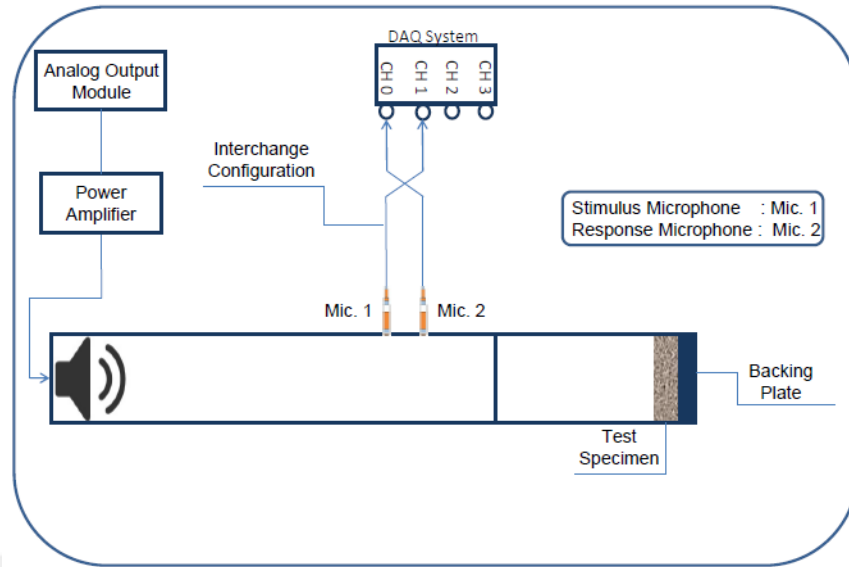


Figure 2.11 Measurement setup of two-microphone method

Microphone diameter should be smaller than 20% of highest frequency wavelength. The distance between nearest microphone and specimen should be three times greater than the diameter of the tube. The distance between microphones ( $s$ ) should satisfy the following equality;

$$s \ll \frac{c}{2f_u} \quad . \quad (2.32)$$

Reflection coefficient can be calculated as

$$R = |R|e^{j\phi R} = R_r + jR_i = \frac{H - e^{-jks}}{e^{jks} - H} e^{j2k(l+s)} \quad . \quad (2.33)$$

Here,  $l$  is the distance between test specimen and the response microphone (Mic. 2).  $H$  is a complex frequency response and it is given as,

$$H = \frac{P_2}{P_1} \quad . \quad (2.34)$$

e wavenumber  $k$  is calculated by,

$$k = k' + jk'' , \quad (2.35)$$

where  $k'$  is the complex wave number,  $k''$  is the tube attenuation and it can be calculated empirically. Attenuation of the impedance tube will be calculated in next chapters. Using reflection coefficient information, normal specific acoustical impedance ratio, normal specific acoustical resistance ratio, normal specific acoustical reactance ratio, normal specific acoustical admittance ratio, normal acoustical conductance ratio and normal specific susceptance ratio can be calculated respectively (ASTM E-1050, 1998);

$$\alpha = 1 - |R|^2 , \quad (2.36)$$

$$\frac{z}{\rho c} = \frac{1+R}{1-R} , \quad (2.37)$$

$$\frac{r}{\rho c} = \frac{\alpha}{2(1-R_r) - \alpha} , \quad (2.38)$$

$$\frac{x}{\rho c} = \frac{2R_i}{2(1-R_r) - \alpha} , \quad (2.39)$$

$$y\rho c = \frac{\rho c}{z} , \quad (2.40)$$

$$g\rho c = \frac{r/\rho c}{(r/\rho c)^2 + (x/\rho c)^2} , \quad (2.41)$$

$$b\rho c = \frac{x/\rho c}{(r/\rho c)^2 + (x/\rho c)^2} . \quad (2.42)$$

All variables are defined in Symbols section in the beginning of the Thesis.

### ***2.4.2 ASTM E 2611-09 - Standard Test Method for Measurement of Normal Incidence Sound Transmission of Acoustical Materials Based on Transfer Matrix Method***

Analytical determination of transfer matrix elements of complex systems is very difficult. Therefore, experimental transfer matrix method is the best way for this purpose. ASTM E 2611-09 is a standard that is a guide for experimental transfer matrix method. In this method, four pole parameters of a material or a silencer are determined with four microphones. Two of them are positioned in front of the material and the other two are positioned behind of the material. Distance between microphones 1-2 and 3-4 should be less than half of the minimum wavelength for no flow (ASTM E2611, 2009). Distance can be calculated using Equation 2.32.

There are three different experimental methods for the determination of transmission loss coefficients; decomposition, two-load and two-source methods. In this thesis, only two-load method is briefly explained and used in experiments.

#### ***2.4.2.1 Two Load Method***

The measurement setup of two-load method is shown in Figure 2.12. Two different end conditions are provided in the measurement. Using the transfer matrix method, four pole equations for the straight tube elements between microphone 1-2 and 3-4 are calculated. Then four pole elements of muffler or material between microphones 2-3 are determined via 1) Four pole parameters signal processing or 2) Wave decomposition signal processing.

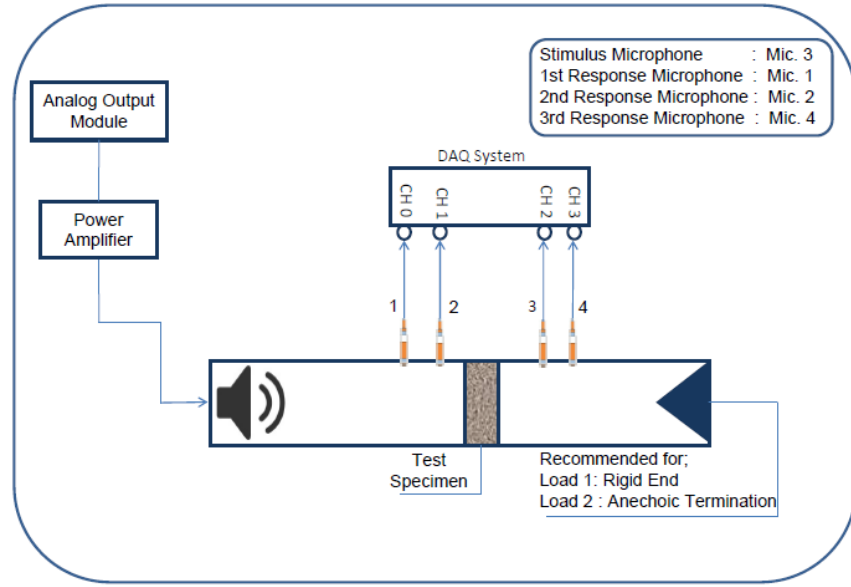


Figure 2.12 Measurement setup of two-load method

2.4.2.1.1 *Four Pole Parameters Signal Processing Method.* The transfer matrix elements of muffler or material between 2-3 microphones can be determined with the following equations:

$$T_{11}^{(23)} = \frac{(H_{32a}H_{34a} - H_{32b}H_{34a})}{(H_{34b} - H_{34a})} + \frac{T_{22}^{(34)}(H_{32b} - H_{32a})}{\Delta_{34}(H_{34b} - H_{34a})}, \quad (2.43)$$

$$T_{12}^{(23)} = \frac{T_{12}^{(34)}(H_{32a} - H_{32b})}{\Delta_{34}(H_{34b} - H_{34a})}, \quad (2.44)$$

$$T_{21}^{(23)} = \frac{(H_{31a} - T_{11}^{(12)}H_{32a})(\Delta_{34}H_{34b} - T_{22}^{(34)}D_{34})}{T_{12}^{(12)}\Delta_{34}(H_{34b} - H_{34a})} - \frac{(H_{31b} - T_{11}^{(12)}H_{32b})(\Delta_{34}H_{34a} - T_{22}^{(34)})}{T_{12}^{(12)}B_{12}\Delta_{34}(H_{34b} - H_{34a})}, \quad (2.45)$$

$$T_{22}^{(23)} = T_{12}^{(34)} \left( \frac{H_{31a} - H_{31b}}{T_{12}^{(12)}\Delta_{34}(H_{34b} - H_{34a})} + \frac{T_{11}^{(12)}(H_{32b} - H_{32a})}{T_{12}^{(12)}\Delta_{34}(H_{34b} - H_{34a})} \right). \quad (2.46)$$

Here,  $T_{11}^{(ij)}$ ,  $T_{12}^{(ij)}$ ,  $T_{21}^{(ij)}$  and  $T_{22}^{(ij)}$  are transfer matrix elements.  $\Delta_{ij}$  is the determinant of the transfer matrix between  $i$  and  $j$  microphones. Subscript  $a$  represents the first load and subscript  $b$  denotes second load configuration. In addition,  $H_{ij}$  is a transfer function, and it can be calculated as

$$H_{ij} = \frac{P_j}{P_i} . \quad (2.47)$$

2.4.2.1.2 *Wave Decomposition Signal Processing Method.* The transfer matrix elements of muffler or material between 2-3 microphones can also be determined via wave decomposition method with the following equations.

$$A = j \frac{H_{13}e^{-jkl_1} - H_{23}e^{-jk(l_1+s_1)}}{2 \sin(ks_1)} , \quad (2.48)$$

$$B = j \frac{H_{23}e^{jk(l_1+s_1)} - H_{13}e^{jkl_1}}{2 \sin(ks_1)} , \quad (2.49)$$

$$C = j \frac{H_{33}e^{jk(l_2+s_2)} - H_{43}e^{jkl_2}}{2 \sin(ks_2)} , \quad (2.50)$$

$$D = j \frac{H_{43}e^{-jkl_2} - H_{33}e^{-jk(l_2+s_2)}}{2 \sin(ks_2)} , \quad (2.51)$$

$$p_0 = A + B , \quad (2.52)$$

$$p_d = Ce^{-jkd} + De^{jkd} , \quad (2.53)$$

$$u_0 = (A - B) / \rho c , \quad (2.54)$$

$$u_d = (Ce^{-jkd} - De^{jkd}) / \rho c , \quad (2.55)$$

$$T_{11}^{(23)} = \frac{P_{0a}u_{db} - P_{0b}u_{da}}{P_{da}u_{db} - P_{db}u_{da}} , \quad (2.56)$$

$$T_{12}^{(23)} = \frac{P_{0b}P_{da} - P_{0a}P_{db}}{P_{da}u_{db} - P_{db}u_{da}} , \quad (2.57)$$

$$T_{21}^{(23)} = \frac{u_{0a}u_{db} - u_{0b}u_{da}}{P_{da}u_{db} - P_{db}u_{da}} , \quad (2.58)$$

$$T_{22}^{(23)} = \frac{P_{da}U_{0b} - P_{db}U_{0a}}{P_{da}U_{db} - P_{db}U_{da}} . \quad (2.59)$$

Here,  $l_1$  and  $l_2$  represent the distances between the surface of the test material and microphones 2 and 3, respectively.  $s_1$  and  $s_2$  indicate the distances between microphones 1-2 and 3-4.  $d$  is the thickness of the test material.

Using transfer matrix elements, the transmission loss, insertion loss and noise reduction can be calculated from Equations 2.26, 2.27 and 2.31. In addition, transmission coefficient ( $t$ ), propagation wave number in material ( $k_m$ ) and characteristic impedance in material ( $Z_m$ ) can be calculated via following equations:

$$t = \frac{2e^{jkd}}{T_{11}^{(23)} + \frac{T_{12}^{(23)}}{\rho c} + \rho c T_{21}^{(23)} + T_{22}^{(23)}} , \quad (2.60)$$

$$TL = 20 \log_{10} \left| \frac{1}{t} \right| , \quad (2.61)$$

$$k_m = \frac{1}{d} \cos^{-1} (T_{11}^{(23)}) , \quad (2.62)$$

$$z = \sqrt{T_{12}^{(23)} / T_{21}^{(23)}} . \quad (2.63)$$

## 2.5 Determination of Surface Impedances of Tubes

The mode shapes of acoustic cavities are very similar to standing wave of plane waves. So surface impedance of tube walls can be computed via phase shift from experimental results and analytical value that is based on the standing wave theory. Sound pressure of a propagated sound wave can be written;

$$p(x, t) = Ae^{i(\omega t - kx)} + Be^{i(\omega t + kx)} , \quad (2.64)$$

and using Euler equation and Equation 2.64, particle velocity can be computed as;



$$u(x,t) = \frac{1}{\rho c} \left( A e^{i(\omega t - kx)} + B e^{i(\omega t + kx)} \right) . \quad (2.65)$$

Assuming that the surface velocity is equal to the particle velocity at the boundary, the mechanical impedance of the plane wave can be written as;

$$Z = \frac{pS}{u_n} = \rho c S \left[ \frac{1 + \frac{B}{A} e^{i\theta}}{1 - \frac{B}{A} e^{i\theta}} \right] , \quad (2.66)$$

where  $\theta$  is phase shift and it can be computed as;

$$\theta_n = 2k\delta_n + \pi(k-1) . \quad (2.67)$$

Here  $n$  is the minimum peak number,  $\delta_n$  is the shift of the  $n$ th peak and  $k$  is the wave number. Wave number is defined as;

$$k = \frac{2\pi f}{c} . \quad (2.68)$$

## 2.6 Tube Attenuation

The incident and reflected sound waves that propagate within the tube subject to attenuation due to viscous and thermal losses (ASTM E1050, 1998). If the microphone positions are placed closed to the surface of the specimen, the tube attenuation will not affect the test results. However, ASTM E1050 says that, if the distance from the nearest microphone to the surface is three times larger than the tube diameters, the tube attenuation could not be ignored.

Normally,  $k$  is a real variable and it can be computed with Equation 2.68. To eliminate the tube attenuation effect, the wave number should be modified by

replacing the real variable  $k$  by the complex wave number  $k'$  and it can be computed as Equation 2.35.

Here;  $k$  is the normal wave number, and it can be computed with Equation 2.68.  $k''$  is the attenuation constant, and it can be determined empirically as;

$$k'' = A \frac{\sqrt{f}}{cd} \quad . \quad (2.69)$$

Here  $d$  is the diameter of the tube and  $A$  is a constant and generally it is taken 0,02203. On the other hand, there is an experimental method to determination of attenuation constant. Reflection coefficient  $r$  equals to 1 for rigid end termination. Therefore  $k''$  can be determined with measuring of transfer function and using Newton Raphson method;

$$r = \frac{H - e^{-jks}}{e^{jks} - H} e^{j2k(l+s)} = 1 \quad . \quad (2.70)$$

Equation 2.70 leads to

$$e^{jks} + e^{jk(2l+s)} = H(1 + e^{j2k(l+s)}) \quad . \quad (2.71)$$

Using Newton Raphson Method given by following equations, one can end up with the attenuation constant:

$$\frac{\partial f_1}{\partial k''} \varepsilon_{k''} = f_1 \quad , \quad (2.72)$$

$$f_1 = H(1 + e^{j2k'(l+s) + 2k''(l+s)}) - e^{jk's + k''s} - e^{jk'(2l+s) + k''(2l+s)} = 0 \quad , \quad (2.73)$$

$$\frac{\partial f_1}{\partial k''} = H2(l+s)e^{j2k'(l+s)+2k''(l+s)} - se^{jk's+k''s} - (2l+s)e^{jk'(2l+s)+k''(2l+s)} . \quad (2.74)$$

The experimental method for the determination of attenuation constant is more accurate than empirical one (Han, Herrin & Seybert, 2007). So in this thesis the experimental method is used because of accuracy.

## 2.7 Sound Absorption Coefficient as a Function of Angle of Incidence

Sound absorption coefficient of materials for normal incidence waves is described in Chapter 2.2.1. Also sound absorption coefficient could be calculated empirically as a function of angle of incidence wave (Figure 2.13) (Fahy, 2000):

$$\alpha(\phi) = \frac{4r' \cos(\phi)}{(1 + r' \cos(\phi))^2 + (x' \cos(\phi))^2} . \quad (2.75)$$

where;  $r'$  and  $x'$  are real and imaginary parts of measured normal specific acoustical impedance ratios respectively, and they can be computed via Equations 2.38 and 2.39.

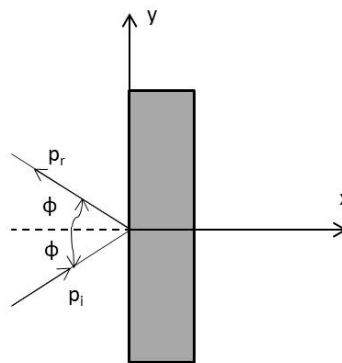


Figure 2.13 Random incidences and reflected a sound wave

## **CHAPTER THREE**

### **DEVELOPMENT OF THE IMPEDANCE TUBE APPARATUS AND SOFTWARE**

This section presents development of a new impedance tube apparatus and determines acoustic performance parameters of materials via this apparatus. Conventional impedance tubes are generally made of brass or other heavy materials to provide rigid guide for better standing wave performance. However, the impedance tube that is made of composites could be a good alternative since brass tubes are heavy and expensive to manufacture. Composite materials are preferred in aerospace and automotive industries because of high strength-weight ratio of them. The tube designed in this study also has an air-conditioning system and rotation apparatus which makes itself unique among the available impedance tubes.

Impedance tubes should be smooth, have constant cross section and their walls must be non-porous, durable and rigid since they should have low vibration amplitudes at walls and low leak in terms of acoustics. Therefore, determination of vibro-acoustic performances of composite tubes is significant. For this purpose a composite hollow tube is designed and manufactured in this study. Then, the tubes developed step by step according to obtained results.

A list of performed studies will be helpful for this section:

1. An insulated cabin is constructed for the outer surface sound pressure measurements.
2. A composite tube that is labeled as “first prototype tube”, is manufactured and its vibro-acoustic performance is measured with several tests.
3. “Second prototype tube” is manufactured and the same vibro-acoustic performance parameters are measured again.
4. Then attenuation for tube is measured and is seen that the second prototype tube has larger tube attenuation even though it has better vibro-acoustic performance.

5. Therefore, a new impedance tube is constructed and its tube attenuation is measured.
6. After that, the software is developed for the measurement and the calculation of acoustic performance parameter.
7. The air conditioning system is designed.
8. Finally, a rotation apparatus for measuring angle incidence sound absorption coefficient is designed.

These studies and three different impedance tube set are presented in next sections.

### **3.1 Designing and Manufacturing of an Insulated Cabin**

Accurate acoustical tests should be performed in an insulated cabin. Therefore a low-cost insulated cabin is designed and manufactured. Oriented Strand Board (OSB) plates for cabin walls and fiberglass are used for insulation. The insulated cabin is manufactured as shown in Figure 3.1 and it is ready for the acoustic tests of the tubes.



Figure 3.1 Insulated acoustic cabin (Personal archive, 2015)

### 3.2 Designing, Manufacturing and Analyzing of the “First Prototype Tube Kit”

The “First prototype tube” is designed and manufactured for low frequency range measurements (63 - 1000 Hz). Figure 3.2 and Figure 3.3 show the designed tube and manufactured tube, respectively.

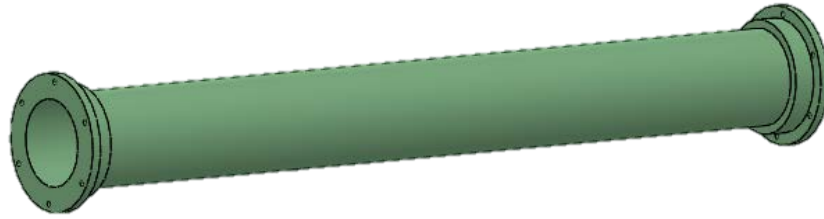


Figure 3.2 3-D design of the “first prototype tube”



Figure 3.3 The “first prototype tube” (Personal archive, 2015)

The vibro-acoustic tests of the tube are performed to investigate whether the composite tubes can be used as an impedance tube kit or not.

#### 3.2.1 *Vibro-Acoustic Properties of the “First Prototype Tube”*

Rigidity of tube walls may be showed via surface impedance measurements. Structural and acoustical modal analysis tests have been performed for determination of surface impedance. Before starting determination of surface impedances, structural and acoustic modal analysis tests are also performed to determine critical frequencies of structures. Then surface vibrations and sound transmission of a composite tube are measured under acoustical excitation at resonance frequencies in insulated cabin. Note that all tests are also performed for brass tube in order to compare the results.

### 3.2.1.1 Cavity Frequencies of the “First Prototype Tube”

Acoustic modal analysis is performed with the procedure given in Section 2.1.2 for the composite and brass tubes and natural frequencies of duct are called as “cavity frequencies”. Experimental setup is shown in Figure 3.4. Boundary conditions are applied to be as closed-closed ends and closed-open ends. Experimental natural frequencies are also compared with analytical natural frequencies that are expressed in Table 2.1. The results are tabulated in Table 3.1 - 3.4. Note that, each experiment is repeated three times for repeatability.



Figure 3.4 Experimental setup of acoustical modal analysis (Personal archive, 2015)

Table 3.1 Cavity frequencies of the “first prototype tube” set for closed-closed boundary condition

Order	Experiment 1	Experiment 2	Experiment 3	Average	Analytical
1	148	148	150	148.6	153.3
2	336	334	335	335	306.7
3	476	475	474	475	460
4	621	620	620	620.3	613.4
5	767	766	767	766.7	766.7
6	913	913	912	912.6	920
7	1058	1059	1060	1059	1073

Table 3.2 Cavity frequencies of the “first prototype tube” set for closed-open boundary condition

Order	Experiment 1	Experiment 2	Experiment 3	Average	Analytical
1	86	86	86	86	85.92
2	269	268	267	269	257.76
3	419	415	415	419	429.6
4	574	570	569	574	601.44
5	780	782	784	780	773.28
6	920	921	920	920,3	945.12
7	1032	1032	1032	1032	1117

Table 3.3 Cavity frequencies of the brass tube set for closed-closed boundary condition

Order	Experiment 1	Experiment 2	Experiment 3	Average	Analytical
1	169	171	170	170.5	171.8
2	350	348	349	349	343.5
3	505	508	507	506.7	515.3
4	661	662	662	661.7	687
5	817	820	819	818.7	858.8
6	978	980	979	979	1030.5
7	1136	1140	1141	1139	1202.3

Table 3.4 Cavity frequencies of the brass tube set for closed-open boundary condition

Order	Experiment 1	Experiment 2	Experiment 3	Average	Analytical
1	86	87	85	86	85.92
2	268	266	265	266.3	257.76
3	418	417	415	416.6	429.6
4	576	577	576	576.3	601.44
5	730	731	730	730	773.28
6	912	910	911	911	945.12
7	1043	1048	1050	1047	1117

As shown in Tables 3.1-3.4, there are little discrepancies between analytical and experimental results. There should be two reasons for this condition.



- 1) Analytical formulas have been derived from assumption that the tube walls are rigid. However, it could not be completely rigid in practice.
- 2) One side of the tube is connected loudspeaker for closed-closed and closed-open conditions and the loudspeaker could not provide close end condition.

Acoustical mode shapes have been determined to execute the reasons of discrepancies and determine the standing wave distributions of tubes under critical frequencies via experimental method and analytical calculations.

### 3.2.1.2 Acoustical Mode Shapes of the “First Prototype Tube”

Mode shapes of composite and brass tubes under their cavity frequencies are obtained for closed-closed condition.

The results are showed in Figures 3.5 – 3.6. There are different shifting values from analytical and experimental results giving information about rigidity of tube walls. The shifts show the attenuation of the tubes and source impedances which are not wanted indeed.

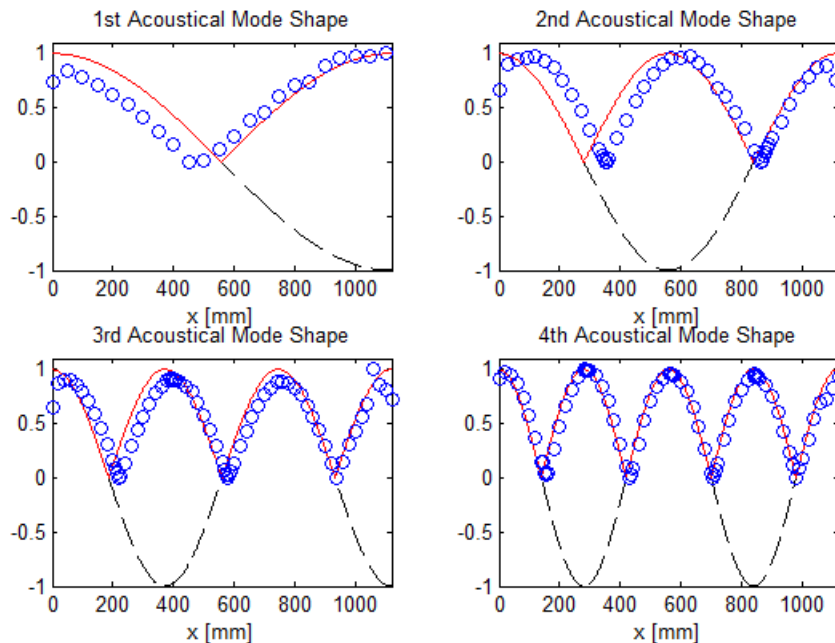


Figure 3.5 Acoustical mode shapes of the “first prototype tube” set for closed-closed condition (‘—’: absolute of analytical results, ‘--’: analytical result, ‘o’: experimental results)

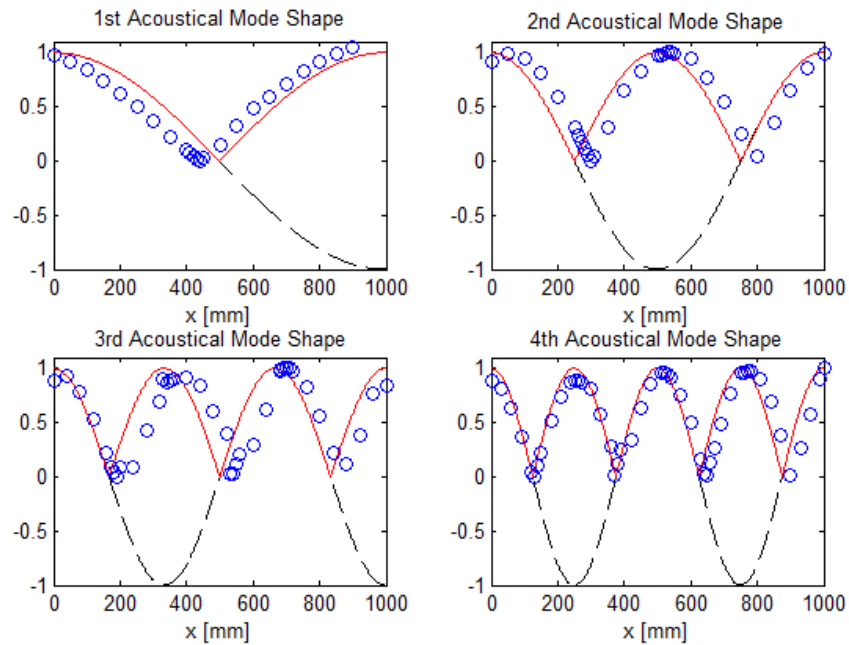


Figure 3.6 Acoustical mode shapes of the brass tube set for closed-closed condition (‘—’: absolute of analytical results, ‘--’: analytical result, ‘o’: experimental results)

### 3.2.1.3 Inner Surface Impedances of the “First Prototype Tube Set”

Theoretically, surface impedance of a rigid tube should be infinite, since surface velocity is zero. Therefore, surface impedance of an impedance tube should be as large as possible in practice. Surface impedances and phase shifting of composite and brass tubes are computed at their cavity frequencies for closed-closed end condition with the procedure given in Section 2.5.

The calculated results are presented in Table 3.5. It is seen from the table that, surface impedances of tubes are close to each other apart from second cavity frequency. According the results, surface impedances of composite tube are in same order with brass ones. Therefore composite structures have good results for surface impedance.

Table 3.5 Measured phase shifts and computed surface impedances of the “first prototype and brass tubes”

“First Prototype Tube”				Brass Tube Set			
Frequency [Hz]	Shift ( $\delta n$ )	Phase Shift [Radians]	Surface Impedance [N.s/m]	Frequency [Hz]	Shift ( $\delta n$ )	Phase Shift [Radians]	Surface Impedance [N.s/m]
148	$\delta 1$	5.98	2.31E+03	170	$\delta 1$	0.546	1.46E+03
335	$\delta 1$	3.26	6.23E+01	350	$\delta 1$	5.357	8.25E+02
	$\delta 2$	2.727		$\delta 2$	5.357		
476	$\delta 1$	5.946	1.60E+03	505	$\delta 1$	1.818	2.49E+02
	$\delta 2$	6.259		$\delta 2$	2.130		
	$\delta 3$	5.493		$\delta 3$	2.245		
621	$\delta 1$	1.480	5.32E+02	661	$\delta 1$	4.358	3.52E+02
	$\delta 2$	1.389		$\delta 2$	4.685		
	$\delta 3$	1.275		$\delta 3$	4.812		
	$\delta 4$	1.161		$\delta 4$	4.812		

### 3.2.2 Vibro-Acoustic Performance of the “First Prototype Tube”

Vibro-acoustic properties and inner surface impedances of tubes are determined in Chapter 3.2.1. Outer surface impedance of tubes is another important parameter for their vibro-acoustic characteristic.

Under acoustic excitation, surface vibration velocity and surface sound pressure level of an impedance tube should be low for better performance. In this chapter of the thesis, surface vibration velocities and sound pressures of the “first prototype tube” and brass tube are measured under acoustic excitation whose frequencies are selected from cavity and structural resonance frequencies. Outer surface impedances are then obtained by dividing sound pressures by surface vibration velocities. This is called as “specific acoustic impedance”. Larger specific acoustic impedance with smaller surface sound pressure is selected as objective function in this study.

Before measuring the impedances, in-situ structural modal analysis are performed to determine structural natural frequencies. After that, the specific acoustic impedance is measured for specified cavity and in-situ structural natural frequencies. Note that, specific acoustic impedance measurement points at cavity frequencies are selected as maximum pressure amplitude points corresponding to the each cavity mode whereas tubes are scanned by 50 mm intervals for the impedance measurement at structural resonance frequencies.

### *3.2.2.1 In Situ Structural Modal Analysis of the “First Prototype Tube”*

In this chapter, in-situ structural modes of the “first prototype tube” and brass tube are determined via in situ experimental modal analysis. Experimental setups are shown in Figure 3.7 and 3.8. Three points have been selected randomly for excitation and measurements. On the other hand, the symmetry test has been provided to verify the results.

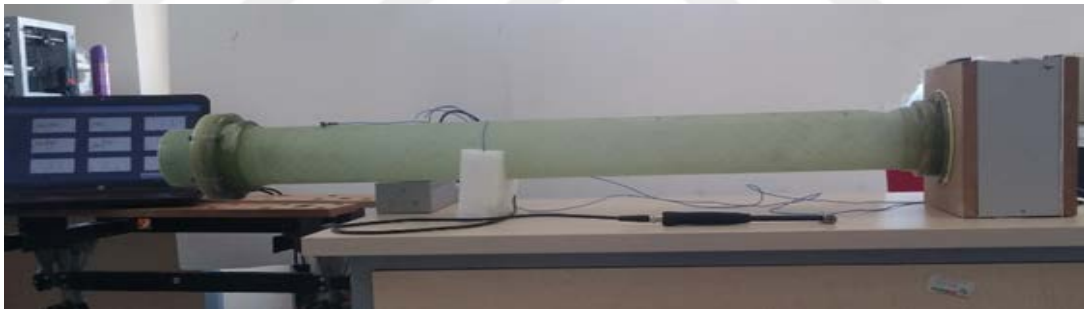


Figure 3.7 Experimental setup of in-situ structural modal analysis of the “first prototype tube” (Personal archive, 2015)



Figure 3.8 Experimental setup of in-situ structural modal analysis of brass tube (Personal archive, 2015)

The results are shown in Figure 3.9 and 3.10.

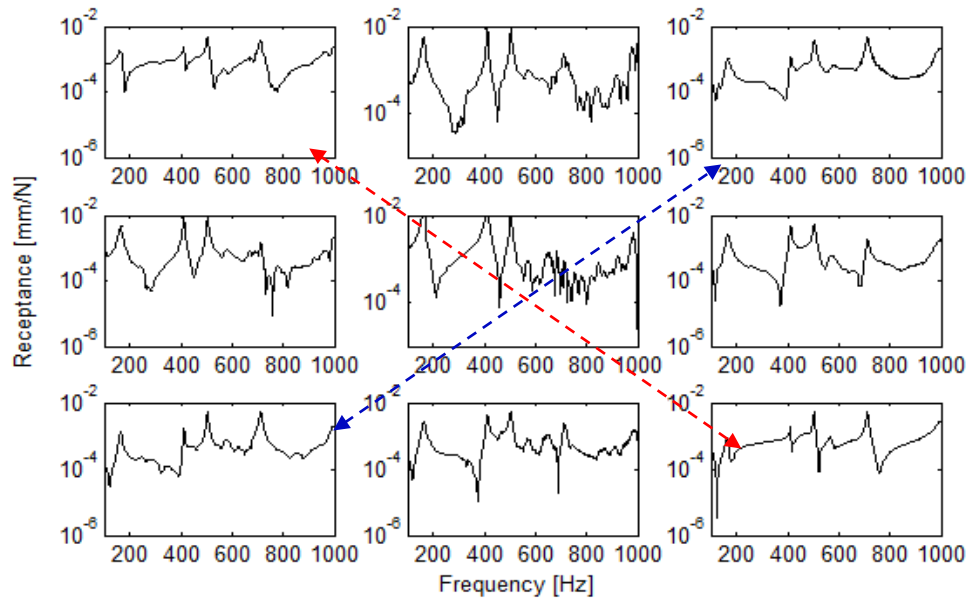


Figure 3.9 Frequency response matrix of the “first prototype tube” for in-situ condition

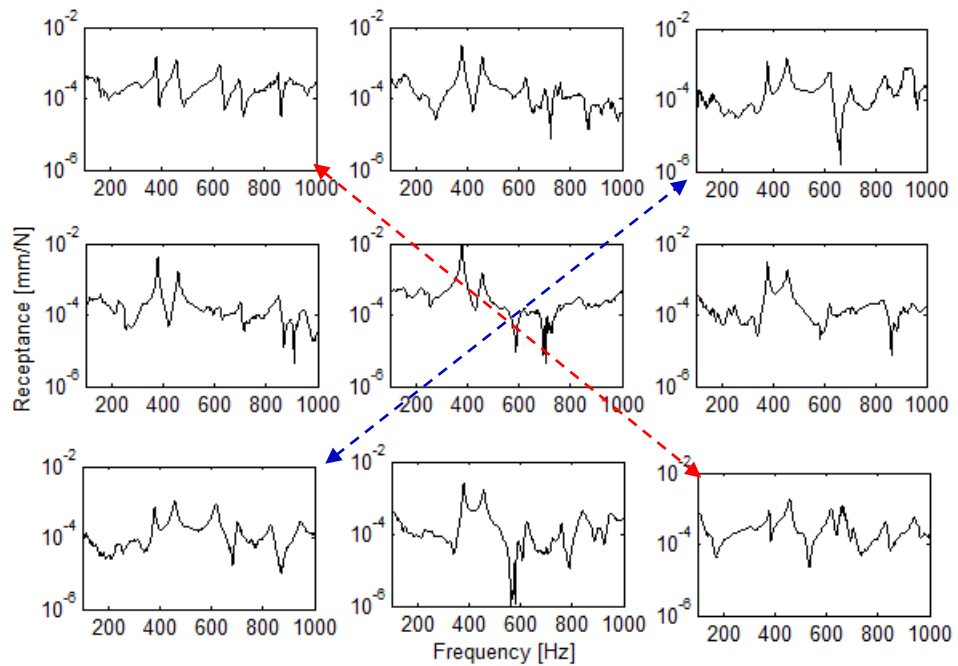


Figure 3.10 Frequency response matrix of brass tube for in-situ condition

Natural frequencies are determined via peak selection method and first two natural frequencies are tabulated in Table 3.6.

Table 3.6 Natural frequencies tubes for in-situ condition

Order	“First Prototype Tube” [Hz]	Brass Tube [Hz]
1	164	380
2	413	458

### 3.2.2.2 Outer Surface Impedances of the “First Prototype Tube”

Here in this section, surface vibration velocities and surface sound pressures of tubes are measured for the cavity frequencies and in-situ natural frequencies. Note that, excitation of the tubes is supplied from loudspeaker. Measurements are repeated three times for repeatability. From the measurements, outer surface specific acoustic impedances of tube are computed via dividing sound pressures by vibration velocities. Surface velocities have been measured with vibrometer and the surface sound pressures have been measured with surface microphone. Devices are shown in Figure 3.11.



Figure 3.11 Laser vibrometer and surface microphone (Personal archive, 2015)

Experiments have been provided in insulated chamber. Experimental setups are shown in Figure 3.12.



Figure 3.12 Experimental setup of outer surface impedance measurements (Personal archive, 2015)

Figures 3.13 - 3.15 show surface velocities, sound pressures and corresponding specific acoustic impedances of tubes subjected to acoustic excitation with first two structural resonance frequencies. Structural natural frequencies have been tabulated in Table 3.6 before.

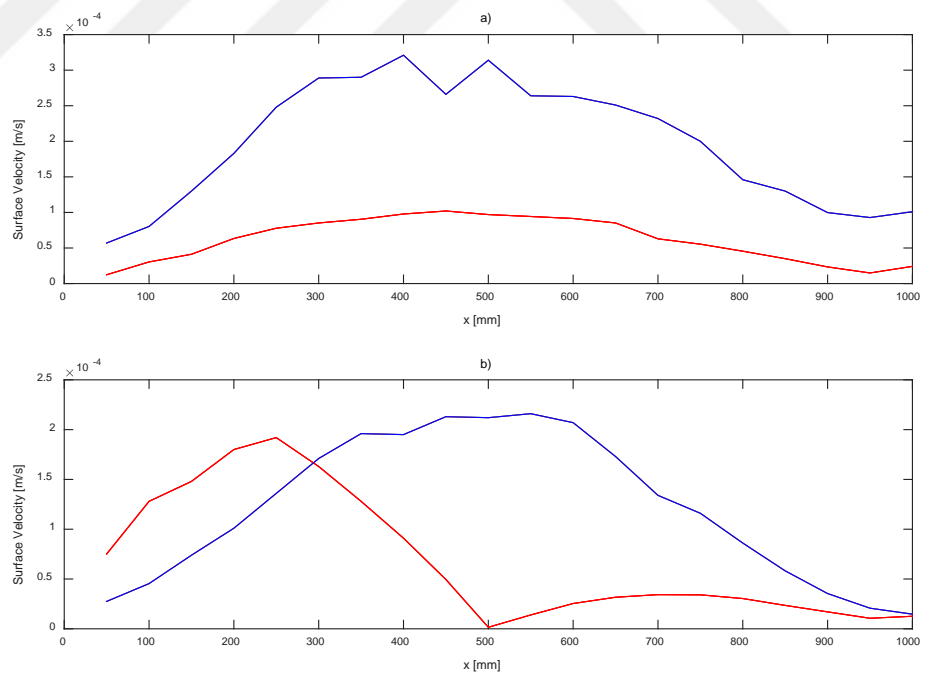


Figure 3.13 Surface vibration velocities of the “first prototype” and brass tubes (red line: brass tube, blue line: “first prototype tube”; a) under first structural natural frequencies b) under second structural natural frequencies)

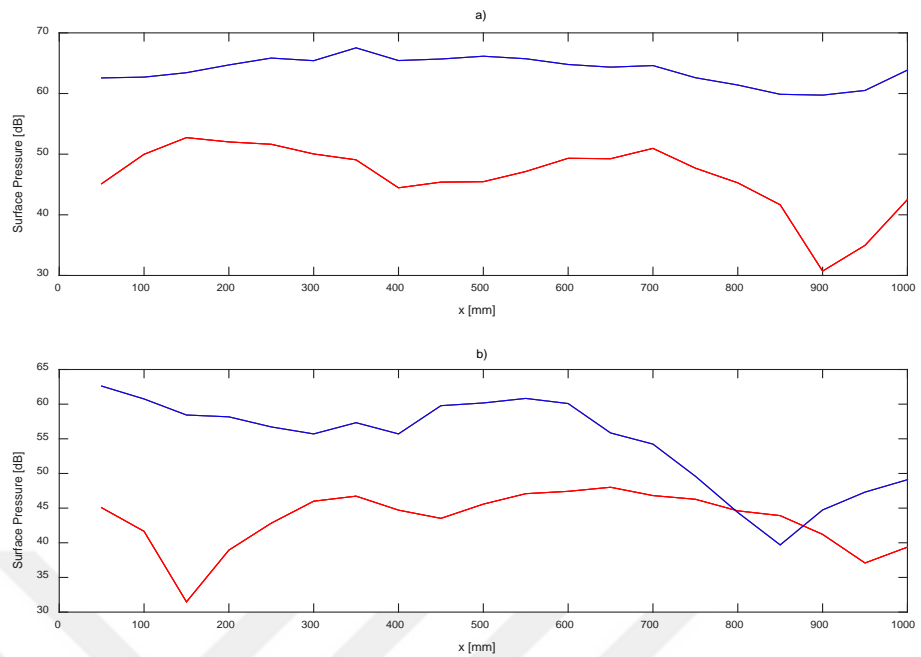


Figure 3.14 Surface sound pressures of the “first prototype” and brass tubes (red line: brass tube, blue line: the “first prototype tube”; a) under first structural natural frequencies b) under second structural natural frequencies)

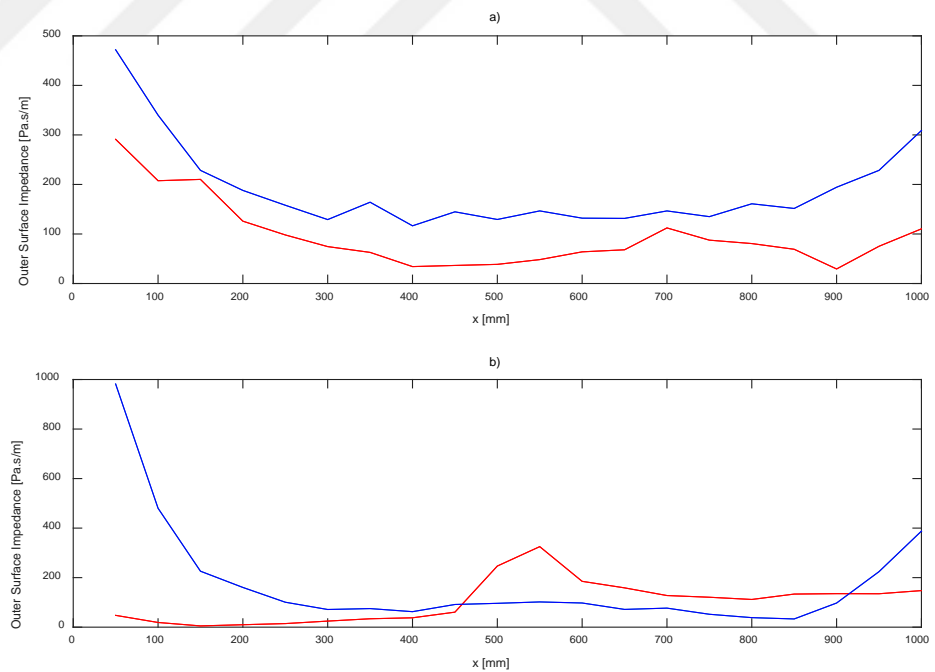


Figure 3.15 Outer surface acoustic impedances of the “first prototype” and brass tubes (red line: brass tube, blue line: the “first prototype tube”; a) under first structural natural frequencies b) under second structural natural frequencies)



It is seen from the figures that vibration levels are very small for both tubes. However, surface sound pressures of the composite tube are much higher than those of the brass tube. This indicates higher sound transmission that is not desired for a tube of impedance measurement apparatus.

Surface velocities, pressures and specific acoustic impedances are measured again at cavity frequencies of tubes and presented in Figures 3.16 – 3.18. Cavity frequencies are tabulated before Table 3.1 and Table 3.3.

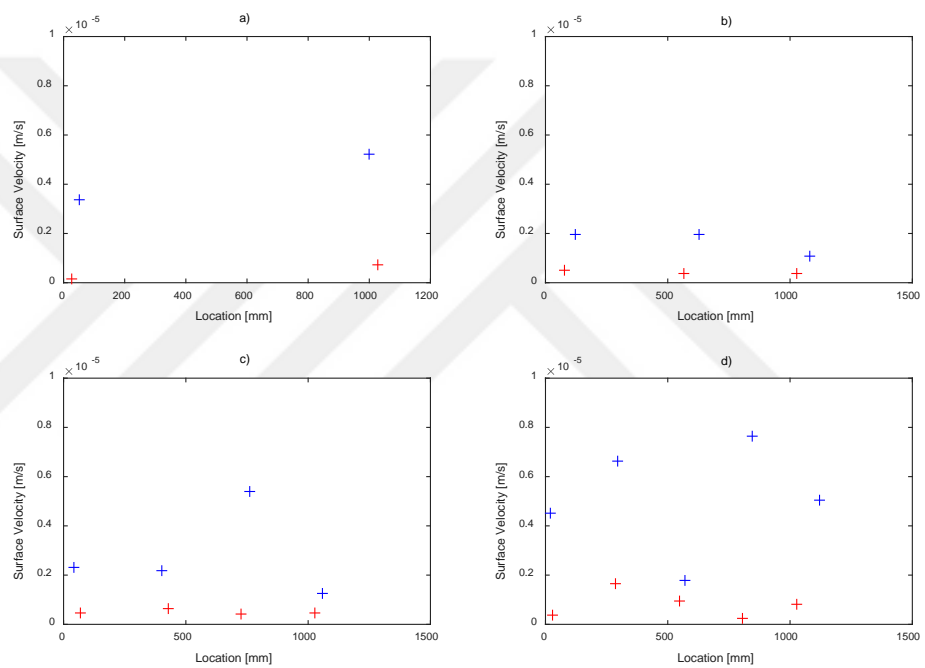


Figure 3.16 Surface vibration velocities of the “first prototype” and brass tubes (red plusses: brass tube, blue plusses: the “first prototype tube”; a) under first cavity frequencies, b) under second cavity frequencies, c) under third cavity frequencies, d) under fourth cavity frequencies)

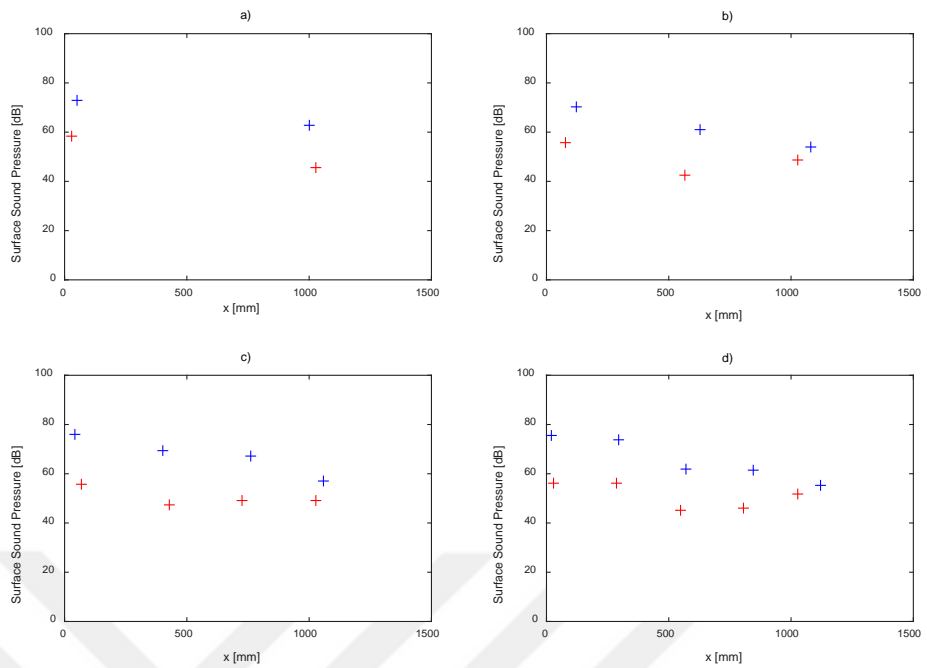


Figure 3.17 Surface sound pressure levels of the “first prototype” and brass tubes (red pluses: brass tube, blue pluses: the “first prototype tube”; a) under first cavity frequencies, b) under second cavity frequencies, c) under third cavity frequencies, d) under fourth cavity frequencies)

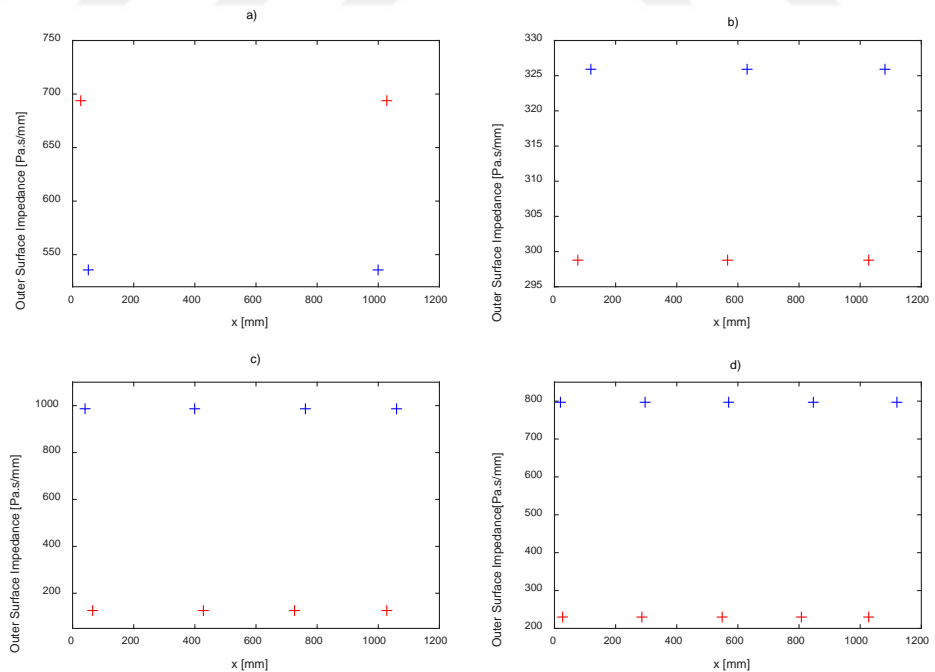


Figure 3.18 Outer surface impedances of the “first prototype” and brass tubes (red pluses: brass tube, blue pluses: the “first prototype tube”; a) under first cavity frequencies, b) under second cavity frequencies, c) under third cavity frequencies, d) under fourth cavity frequencies)

Vibro-acoustic performances of the “first prototype tube” and the brass tube subjected to acoustic excitations have been compared regarding on outer surface impedance and surface sound pressures. Excitation frequencies are selected for structural and acoustic resonance frequencies since they exhibit much larger response amplitudes. It is found that 15 - 20 dB difference on surface pressure levels of the “first prototype tube” compared by the brass tube. This is undesirable situation and it should be eliminated before it is used as professional measurement equipment. However, since it exhibits larger impedance values it promises to be a good alternative to the brass tube after improving its sound insulation property.

### **3.3 Designing, Manufacturing and Analyzing of the “Second Prototype Tube Kit”**

The results of vibro-acoustic tests show that, inner surface impedance values of composite tube are suitable for impedance tube kits. However, outer surface sound pressure levels of composite one is higher than brass one. Therefore, the composite tube should be insulated for comfortable measurements with no sound leakages. In this stage of study, a sandwich composite tube set is designed and manufactured for this aim.

In design of the “second prototype tube kit”, styrofoam peanut have been filled up between nested composite tubes. In addition, the “second prototype tube” is designed and manufactured in accordance with standards. Designed impedance tube kit is a modular system. It can be used for two different types of measurement i.e, four-pole method for transmission loss and noise reduction measurements of materials and two-microphone method for sound absorption coefficient and surface impedance measurements. Besides that, two types of tube diameter for each measurement technique are valid. For low frequency measurements (100 Hz - 1000 Hz) larger diameter duct (100 mm) should be used and for high frequency measurements (1000 Hz – 5000 Hz) smallest diameter duct (29 mm) should be used.

Distances between microphones are computed via Equation 2.32. In this equation  $f_u$  represents upper frequency limit also it is called as cut off frequency. For the diameter of 100 mm, cut off frequency is computed as 1000 Hz whereas it is 5000 Hz for the diameter of 29 mm. Therefore, distance between microphones is computed 75 mm for low frequency measurements and 20 mm for high frequency measurements.

The designed tubes are manufactured and they are shown in Figures 3.19 and Figure 3.20.



Figure 3.19 Low frequency sound absorption coefficient measurement tube kit of the “second prototype tube” (Personal archive, 2016)



Figure 3.20 All parts of the “second prototype tube” (Personal archive, 2016)

In next sections, modal analyses of tubes, inner and outer surface impedance measurements are performed for the “second prototype tube” sets.

### ***3.3.1 Vibro-Acoustic Properties of the “Second Prototype Tube Kit”***

In this section of the thesis, vibro-acoustic performances of manufactured the “second prototype tube” are performed in terms of natural frequencies, inner surface

impedance and outer surface impedance as done for the “first prototype tube”. Calculated results are compared with the brass and the “first prototype tube”. First of all, acoustical modes are determined experimentally and then inner surface impedance values are computed. Moreover, in-situ structural modal analysis has been performed and outer surface impedance values are calculated under acoustical excitations at cavity and structural natural frequencies.

### 3.3.1.1 Cavity Frequencies of the “Second Prototype Tube”

Acoustical modal analysis of the “second prototype tube” is performed via experimental method which is explained in Chapter 2.1.2. Tests are only performed for closed-closed boundary condition. Cavity frequencies of tube are tabulated in Table 3.7 and also acoustical mode shapes are shown in Figure 3.21. Note that the results are compared with the analytical ones.

Table 3.7 Cavity frequencies of the “second prototype tube” for closed-closed boundary condition

Order	Experiment 1	Experiment 2	Experiment 3	Average	Analytical
1	155	154	155	154.6	172
2	298	297	297	297.3	345
3	548	547	547	547.3	517
4	710	707	708	708.3	690

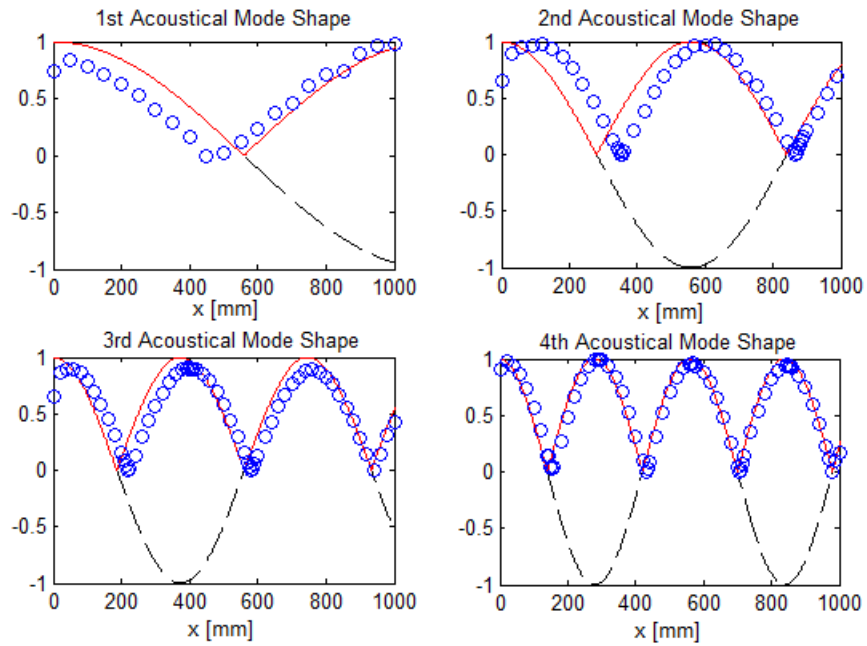


Figure 3.21 Acoustical mode shapes of the “second prototype tube” set for closed-closed condition (‘—’: absolute of analytical results, ‘--’: analytical result, ‘o’: experimental results)

It is seen from the results that, there are some deviations in measured natural frequencies but mode shapes are more closer to analytical ones.

### 3.3.1.2 Inner Surface Impedances of the “Second Prototype Tube”

Inner surface impedance of the “second prototype tube” is determined as described in Chapter 2.5 by using experimental cavity frequencies and mode shapes.

The calculated inner surface impedances are presented in Table 3.8. It is seen from the Table that, the results are generally in same order with the “first prototype tube” and brass tube.

Table 3.8 Measured phase shifts and computed surface impedances of the “second prototype tube”

Frequency [Hz]	Shifting [m]	Phase Shifting ( $\Theta$ ) [rad]	Acoustical Impedance (ZL) [N.s/m]	Average (ZL) [N.s/m]	
155	$\delta_1$	0.113	-5.13	198.709 + 591.580i	624.06
298	$\delta_1$	0.12	-12.644	5226.01 - 4618.167i	4021.26
	$\delta_2$	0.06	-13.297	140.354 - 1059.113i	
547	$\delta_1$	0.043	-27.475	25.728 - 173,084i	116.03
	$\delta_2$	0.03	-27.736	23.506 - 113,123i	
	$\delta_3$	0.016	-28.016	22.216 - 53,119i	
709	$\delta_1$	0.035	-36.695	59.318 + 746.177i	1252.20
	$\delta_2$	0.025	-36.954	103.41 + 1045.002i	
	$\delta_3$	0.016	-37.188	212.176+ 1547.797i	
	$\delta_4$	0.015	-37.214	234.52 + 1631.123i	

### 3.3.2 Vibro-Acoustic Performance of the “Second Prototype Tube”

In this chapter of the thesis, outer surface vibration velocities and outer sound pressures of the “second prototype tube” are measured under acoustic excitation whose frequencies are specified from cavity and structural modes. Outer surface impedances are then obtained by dividing sound pressures by surface vibration velocities.

Acoustic excitation frequencies are selected from acoustical and structural natural frequencies of tube. The cavity frequencies are determined in previous section whereas structural modes are determined by in-situ modal analysis.

#### 3.3.2.1 In Situ Structural Modal Analysis of the “Second Prototype Tube”

In this chapter, in situ structural modal analysis of “second prototype tube” has been performed. Impact test has been performed for three different points. Experimental setup is shown in Figure 3.22. Symmetry test has been carried out for

verification of test. 3 x 3 FRF matrix is shown in Figure 3.23 and first two structural natural frequencies are tabulated in Table 3.9.



Figure 3.22 In situ modal test setup of the “second prototype tube” (Personal archive, 2016)

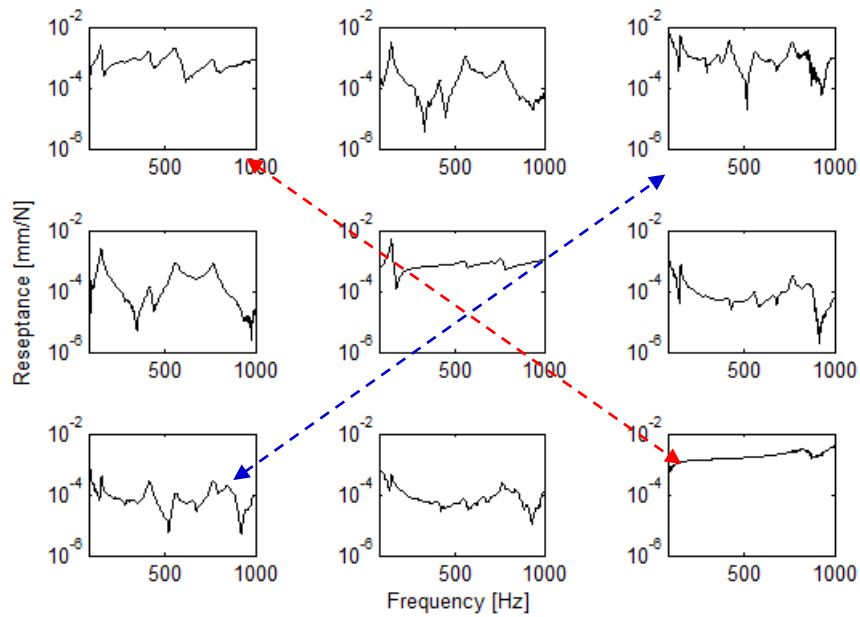


Figure 3.23 3x3 frequency response matrix of the “second prototype tube” for in-situ condition

Table 3.9 Natural frequencies of the “second prototype tube” for in-situ condition

Order	“Second Prototype Tube” [Hz]
1	148
2	418



### 3.3.2.2 Outer Surface Impedances of the “Second Prototype Tube”

Here, the outer surface sound pressures and outer surface vibration velocities of the “second prototype tube” are measured under acoustic excitations with different frequencies. Then, outer surface specific acoustic impedances of tube are computed via dividing sound pressures by vibration velocities. The measurement setup is shown in Figure 3.24.

The tube has been excited under its acoustical and structural natural frequencies. Figures 3.25 shows surface velocities and sound pressures of tubes subjected to acoustic excitation with first two structural resonance frequencies and outer surface impedances of tubes subjected to acoustic excitation at first two structural resonance frequencies are shown in Figure 3.26. Besides that, measurements at first four cavity frequencies are shown are Figures 3.27 - 3.29. Note that, the results are compared with brass and the “first prototype tube”.



Figure 3.24 Outer surface impedance measurements setup (Personal archive, 2016)

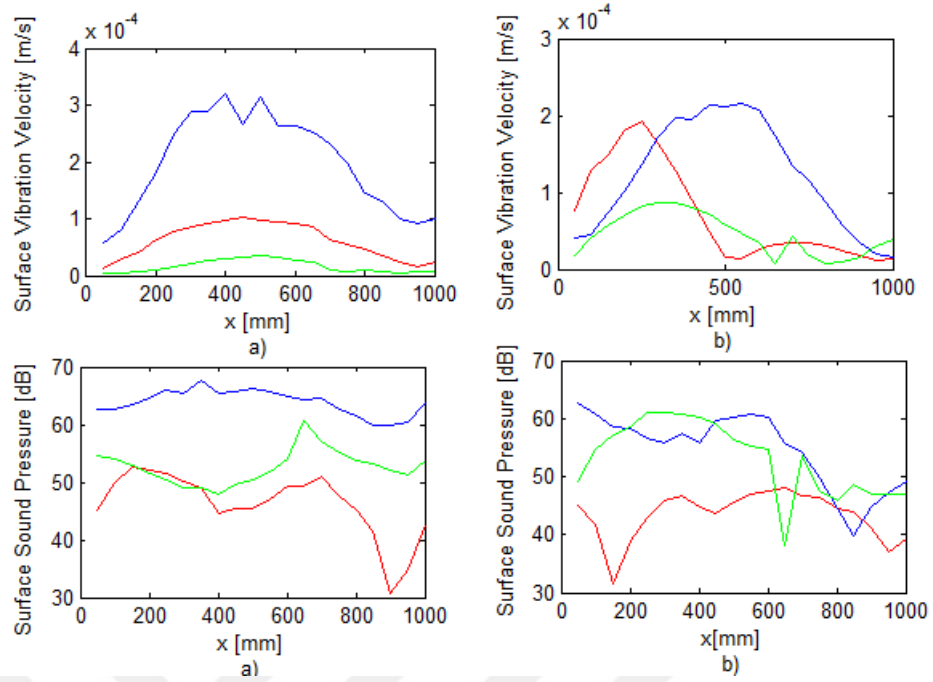


Figure 3.25 Outer surface vibration velocities and surface sound pressures of tubes, a) at first structural natural frequencies b) at second structural natural frequencies (red line: brass tube, blue line: the “first prototype tube”, green line: the “second prototype tube”)

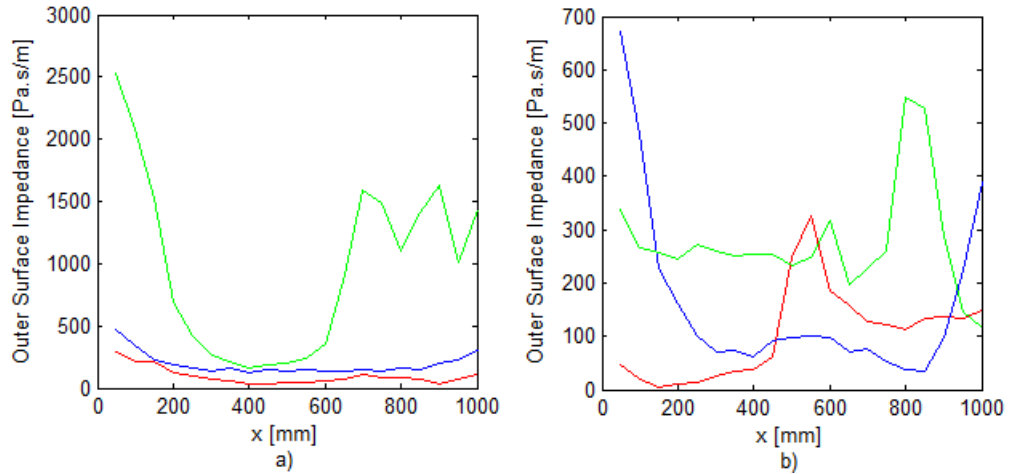


Figure 3.26 Outer surface impedance values of tubes, a) at first structural natural frequencies b) at second structural natural frequencies (red line: brass tube, blue line: the “first prototype tube”, green line: the “second prototype tube”)

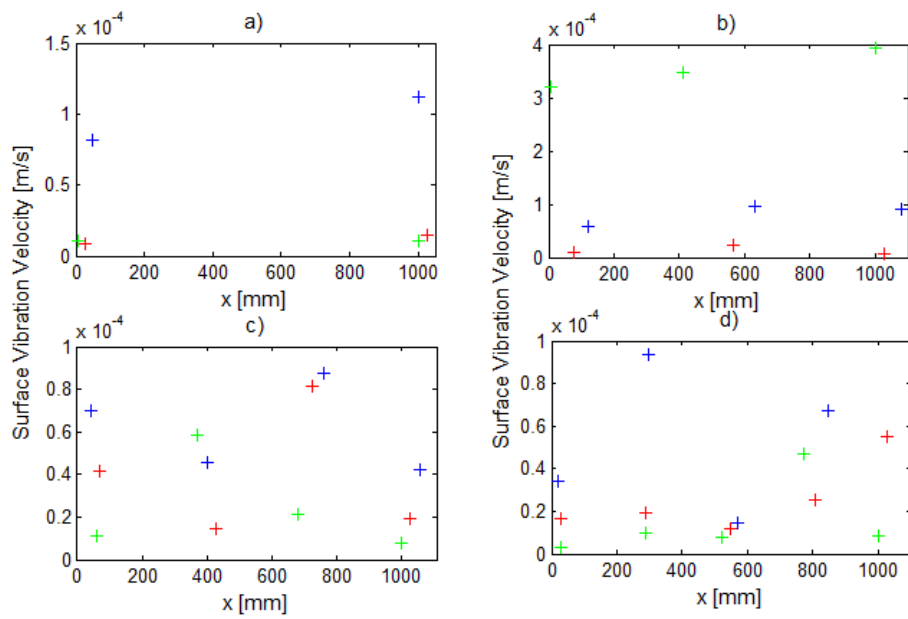


Figure 3.27 Surface vibration velocity values of tubes. a) at first structural natural frequency, b) at second cavity frequency, c) at third cavity frequency, d) at fourth cavity frequency (red plus: brass tube, blue plus: the “first prototype tube”, green plus: the “second prototype tube”)

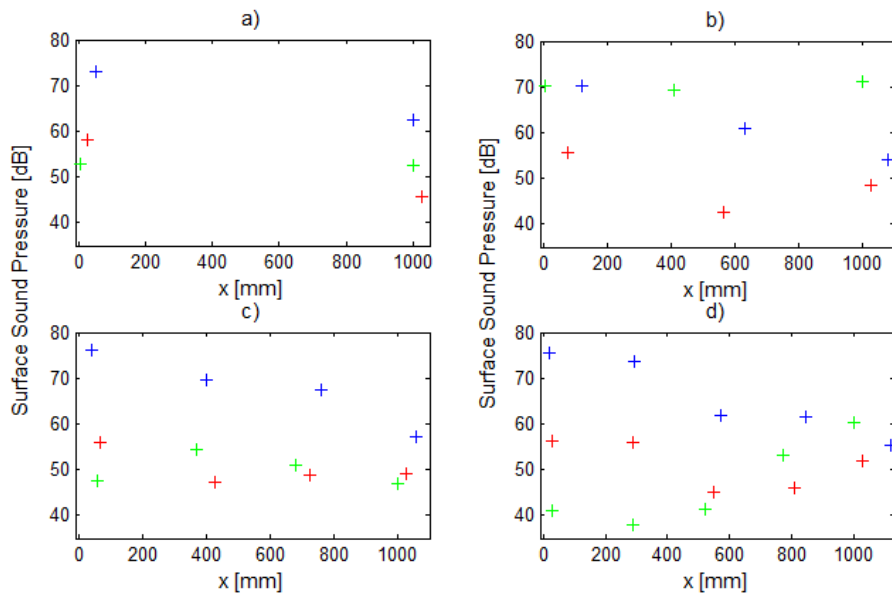


Figure 3.28 Surface sound pressures of tubes. a) at first structural natural frequency, b) at second cavity frequency, c) at third cavity frequency, d) at fourth cavity frequency (red plus: brass tube, blue plus: the “first prototype tube”, green plus: the “second prototype tube”)

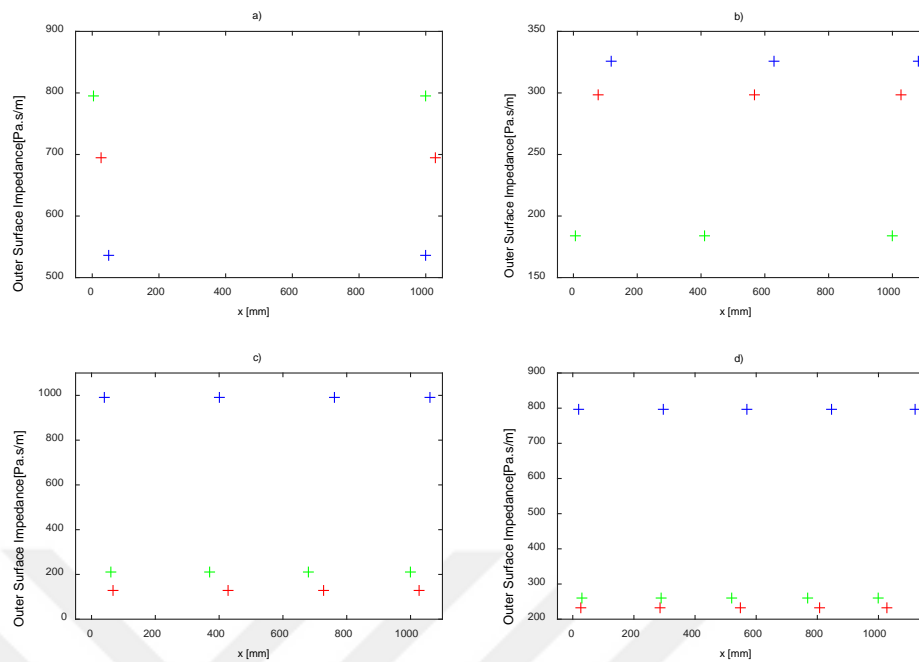


Figure 3.29 Outer surface impedance values of tubes. a) at first structural natural frequency, b) at second cavity frequency, c) at third cavity frequency, d) at fourth cavity frequency (red plus: brass tube Hz, blue plus: the “first prototype tube”, green plus: the “second prototype tube”)

Results show that the “second prototype tube” is generally better than the brass tube whereas it has lower impedance with respect to the “first prototype tube”. However, it is seen from the figures that measured outer sound pressures of the “second prototype tube” is lower than the “first prototype tube” results.

### 3.4 Sound Absorption Coefficient Measurements via “First and Second Prototype Tubes”

In this chapter, sound absorption coefficient of a material is measured and results are compared for the “first and second prototype” and brass tube.

According to ASTM E 1050-98, the impedance tubes should have low tube attenuation. Tube attenuations are determined by measuring sound absorption coefficient of tube with rigid end condition. Tube attenuations of “first and second prototype tubes” are determined via two-microphone method and standing wave

method was used for brass tube. Sound absorption measurement at 1/3 octave band are presented in Figures 3.30-3.32.

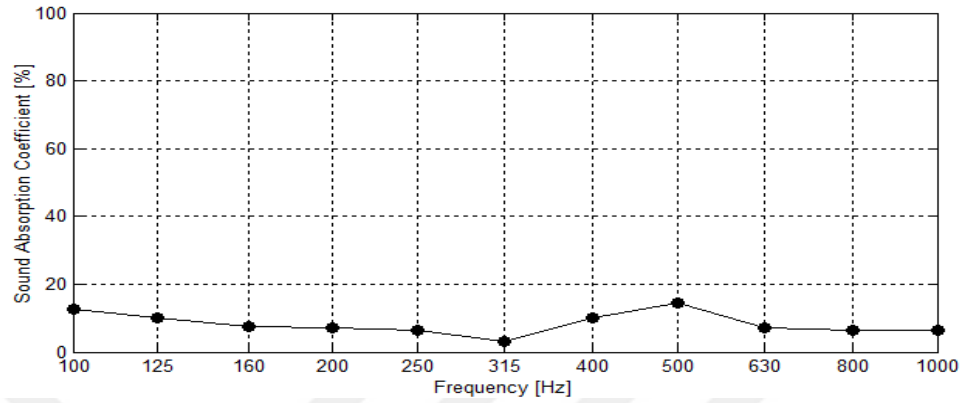


Figure 3.30 Sound absorption coefficient of the “first prototype tube” for rigid end condition

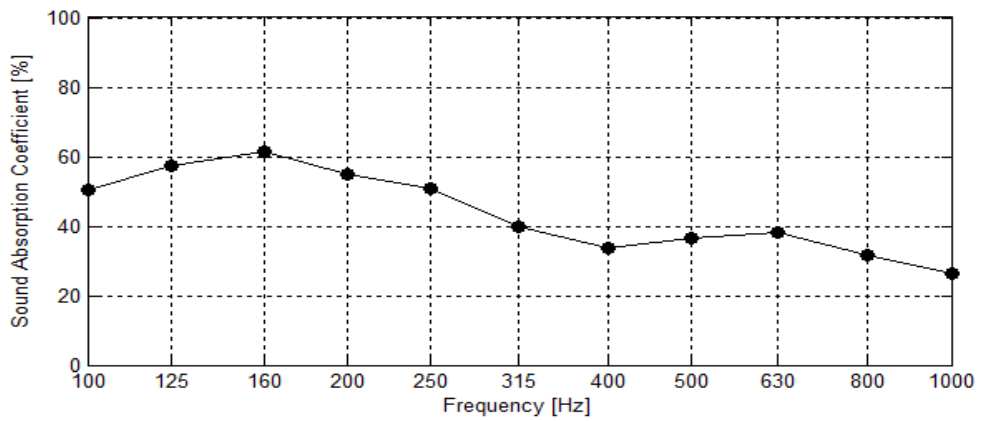


Figure 3.31 Sound absorption coefficient of the “second prototype tube” for rigid end condition

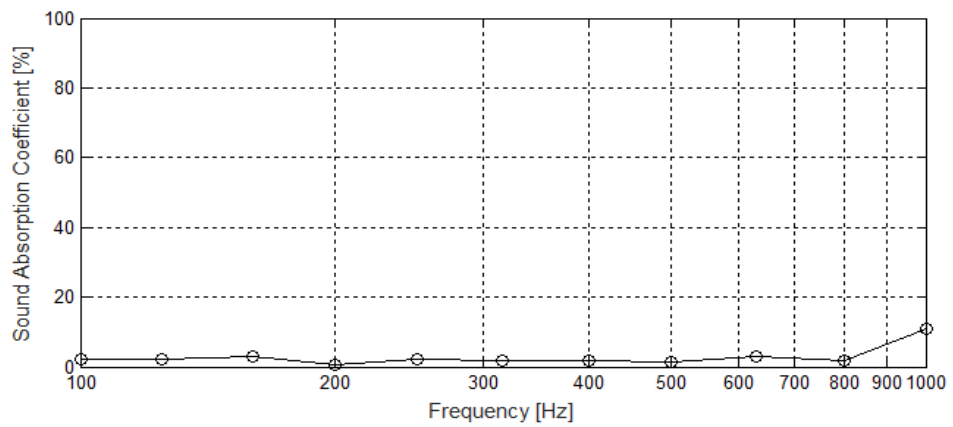


Figure 3.32 Sound absorption coefficient of brass tube for rigid end condition

Figure 3.30 shows that, averaged tube attenuation of the “first prototype tube” is %8 but it increases up to %20 for 400 – 500 Hz band and the “second prototype tube” set has the highest tube attenuation. This may be the result of the leakage at the connections. Besides that, tube attenuation of the brass tube is very low.

ASTM E 1050-98 recommends that, if distance of the nearest microphone to face of specimen is greater than three times of tube diameter, the tube attenuation needs to be taken into account. To eliminate the tube attenuation effect, wave number should be modified. This may be done by the given process in Chapter 2.6. Tube attenuation coefficients of “first and second prototype tube” are computed via mentioned methodology and computed coefficients are shown in Figure 3.33.

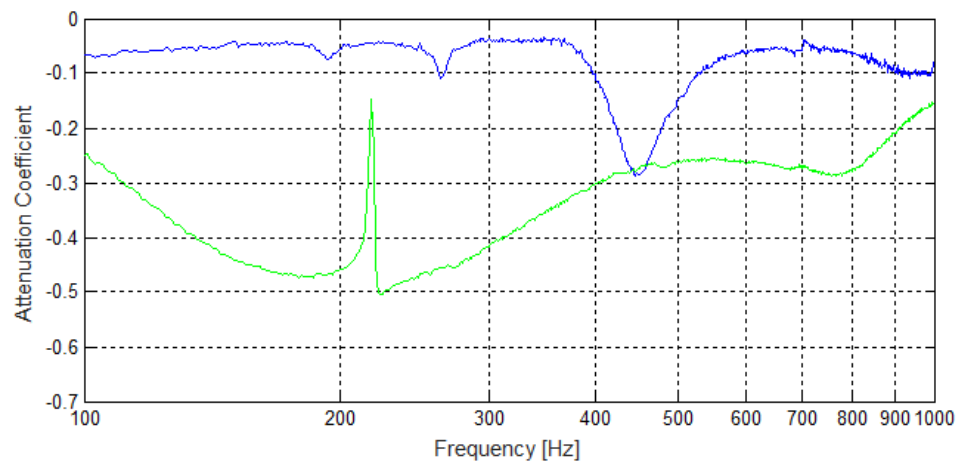


Figure 3.33 Attenuation coefficients of the “first and second prototype tubes” (blue line: the “first prototype tube”, green line: the “second prototype tube”)

Wave numbers have been manipulated via computed tube attenuation as Equation 2.70. Then, sound absorption coefficients of a felt material have been measured with the prototype tubes via two-microphone method and with the brass tube via standing wave method. Figure 3.34 shows sound absorption coefficient measurement results of the felt material.

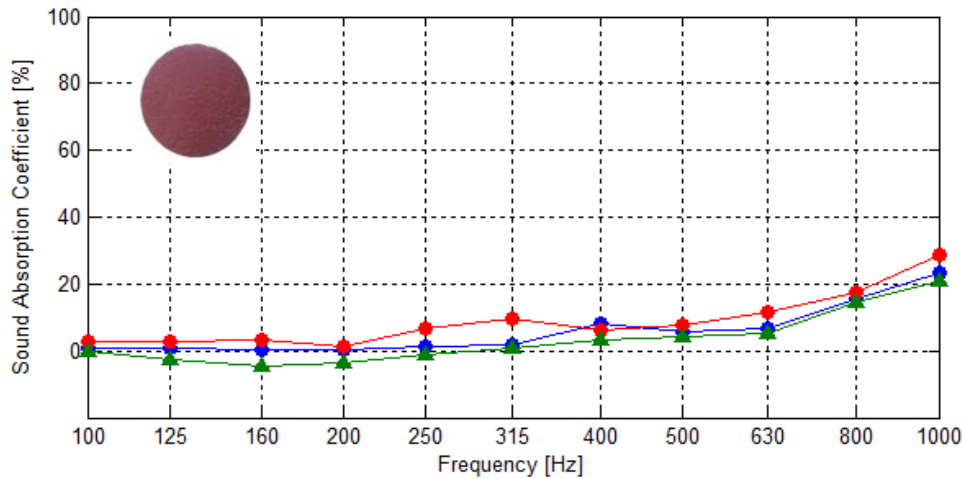


Figure 3.34 Sound absorption coefficient measurement results of a felt material (red circles: brass tube, blue line: the “first prototype tube”, green line: the “second prototype tube”)

The results show that, characteristics of sound absorption coefficient measurements are coherent with each other. However, sound absorption coefficients measured with the “first prototype tube” is greater than the ones with brass tube at 400-500 Hz band. Besides that, negative sound absorption coefficients are measured at 100-300 Hz band with the “second prototype tube”. Since sound absorption coefficient could not be negative, leakages and high tube attenuation may cause this situation. Therefore, a new tube set has been designed and manufactured.

### 3.5 Designing, Manufacturing and Analyzing of “New Impedance Tube Set”

The “new impedance tube set” has been designed as a sandwich composite structure to reduce the leakages. Inner tube has been designed again epoxy-glass composite because of its mechanic advantages. However, outer tube has been selected to be as aluminum since it is cheaper and easy to manufacture than composite ones. In addition, space between aluminum and composite tubes has been filled with fiberglass material for acoustic and thermal insulation.

On the other hand, the leakage problem of the “second prototype tube” has been tried to be overcome in new design. Delrin materials have been used for flanges. Therefore, there are not any axial imperfections and leakages from connections. All

other parameters, i.e., distance between microphones, tube length and tube diameter, are specified according to the standards.

The “new impedance tube set” is designed and manufactured modular for four different measurement types as the “second prototype tube”. The designed and manufactured tubes are shown in following Figures 3.35-3.48.



Figure 3.35 Low frequency sound absorption coefficient measurement set (a: 3-D design model, b: manufactured system, c: painted system) (Personal archive, 2016)



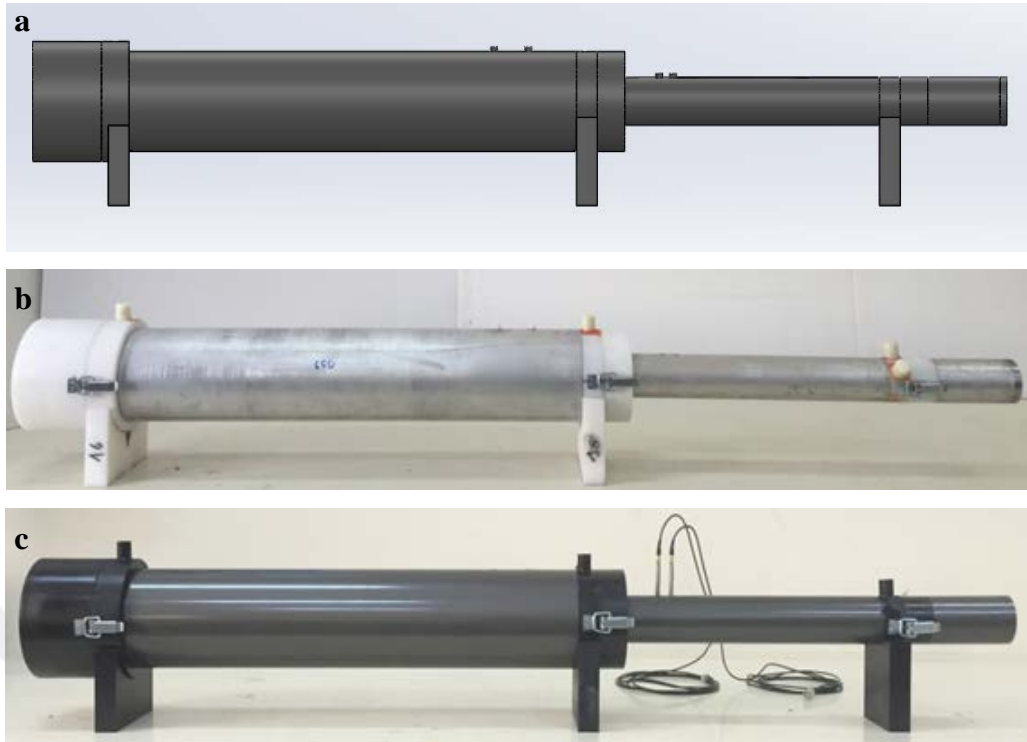


Figure 3.36 High frequency sound absorption coefficient measurement set (a: 3-D design model, b: manufactured system, c: painted system) (Personal archive, 2016)

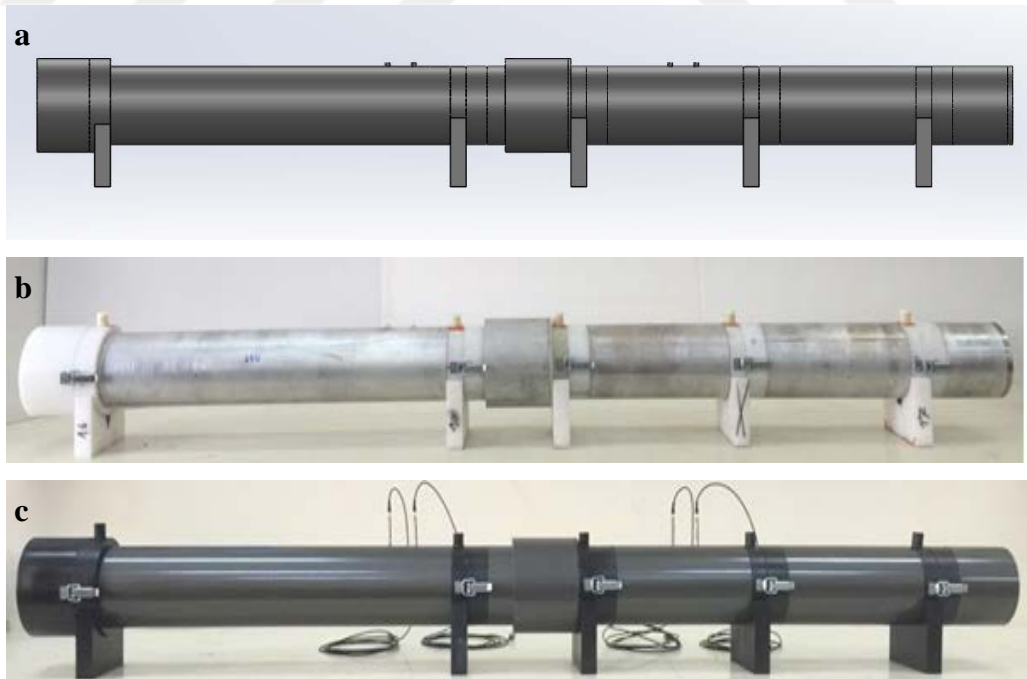


Figure 3.37 Low frequency transmission loss measurement set (a: 3-D design model, b: manufactured system, c: painted system) (Personal archive, 2016)



Figure 3.38 High frequency transmission loss measurement set (a: 3-D design model, b: manufactured system, c: painted system) (Personal archive, 2016)

The vibro-acoustic performance tests are not repeated for the “new impedance tube set” since the structure is the same of the “second prototype tube” and it has good results from vibro-acoustic performance point of view. The tube attenuation of the “new impedance tube set” has been determined for low and high frequency sound absorption coefficient measurement systems. The method which is explained in Chapter 2.6 has been used for determination of tube attenuations. Imaginary parts of wave numbers are presented in Figures 3.39 and 3.40.

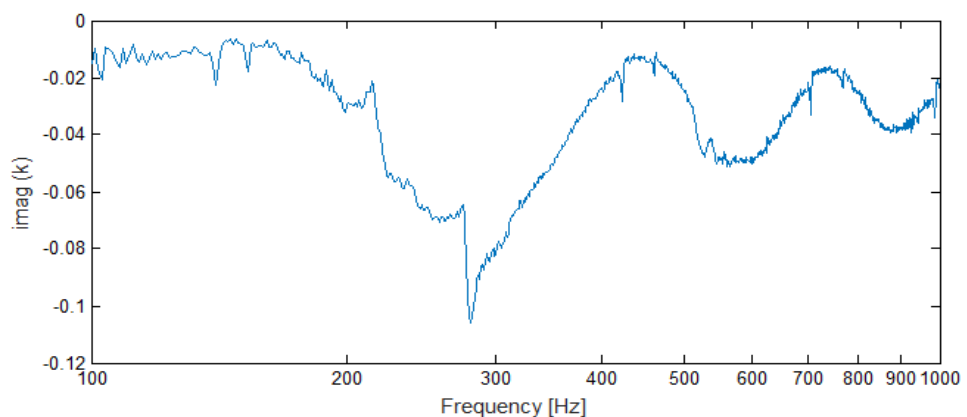


Figure 3.39 Imaginary part of wave number that has been determined for tube attenuation of the “new impedance tube set” (100 Hz – 1000 Hz)

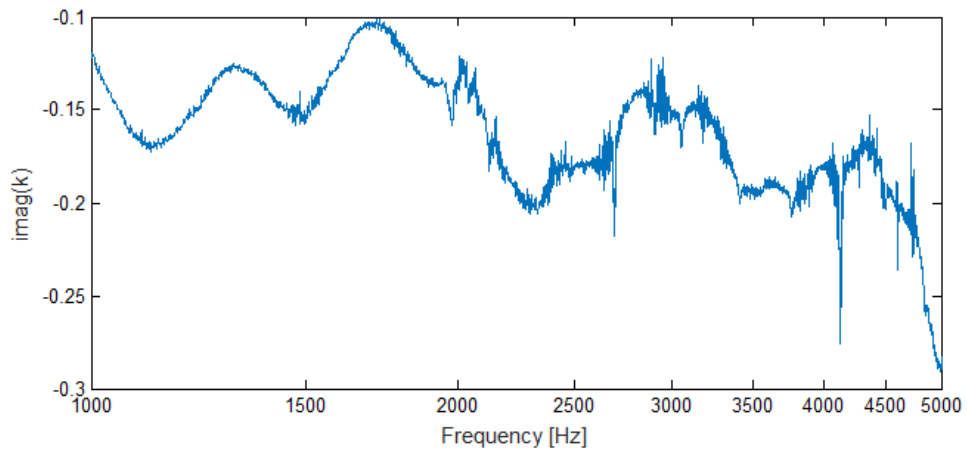


Figure 3.40 Imaginary part of wave number that has been determined for tube attenuation of the “new impedance tube set” (1 kHz- 5 kHz)

It is seen from the figures that, the tubes have higher attenuation in higher frequencies since the imaginary part of wave number is lower in the mentioned range.

Also sound absorption coefficients have been measured for rigid end. The measured results are shown in Figures 3.41 and 3.42. Then, the sound absorption coefficients have been manipulated with modified wave numbers in compliance with the measured tube attenuations. Modified results are also shown in Figures 3.41-3.42.

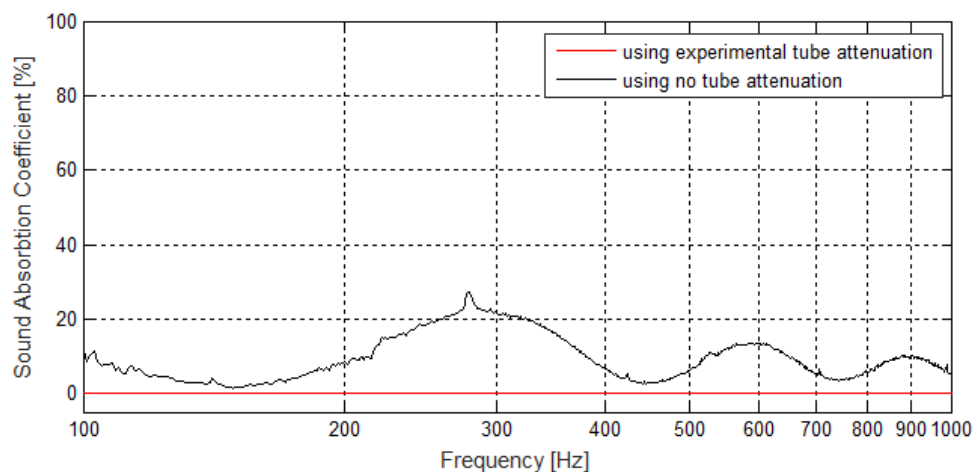


Figure 3.41 Sound absorption coefficient of the “new impedance tube set” for rigid end condition (100 Hz- 1000 Hz)

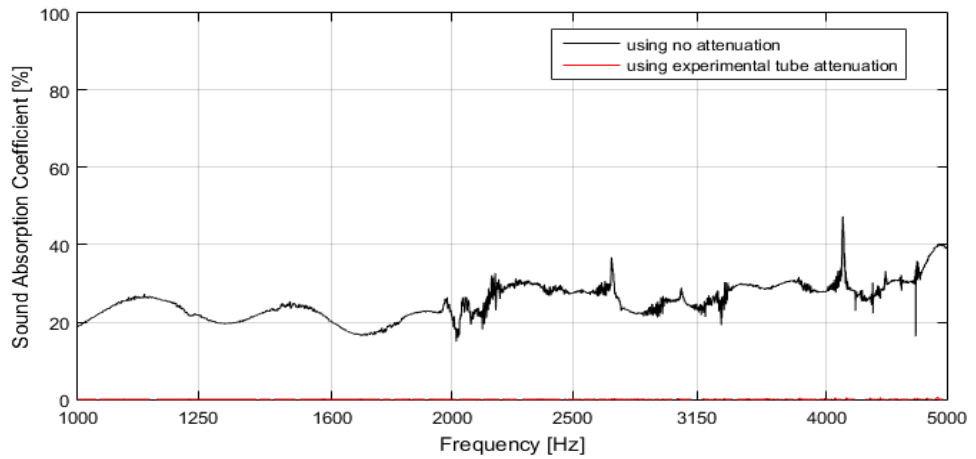


Figure 3.42 Sound absorption coefficient of the “new impedance tube set” for rigid end condition (1 kHz- 5 kHz)

Figure 3.41 shows that, the tube has high attenuation at 250 – 350 Hz band in low frequency measurements. However, sound absorption coefficient is calculated as zero after adopting the tube attenuation into the measurements.

Sound absorption coefficient of a felt material is measured for low frequency range (100-1000 Hz) with several tubes i.e., brass tube, the “first prototype tube”, the “second prototype tube” and the “new impedance tube set”. Results are shown in Figure 3.43.

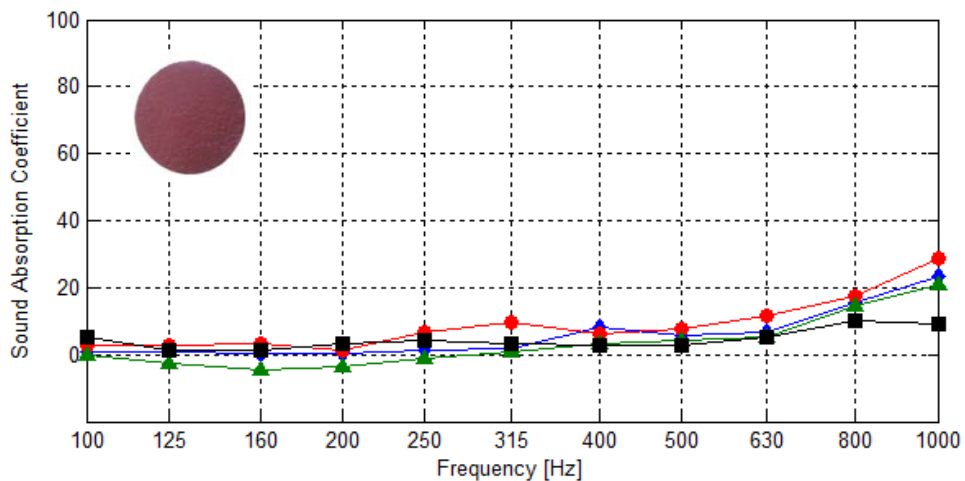


Figure 3.43 Sound absorption coefficient measurement results of a felt material (Red circles: brass tube, blue line: the “first prototype tube”, green line: the “second prototype tube”, black line: the “new impedance tube set”)

Figure 3.43 shows that, sound absorption coefficient of the material which is measured with the “new impedance tube set” are coherent with the other results.

### 3.6 Development of Software

For the determination of acoustic parameters, measurement and calculation software are developed via LabVIEW. The measurements and calculations of acoustical performance parameters can be provided in few seconds via these programs.

Measurement and calculation programs are developed separately. Note that, there are four different programs, i.e, measurement of sound absorption, calculation of sound absorption, measurement of transmission loss, calculation of transmission loss.

#### 3.6.1 Measurement and Calculation Programs

Figure 3.44 represents algorithm of measurement programs. White noise signal is created digitally from program and signal is transmitted to loudspeaker by analog output module. The sound pressure levels are measured by microphones and Frequency Response Function (FRF) is obtained as output of measurement program. By the way, temperature and relative humidity levels of tube inside is measured and monetarized in program.

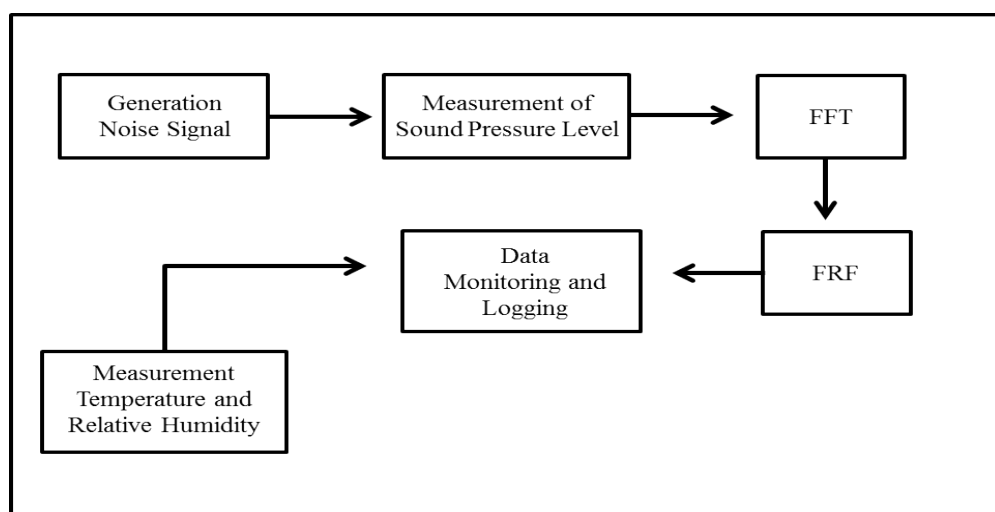


Figure 3.44 Algorithm of measurement programs

### 3.6.1.1 Sound Absorption Coefficient Measurement Program

This program enables to measure the frequency response function (FRF) with respect to measured sound pressures. There are two different tube setups depending on the measurement frequency range, i.e., low (100-1000 Hz) and high frequency (1000-5000 Hz) measurements.

In the measurements, the stimulus microphone and response microphone channels should be selected before the measurement and sensitivities of each microphone are entered. Figure 3.45 shows main page of Sound Absorption Coefficient Set Measurement Program.

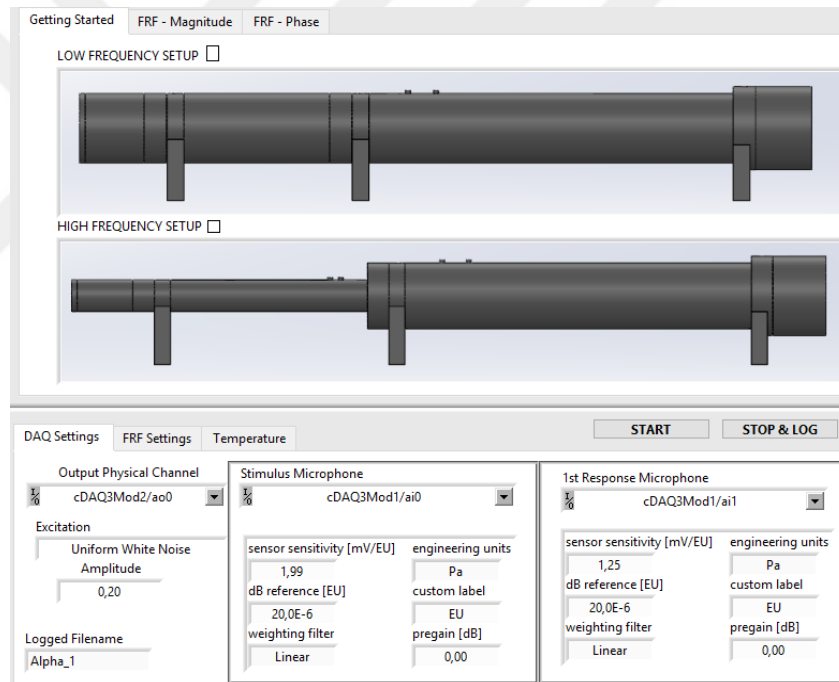


Figure 3.45 Sound Absorption Coefficient Set Measurement Program main pages

### 3.6.1.2 Transmission Loss Measurement Program

This program is similar to Sound Absorption Measurement Program but since four microphones are used in the measurements, there are three different FRFs to measure if one of the microphones are selected as stimulus. Main page is shown in Figure 3.46.

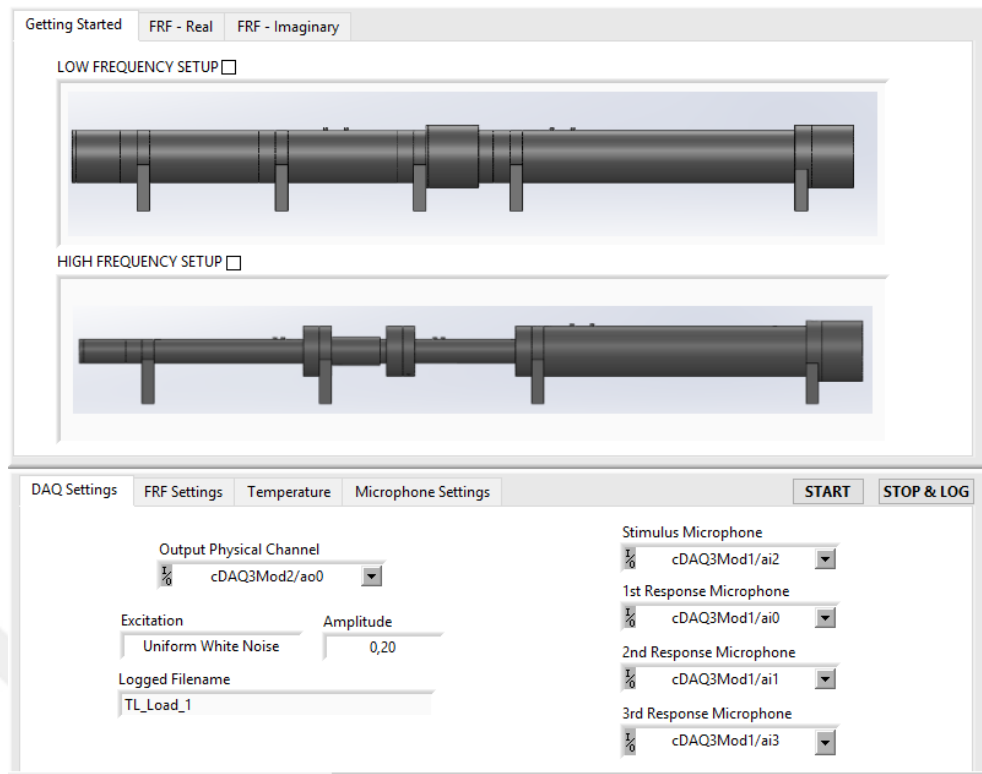


Figure 3.46 Transmission Loss Set Measurement Program main pages

### 3.6.1.3 Sound Absorption Calculation Program

Acoustical performance parameters can be calculated by using the measured frequency response functions. ASTM E 1050-98 standard describes calculation of impedance and absorption of acoustical materials via two microphone method. Details of this method have been described in Chapter 2.4.1.

Sound Absorption Coefficient Calculation Program uses this method and calculates absorption and impedances of acoustical materials. Measured data should be loaded to program in .csv format.

Besides, the user should select the parameters those will be calculated and the frequency range. These parameters are sound absorption coefficient, specific acoustic admittance, reflection coefficient and specific acoustic impedance as specified in standard. Main page of this program is shown in Figure 3.47.

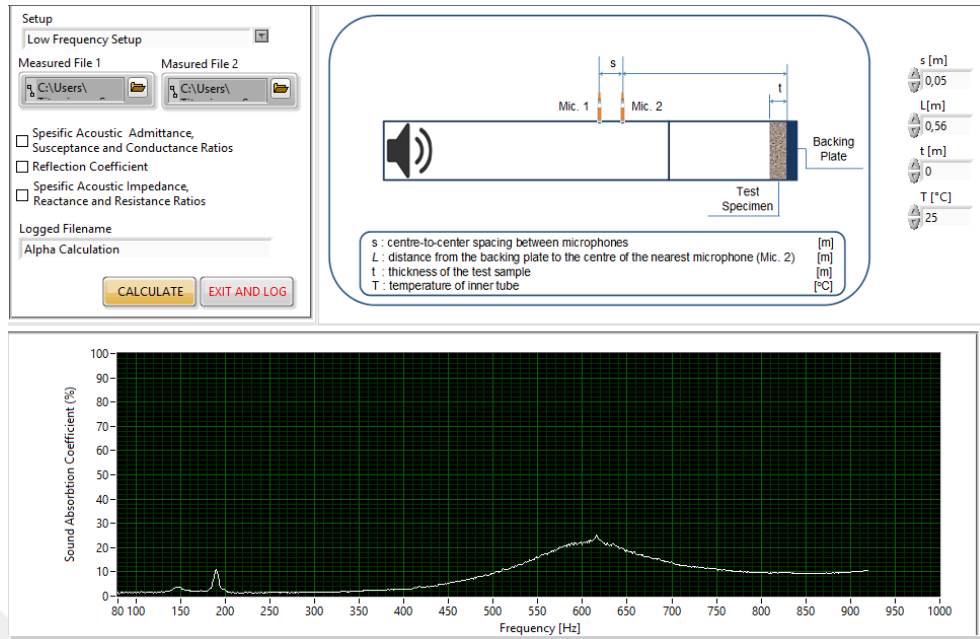


Figure 3.47 Sound Absorption Coefficient Set Calculation Program

### 3.6.1.4 Transmission Loss Calculation Program

ASTM E 2611-09 standard describes calculation of sound transmission loss of acoustical materials via transfer matrix method. Details of this method have been described in Chapter 2.4.2.

The operation method is similar to Sound Absorption Calculation Program. The program interface is shown in Figure 3.48.

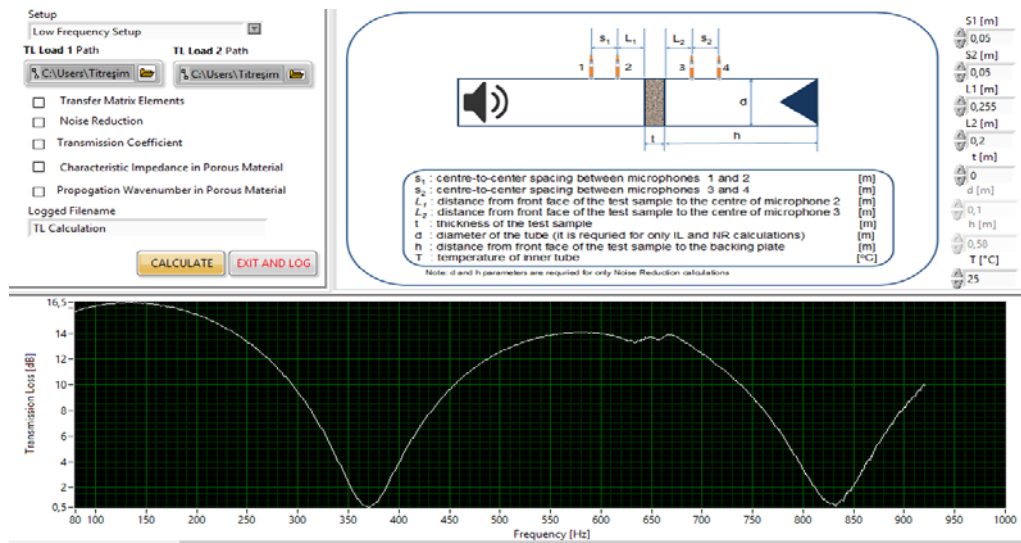


Figure 3.48 Transmission Loss Set Calculation Program



### 3.6.1.5 Verification of Measurement Programs

In this section, measured FRFs are compared with the ones those are obtained by using “Signal Express”. Here, the measurements are performed for the same conditions but at different timelines. In Figures 3.49 and 3.50, real and imaginary parts of FRFs measured via sound absorption measurement program are presented. Note that, the boundary conditions in the measurements are selected as rigid end.

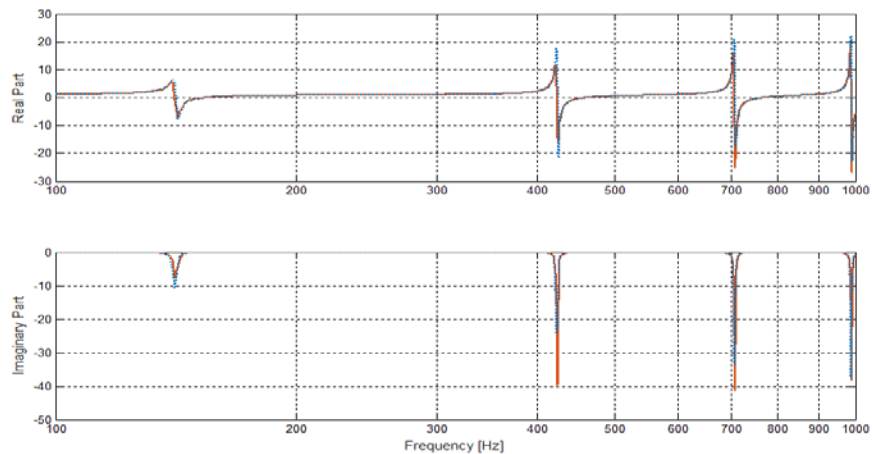


Figure 3.49 Compared results of Signal Express and Sound Absorption Coefficient Set Measurement Program measurements for low frequency bandwidth; 100 Hz – 1000 Hz (red line: Signal Express FRF result; blue line: Alfa Measurement Program FRF result)

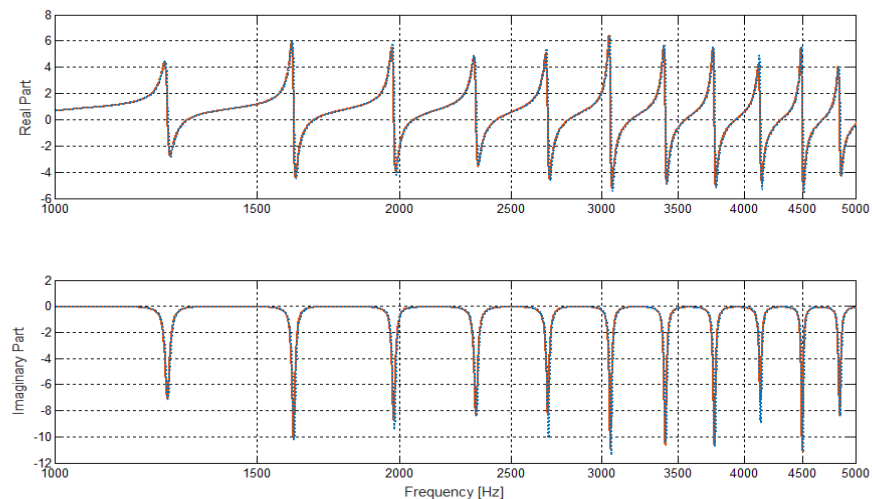


Figure 3.50 Compared results of Signal Express and Sound Absorption Coefficient Set Measurement Program measurements for high frequency bandwidth; 1000 Hz - 5000 Hz (red line: Signal Express FRF result; blue line: Alfa Measurement Program FRF result)

It is seen from the Figures that, measurements are coherent with each other. Therefore, the measurement programs are reliable.

### 3.6.1.6 Verification of Calculation Programs

After verifying the measurement programs, calculation programs are tested. Figure 3.43 is also proof of verification of alfa set calculation program. The “new impedance tube set” results are calculated via this program and results are similar with brass tube result.

The transmission loss calculation program is tested for an expansion chamber. Figure 3.51 shows the considered expansion chamber. Transmission loss of the expansion chamber is measured and calculated by using developed programs and presented in Figure 3.52. Note that, analytical calculation of Transmission Loss is taken from Seçgin et. al. (2013).



Figure 3.51 Expansion chamber (Personal archive, 2015)

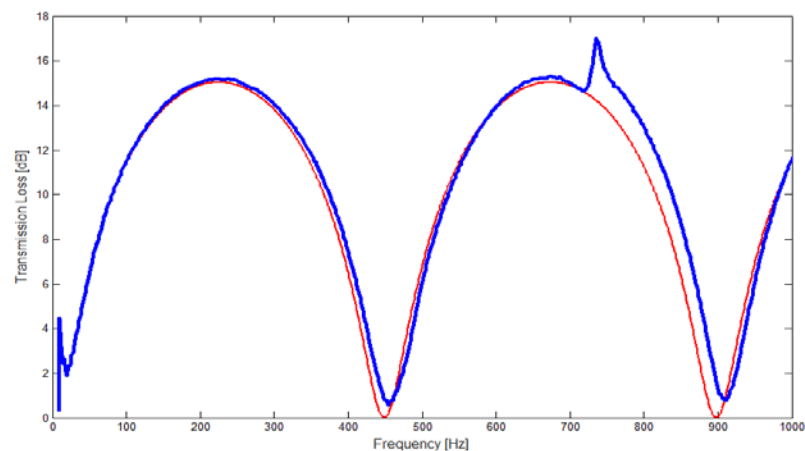


Figure 3.52 Compared results of transmission loss of expansion chamber (red line: analytical result; blue line: calculated result via Transmission Loss Set Calculation Program)

### 3.7 Design and Manufacturing of Conditioning System

Determination of acoustic performance parameters of materials and mufflers depending on temperature and relative humidity is significant especially in aeronautical industry. For this purpose, two different conditions are investigated in this study. First, sound absorption coefficients of materials are determined for different temperature conditions and relative humidity of tube inside, materials are conditioned different temperatures secondly, and their sound absorption coefficients are determined.

An air conditioning system has been designed and manufactured for conditioning of tube inside. Figure 3.53 shows the scheme of system. A compressor is used for refrigerating cycle. Air inside of the tube is sucked by a plug fan for conditioning system and it is cooled by evaporator. Then, it is blown to tube by another fan. Also for heating air, a resistance is used in system. In addition an ultrasonic vapor machine is used for conditioning of humidity inside of the tube.

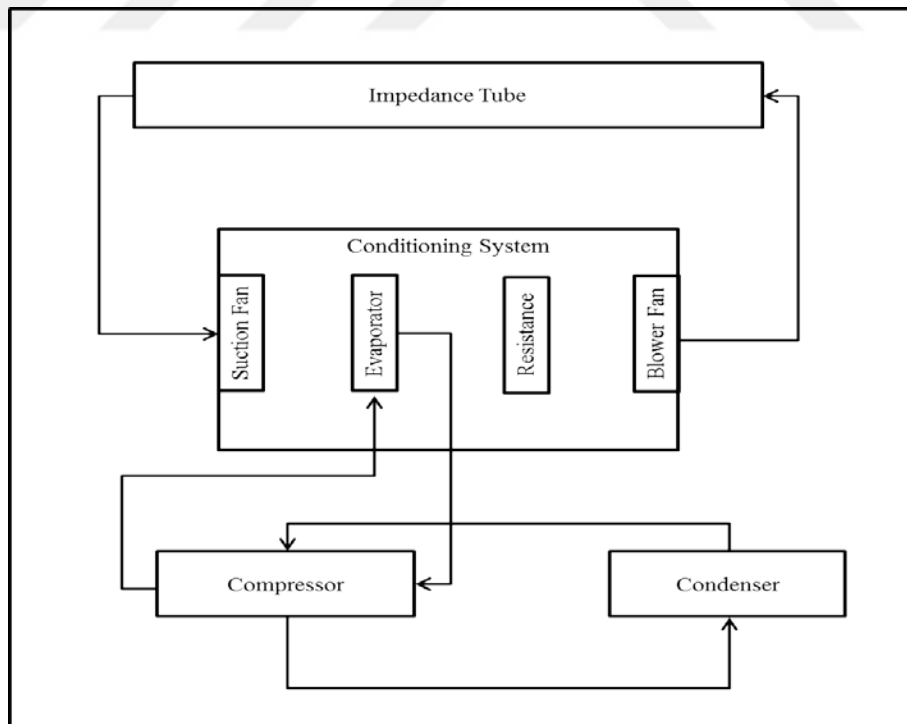


Figure 3.53 Scheme of conditioning system

Manufactured system is shown in Figure 3.54 with low frequency sound absorption coefficient measurement tube set. The tube inside can be conditioned -10 °C to 60 °C via this system. Temperature and relative humidity of tube inside is measured via a probe and results are shown in measurement programs.



Figure 3.54 Conditioning test system (Personal archive, 2016)

Also, materials are conditioned at different temperatures via household refrigerator and furnace. K type thermocouples are used for measuring the temperature of the materials. Note that, temperature measurements are performed from centers of materials.

Sound absorption coefficients are measured under different temperature conditions. The experimental results will be presented and discussed in Chapter 4.

### **3.8 Design and Manufacturing of Specimen Rotation Apparatus**

Acoustical performance parameters of materials are not only measured with impedance tubes, but also they can also be obtained in reverberation rooms. These rooms can simulate the actual conditions of usage of materials. Because in these rooms, sound absorption measurements are performed for random incidence waves whereas normal incidence sound absorption coefficient is measured via impedance tubes. Therefore, impedance tubes cannot simulate the actual conditions. In this study, a rotation apparatus is designed and manufactured for the simulation of the actual conditions. The test specimen can be rotated between 0 to 40 degrees and

sound absorption coefficients of the materials can be determined as a function of incidence angle of sound waves. The designed and manufactured system is shown in Figure 3.55.



Figure 3.55 Rotation apparatus with low frequency sound absorption coefficient measurement set (a: design drawing b: manufactured system c: painted system) (Personal archive, 2016)

Note that, there is an expansion in designed rotation apparatus and it is undesirable situation for the impedance tubes. In order to neglect this effect, tube attenuation is measured and calculated new wave numbers. In addition, three different angled specimen holders are designed and manufactured as shown in Figure 3.56 for the verification of apparatus. Angles of holders are 15, 30 and 40 degrees.

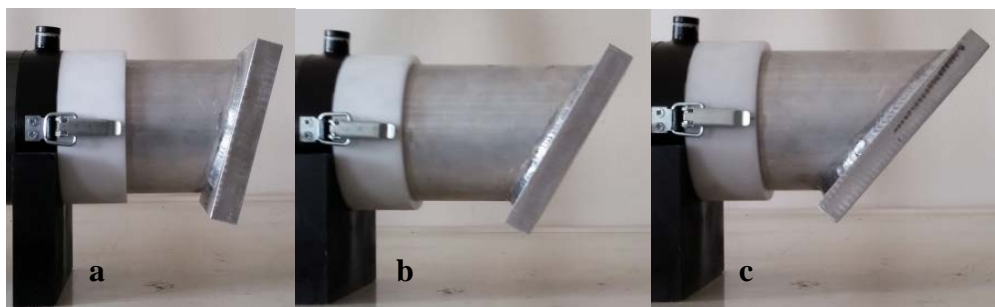


Figure 3.56 Constant angled specimen holders (a: 15° b: 30° c: 40°) (Personal archive, 2016)

The sound absorption coefficients of materials are determined for different angle of incidence of sound waves with rotation apparatus, constant angled holders and analytical methods. Results are given and discussed in Chapter 4.



## **CHAPTER FOUR**

### **EXPERIMENTAL RESULTS**

In this chapter; acoustical performance parameters of materials are determined with the “new impedance tube set” via experimental methods which are explained before in Chapter 2.

Measurements are performed for four different cases. These are;

- 1) Normal incidence sound absorption coefficient, impedance and reflection coefficient measurements of materials are determined with the “new impedance tube set”. These experiments are carried out at room temperature.
- 2) Normal incidence sound absorption coefficient measurements of materials are determined with the “new impedance tube set” under different temperature and relative humidity conditions.
- 3) Varied incidence sound absorption coefficient measurements of materials are determined via the “new impedance tube set” and with rotation apparatus. These results are compared with results of constant angled specimen holders (15°, 30°, 40°) and empirical results.
- 4) Finally, transmission loss of materials is determined via the “new impedance tube set”.

#### **4.1 Measurement Results of Normal Incidence Sound Absorption Coefficient, Impedance and Reflection Coefficient of Materials**

In this section; sound absorption coefficients, impedances and reflection coefficients of different formed materials are determined with the “new impedance tube set”. First, three different types felt materials which are named Ax, Bx, Cx are measured and compared with standing wave method to verification results. Then acoustical performance parameters of a pyramid shaped sponge and petroleum based

insulant material are measured via only the “new impedance tube set”. Low frequency sound absorption coefficient measurement set is used for low frequency measurements (100-1000 Hz) and high frequency sound absorption coefficient measurement set is used for high frequency measurements (1000 Hz - 5 kHz). These tube sets are shown in Figures 3.62 and 3.63.

#### 4.1.1 Normal Incidence Sound Absorption Coefficient Results of Materials

Two-microphone method is used as experimental method. The method has been described in Chapter 2.4.1. Also Alfa Set Measurement and Calculation programs are used.

Sound absorption coefficients of felt materials with a thicknesses of 5 mm, are also determined via standing wave method that has been described in Chapter 2.2. 1/3 octave band results are given in Figures 4.1 – 4.3.

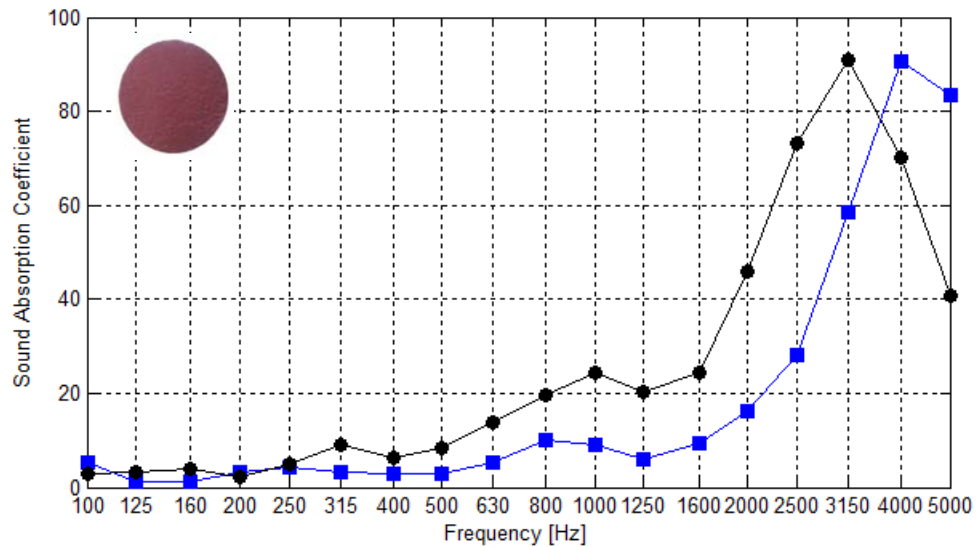


Figure 4.1 Sound absorption coefficient measurement results of Ax (blue line: two-microphone method via the “new impedance tube set”, black line: standing wave ratio method via brass tube)



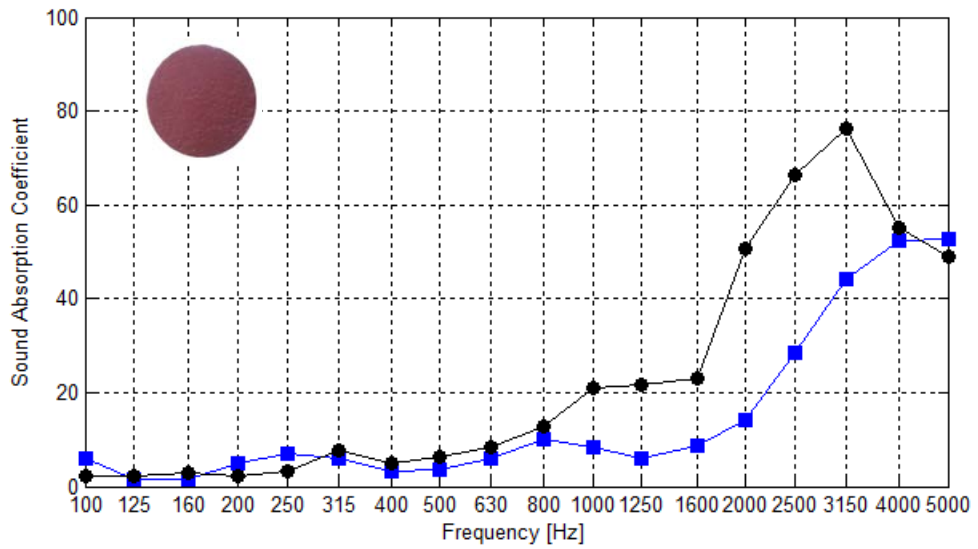


Figure 4.2 Sound absorption coefficient measurement results of Bx (blue line: two-microphone method via the “new impedance tube set”, black line: standing wave ratio method via brass tube)

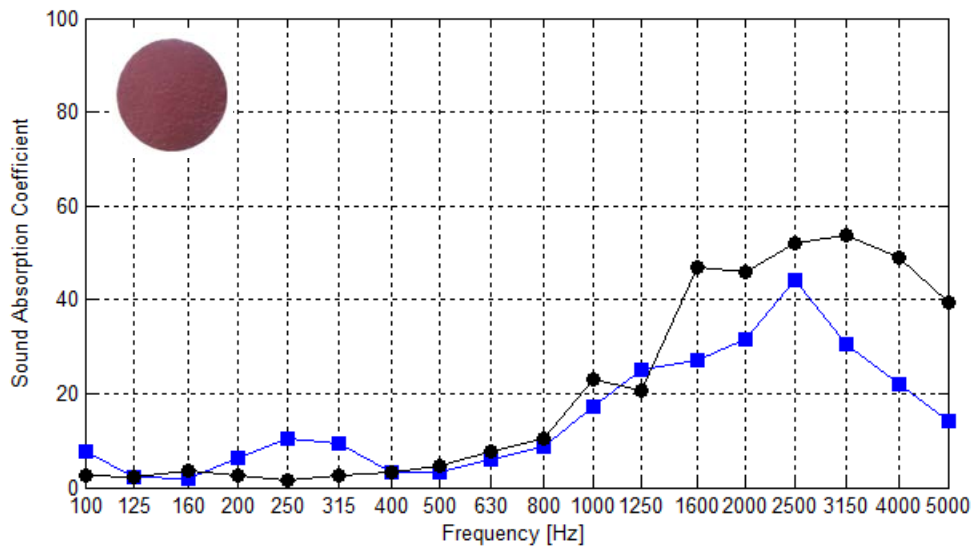


Figure 4.3 Sound absorption coefficient measurement results of Cx (blue line: two-microphone method via the “new impedance tube set”, black line: standing wave ratio method via brass tube)

The results show that, two microphone method and standing wave method are given approximately same results. And also it can be said that the “new impedance tube set” is reliable for acoustical performance parameter measurements.

Sound absorption coefficient result of pyramid shaped sponge material with a thickness of 18 mm, is shown in Figure 4.4.

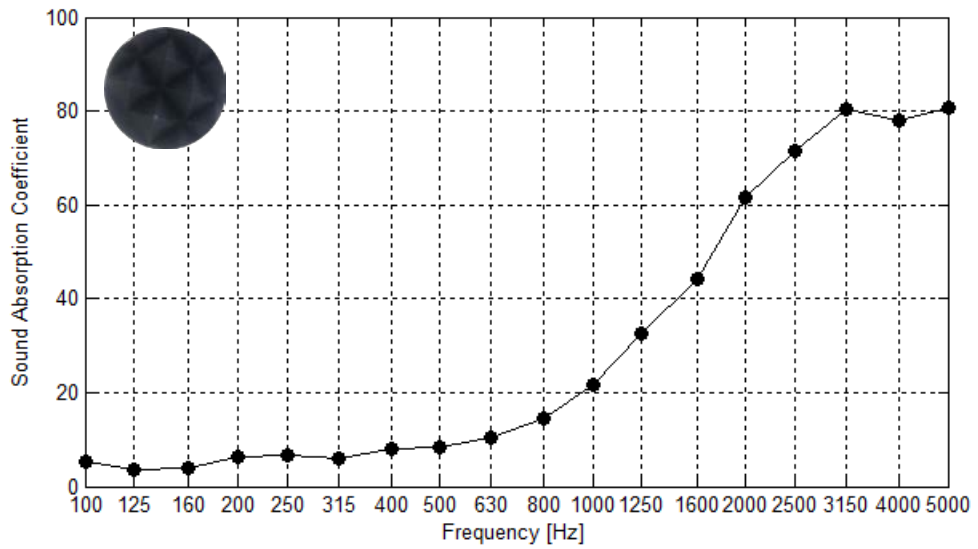


Figure 4.4 Sound absorption coefficient measurement results of pyramid shaped sponge material

Finally; sound absorption coefficient result of petroleum based insulant material with a thickness of 45 mm, is shown in Figure 4.5.

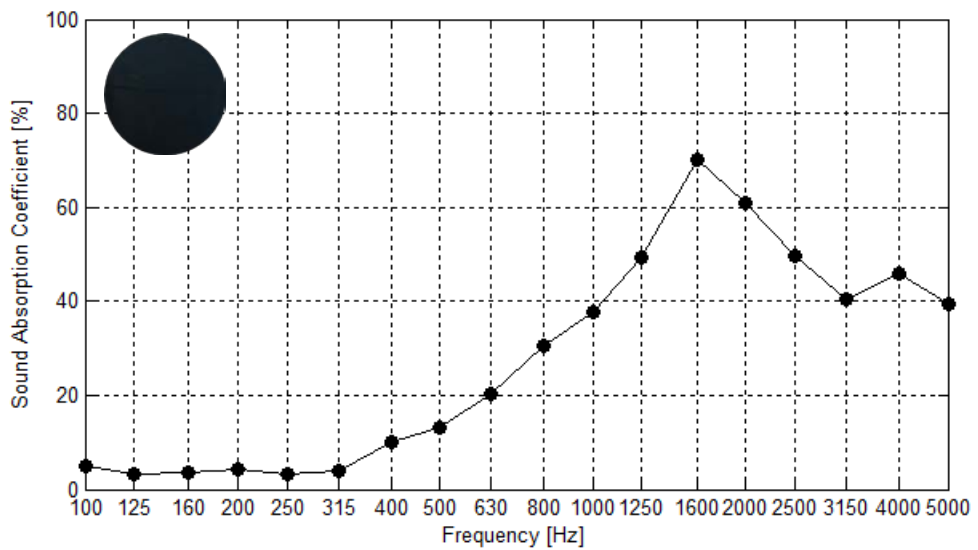


Figure 4.5 Sound absorption coefficient measurement results of petroleum based insulant material

#### 4.1.2 Normal Incidence Reflection Coefficient Results

Normal incidence reflection coefficients of materials are computed via Equation 2.33. Results are given in Figures 4.6 – 4.10.

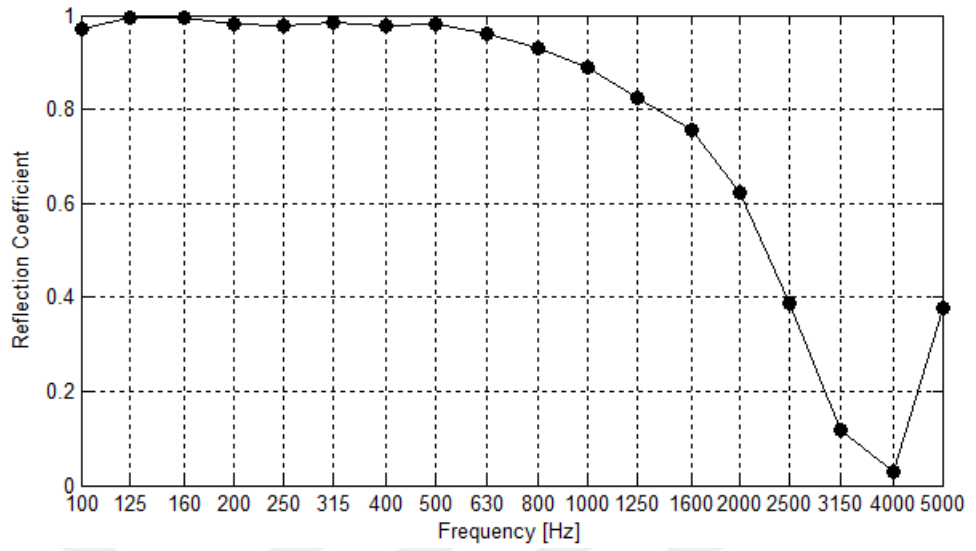


Figure 4.6 Reflection coefficient of Ax

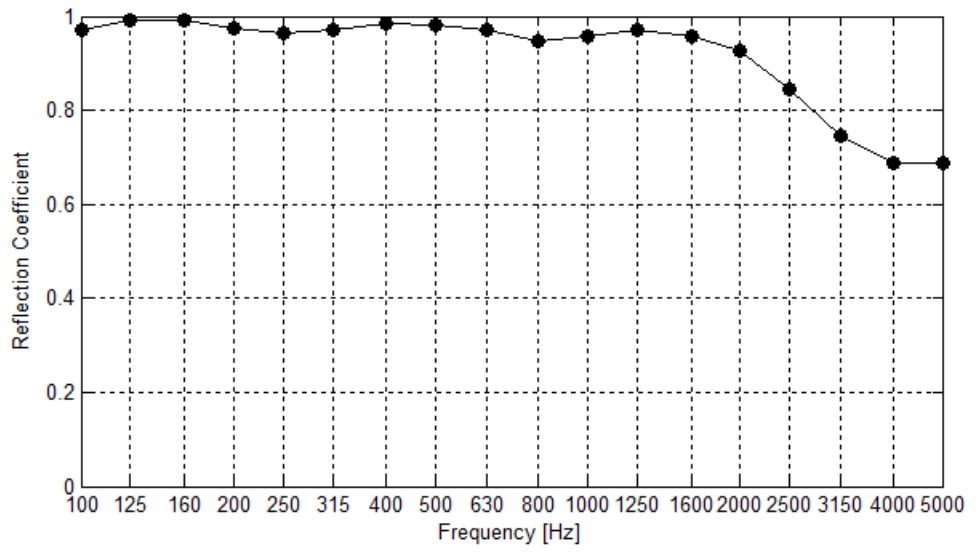


Figure 4.7 Reflection coefficient of Bx

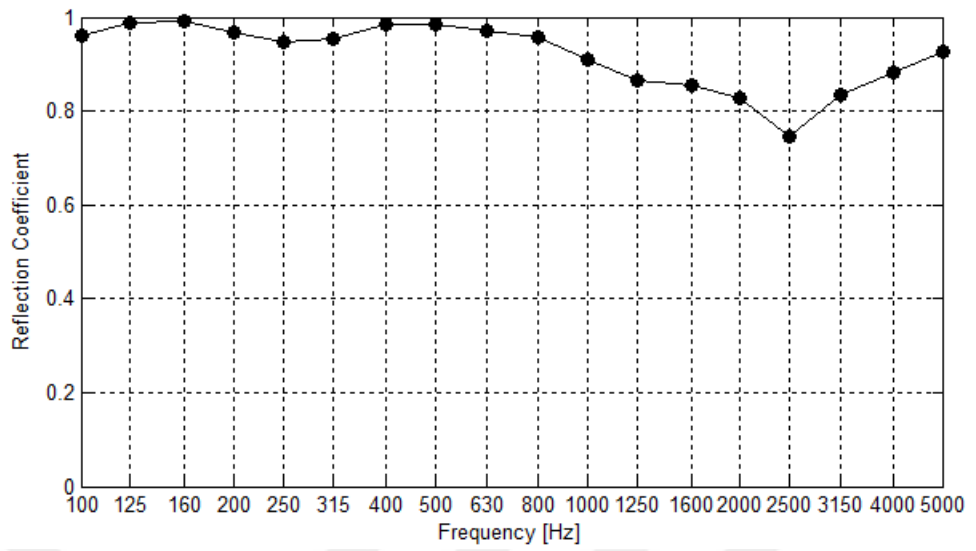


Figure 4.8 Reflection coefficient of Cx

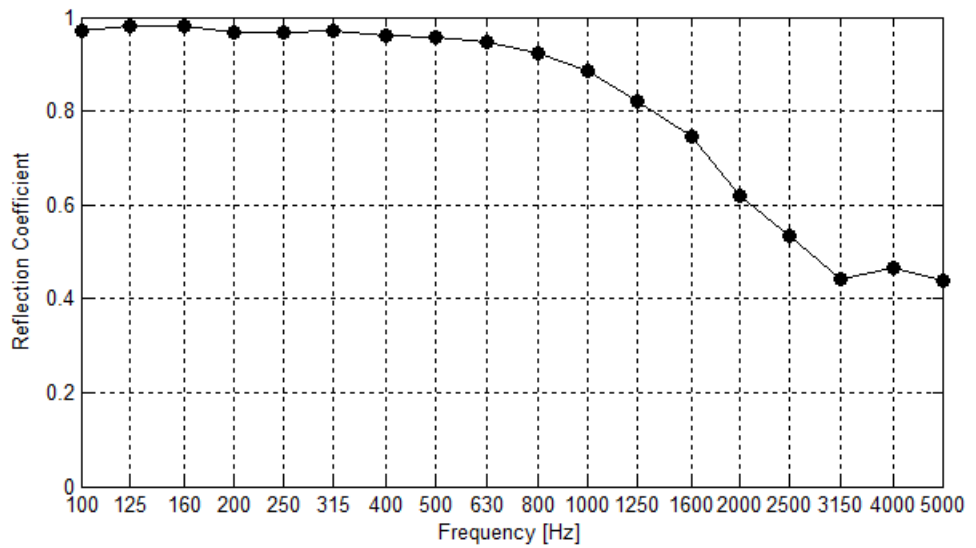


Figure 4.9 Reflection coefficient of pyramid shaped sponge material

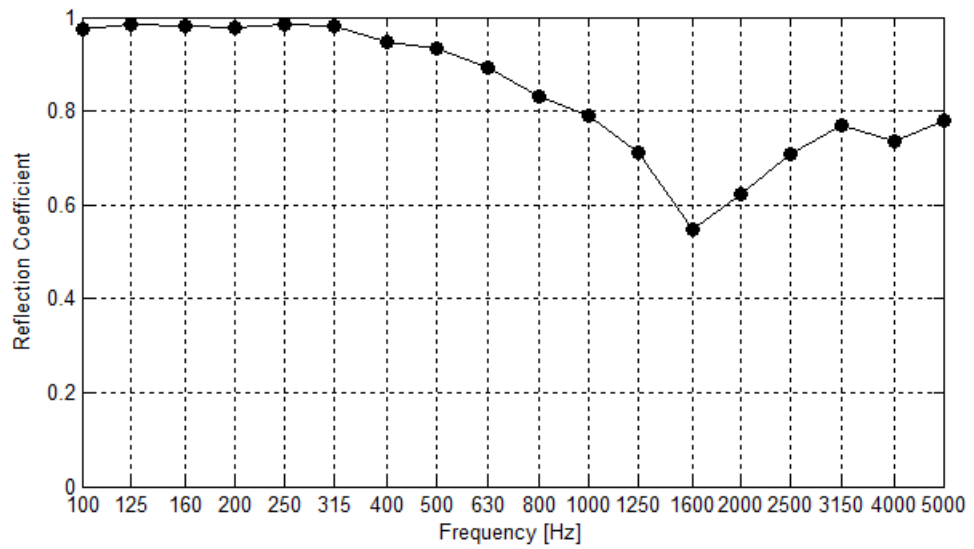


Figure 4.10 Reflection coefficient of petroleum based insulant material

Results show how many percent of sound is reflected from materials.

#### 4.1.3 Normal Incidence Specific Impedance Results

Normal incidence specific impedances of materials are computed via Equation 2.37. Normal specific impedance ratio is a complex number and it is computed sum of reactance and resistance ratios like Equation 4.1. This information will be used for computing empirical random incidence sound absorption coefficients of materials.

$$\frac{z}{\rho c} = \frac{r}{\rho c} + j \frac{x}{\rho c}. \quad (4.1)$$

Here, r is resistance and x is reactance. Results are shown in Figures 4.11 – 4.15.

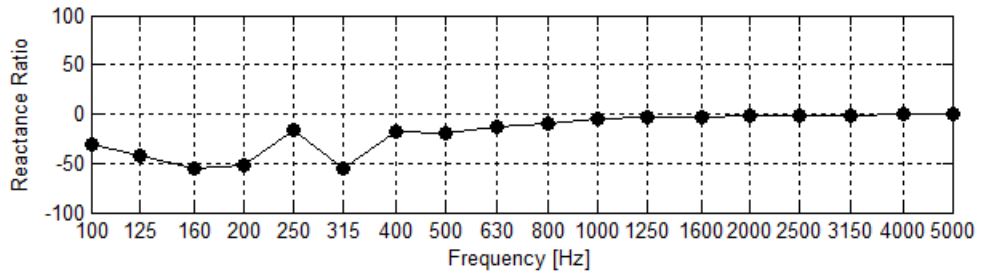
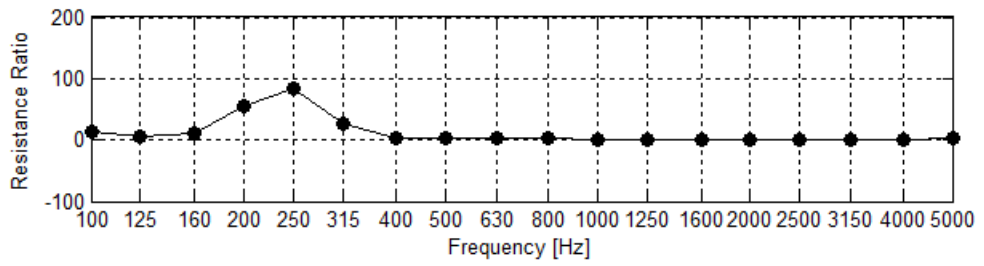


Figure 4.11 Resistance and reactance ratios of Ax

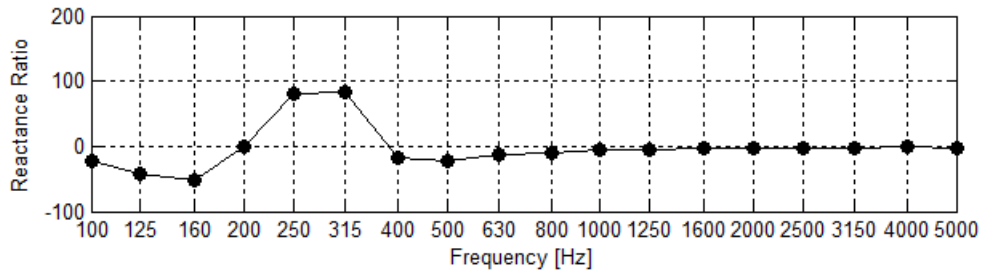
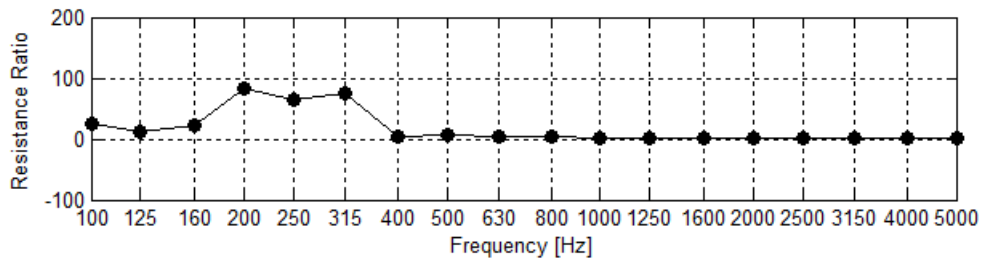


Figure 4.12 Resistance and reactance ratios of Bx

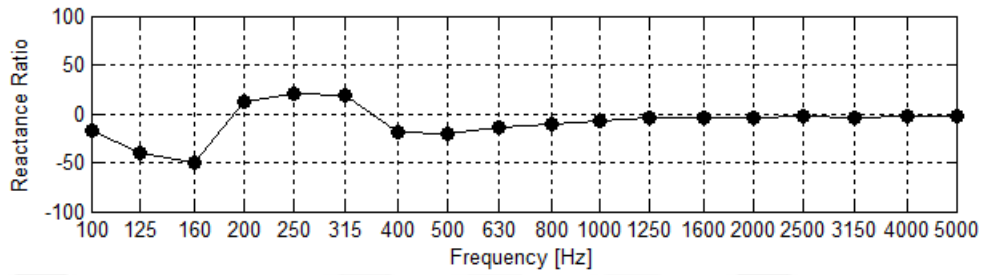
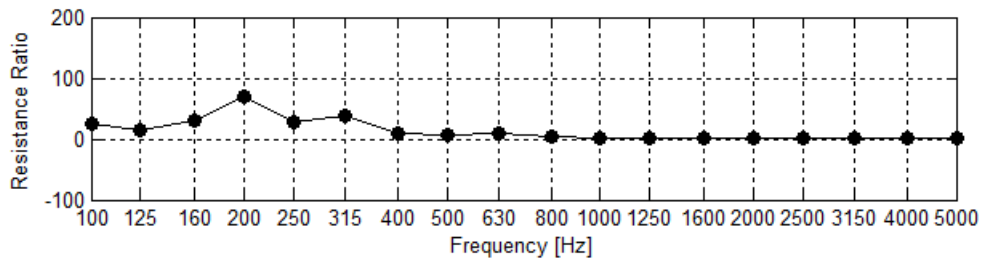


Figure 4.13 Resistance and reactance ratios of Cx

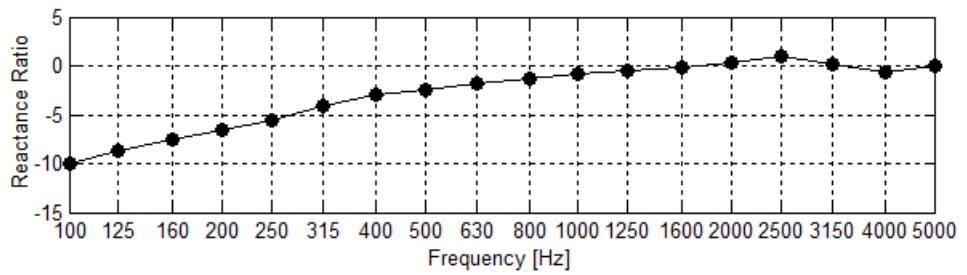
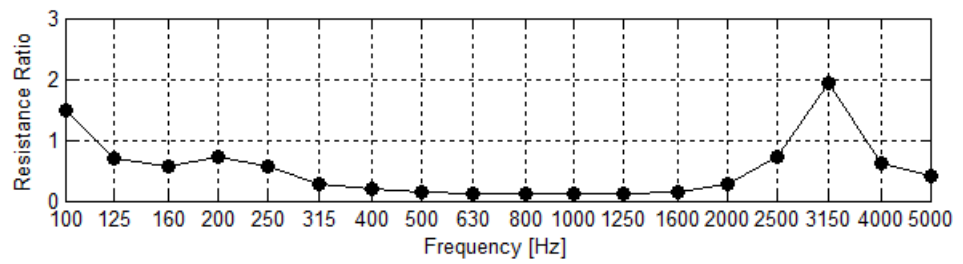


Figure 4.14 Resistance and reactance ratios of pyramid shaped sponge material

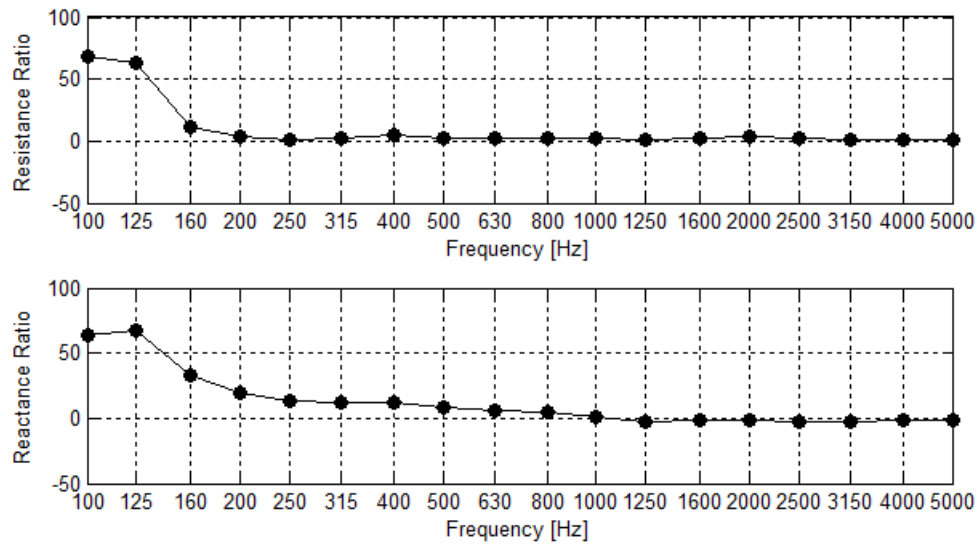


Figure 4.15 Resistance and reactance ratios of petroleum based insulant material

## 4.2 Measurement Results of Normal Incidence Sound Absorption Coefficient of Materials Under Different Temperature Conditions

In this section, sound absorption coefficients of materials are determined as a function of temperature. Two specimens, petroleum based insulant and pyramid shaped sponge materials are selected for these tests. There, two different conditions have been tested. First, inside of the tube is conditioned for different temperatures by conditioning system. Conditioning system has been described before in Chapter 3.8.

Secondly, test materials are conditioned at different temperatures and sound absorption coefficients of materials are determined via the “new impedance tube set”.

### 4.2.1 Sound absorption coefficients of materials at different ambient temperatures and relative humidity

Sound absorption coefficients of petroleum based insulant and pyramid shaped sponge materials at different ambient temperatures are shown in Figures 4.16 and 4.17.



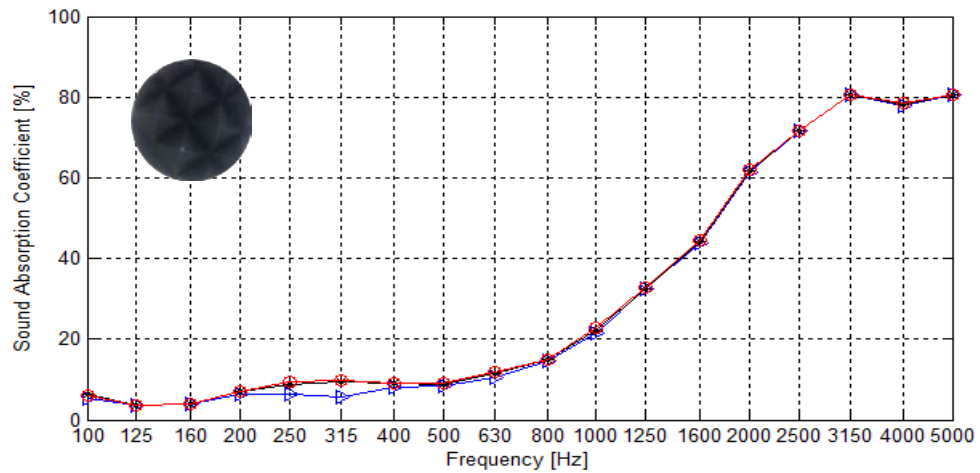


Figure 4.16 Sound absorption coefficient measurement result of pyramid shaped sponge material at different ambient temperatures (black line: temperature of tube inside is 32°C and relative humidity is %36, red line: temperature of tube inside is 42°C and relative humidity is %51, blue line: temperature of tube inside is 19°C and relative humidity is %20)

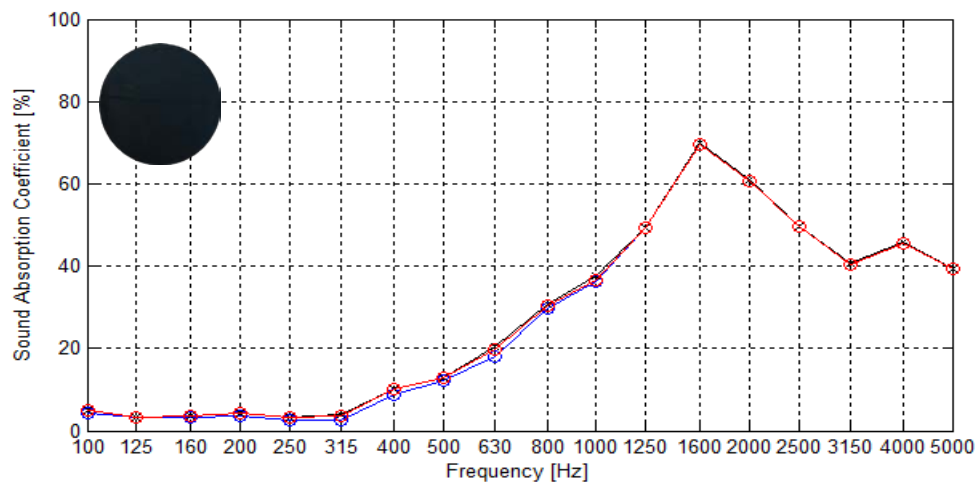


Figure 4.17 Sound absorption coefficient measurement result of petroleum based insulant material at different ambient temperatures (black line: temperature of tube inside is 25°C and relative humidity is %31, red line: temperature of tube inside is 43°C and relative humidity is %48, blue line: temperature of tube inside is 16°C and relative humidity is %17)

In these tests, specimen temperatures are stable, but ambient temperature and relative humidity is variable. Results show that, ambient temperature and relative humidity does not affect sound absorption characteristics of materials in many frequencies. However, it affects to pyramid shape sponge material at 19 °C between 200 and 400 Hz.

#### 4.2.2 Sound absorption coefficients of materials at different specimen temperatures

Sound absorption coefficients of petroleum based insulant and pyramid shaped sponge materials at different specimen temperatures are shown in Figures 4.18 and 4.19. Temperatures of specimens are 50 °C, 25 °C, 10 °C and -9 °C.

Results shows that clearly, specimen temperature level affects sound absorption characteristics of materials. Also it can be said that, sound absorption coefficients of materials increase with increasing of ambient temperature. Therefore, specialist should take cognizance of materials environmental conditions to select a material. Especially in aeronautical industry it is significant, because of the change of planes' environmental conditions during the flight.

It is thought that, because of the inside structure of materials and sound wavelength relation; materials are more effected at higher frequencies than lower ones. In addition, petroleum based material is more effected than sponge one. Since fusion point of petroleum based one is lower, temperature variation affects it further.

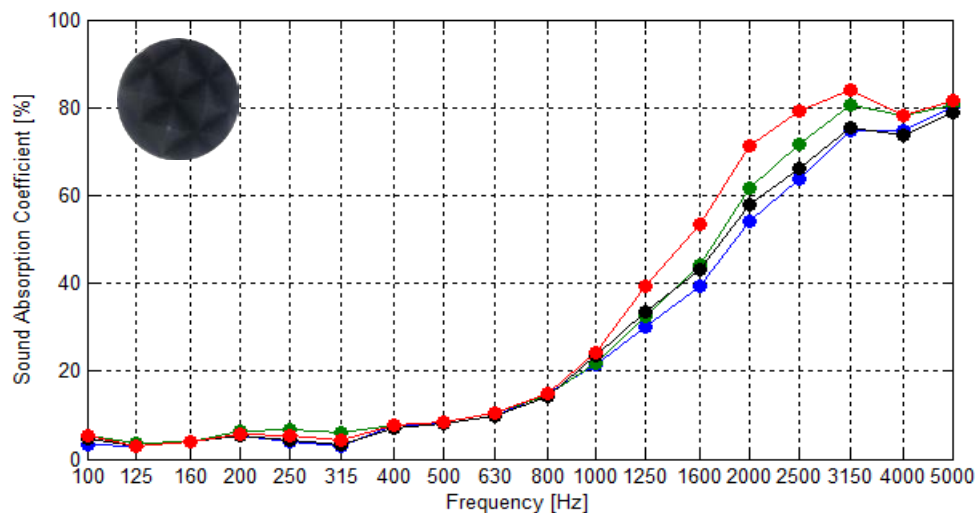


Figure 4.18 Sound absorption coefficient measurement result of pyramid shaped sponge material at different specimen temperatures (red line: temperature of tube inside is 50°C, green line: temperature of tube inside is 25°C, black line: temperature of tube inside is 10°C, blue line: temperature of tube inside is -9°C)

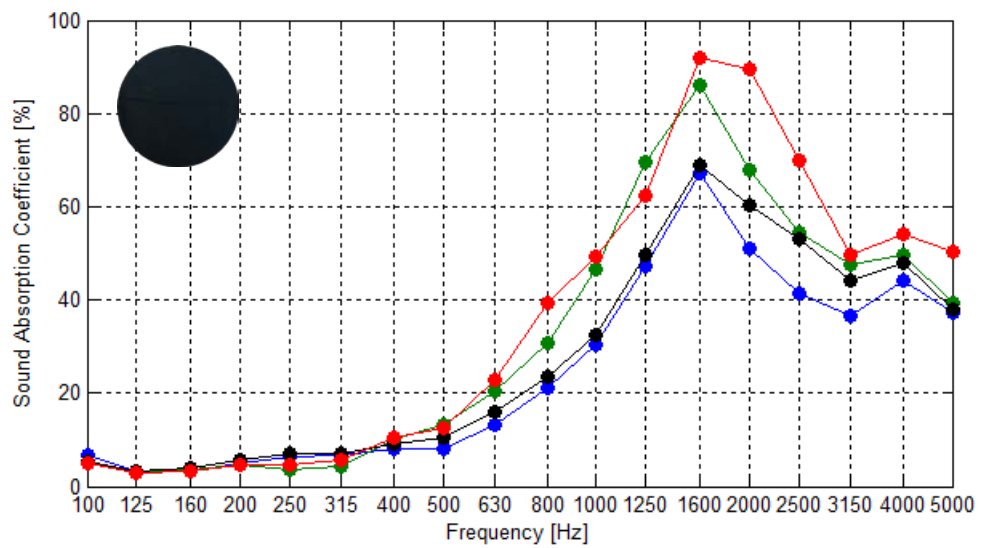


Figure 4.19 Sound absorption coefficient measurement result of petroleum based insulant material at different specimen temperatures (red line: temperature of tube inside is 50°C, green line: temperature of tube inside is 25°C, black line: temperature of tube inside is 10°C, blue line: temperature of tube inside is -9°C)

### 4.3 Measurement Results of Varied Angle Incidence Sound Absorption Coefficient of Materials

In this section, sound absorption coefficients of materials are determined as a function of the incidence of sound wave angle. Three specimens; fiberglass, petroleum based insulant and pyramid shaped sponge materials are selected for these tests. Rotation apparatus which has been described with details in Chapter 3.9, has been used for these tests. In addition, 15°, 30° and 40° constant angled specimen holders are used for verification of rotation apparatus tests. Specimens have been tested by only low frequency sound absorption coefficient apparatus.

All test results are compared with the result of Equation 2.75. This is an empirical formula and uses real and imaginary parts of normal incidence specific impedance ratios of materials.

### 4.3.1 Random incidence sound absorption coefficients of fiberglass material

Compared results of experimental method via constant angled specimen holders and rotation apparatus and empirical ones are shown in Figure 4.20 for fiberglass material.

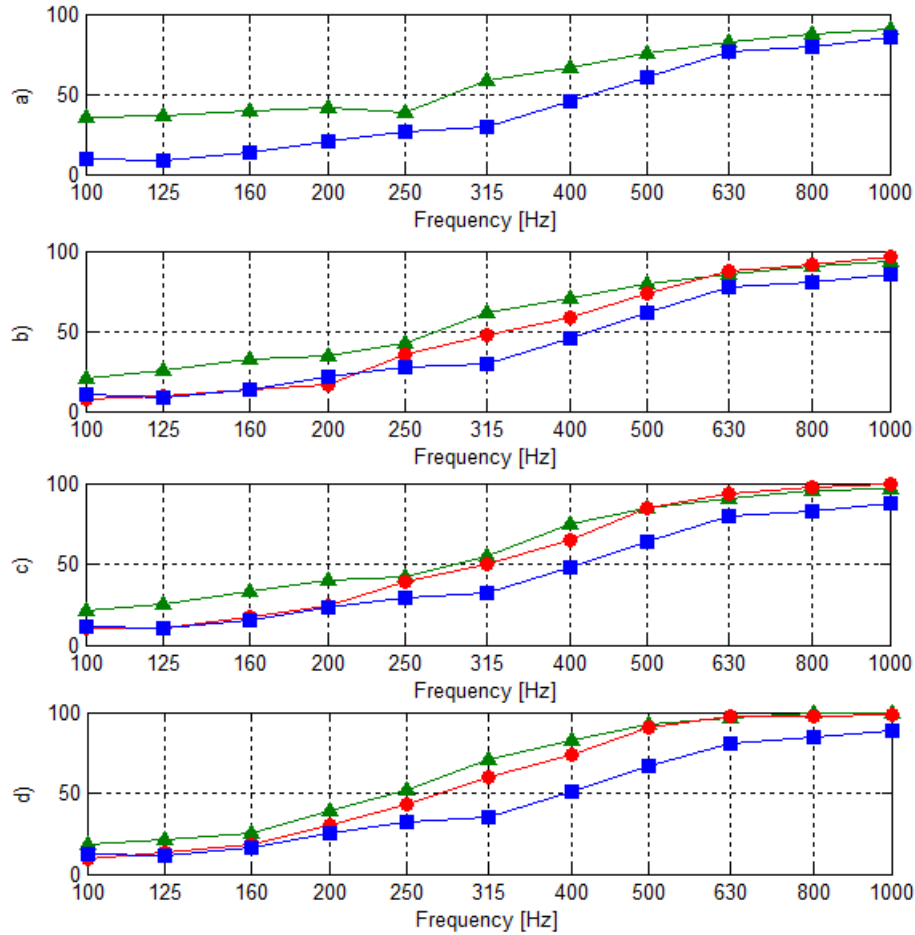


Figure 4.20 Random incidence sound absorption coefficient measurement result of fiberglass material (red lines: results of constant angled specimen holders, green lines: results of rotation apparatus, blue lines: results empirical formula; a) for 0° b) for 15° c) for 30° d) for 40°)

In addition, results are shown again in Figure 4.21 for investigating effect of incidence angle of sound.

Results show that, incidence angle of sound has significant effect on sound absorption coefficient of fiberglass material. For these tests, rotation apparatus and constant angled holders give similar results and behavior.

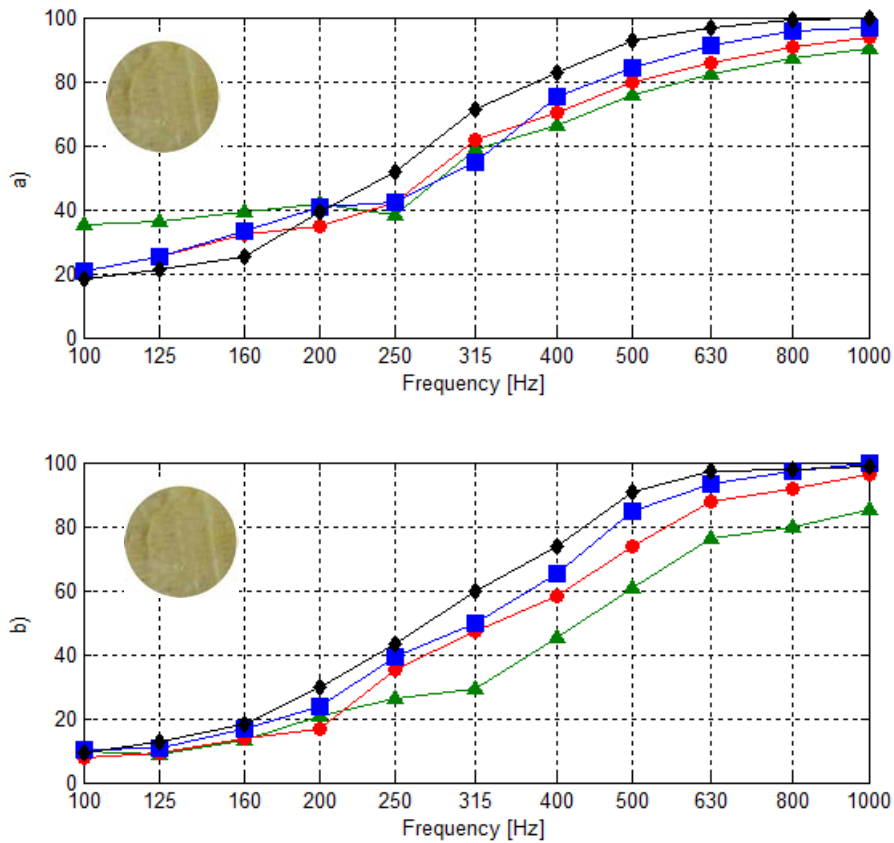


Figure 4.21 Random incidence sound absorption coefficient measurement result of fiberglass material (green lines: for 0°, red lines: for 15°, blue lines: for 30°, black lines: for 40°; a) results of rotation apparatus b) results of constant angled specimen holders)

### 4.3.2 Random incidence sound absorption coefficients of petroleum based insulant material

Compared results of experimental method via constant angled specimen holders and rotation apparatus and also empirical ones for petroleum based insulant material are shown in Figure 4.22. Also results have been shown again in Figure 4.23 for effect of incidence angle of sound.

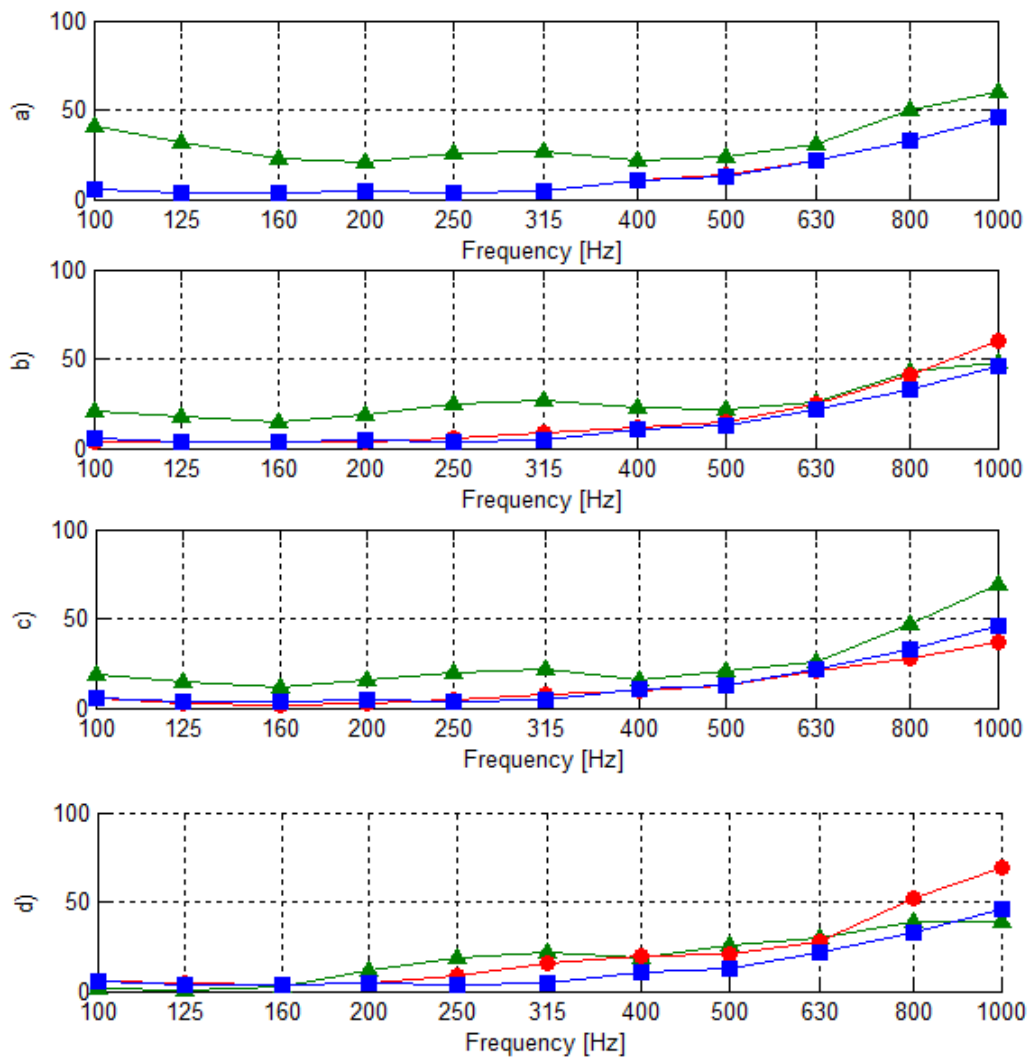


Figure 4.22 Random incidence sound absorption coefficient measurement result of petroleum based insulant material (red lines: results of constant angled specimen holders, green lines: results of rotation apparatus, blue lines: results empirical formula; a) for 0° b) for 15° c) for 30° d) for 40°)

Results show that, incidence angle of sound wave is effective on sound absorption coefficient of petroleum based insulant material especially in high frequencies. Also, experiments with constant angled specimen holders give more reliable and linear results.

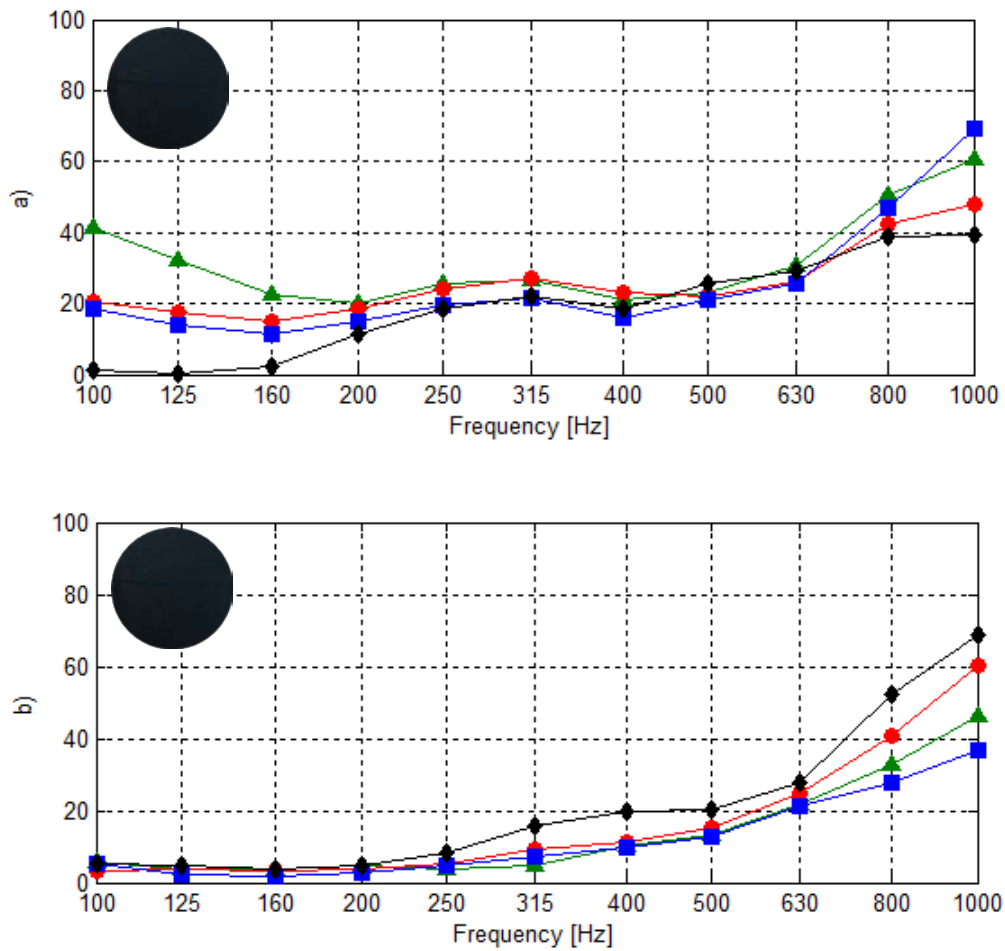


Figure 4.23 Random incidence sound absorption coefficient measurement result of petroleum based insulant material (green lines: for 0°, red lines: for 15°, blue lines: for 30°, black lines: for 40°; a) results of rotation apparatus b) results of constant angled specimen holders)

### 4.3.3 Random incidence sound absorption coefficients of pyramid shaped sponge material

Compared results of experimental method via constant angled specimen holders and rotation apparatus and also empirical ones for pyramid shaped sponge material are shown in Figure 4.24. In addition, results have been shown again in Figure 4.25 for effect of incidence angle of sound.

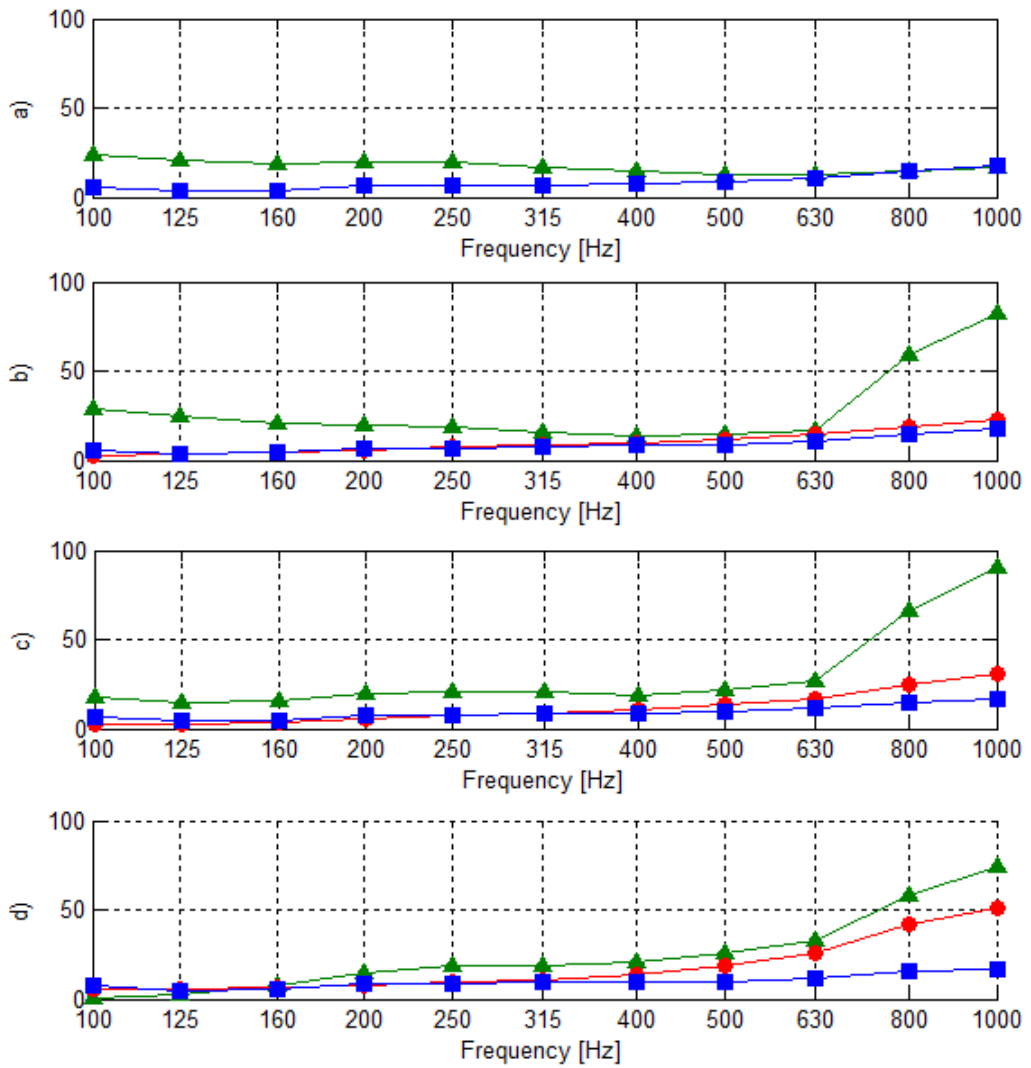


Figure 4.24 Random incidence sound absorption coefficient measurement result pyramid shaped sponge material (red lines: results of constant angled specimen holders, green lines: results of rotation apparatus, blue lines: results empirical formula; a) for 0° b) for 15° c) for 30° d) for 40°)

Results show that, incidence angle of sound wave is again effective on sound absorption coefficient of pyramid shaped sponge material especially in high frequencies. In addition, experiments with constant angled specimen holders give more reliable and linear results. This situation will be discussed in next section.



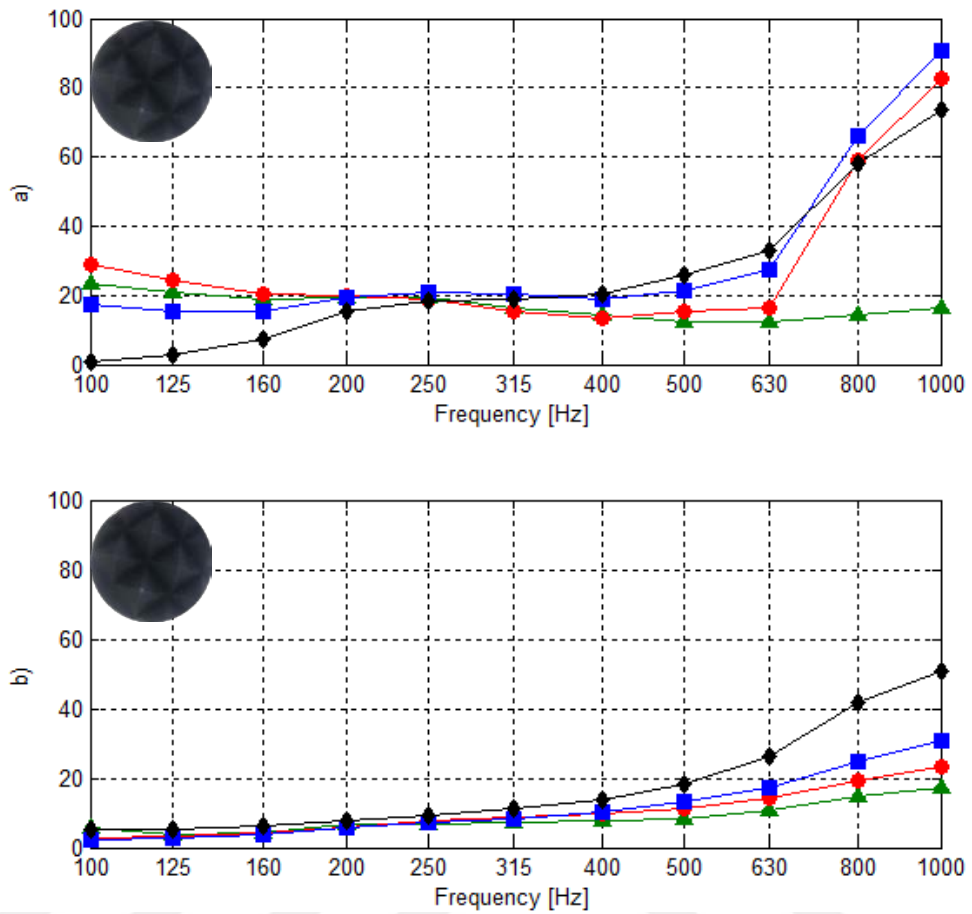


Figure 4.25 Random incidence sound absorption coefficient measurement result of pyramid shaped sponge material (green lines: for 0°, red lines: for 15°, blue lines: for 30°, black lines: for 40°; a) results of rotation apparatus b) results of constant angled specimen holders)

#### 4.3.4 Evaluation of results

Sound absorption coefficients of materials are determined via two different method, reverberation rooms and impedance tubes. Random incidence sound waves are calculated for reverberation room measurements but cannot be simulated in impedance tube kits. This study show that, sound absorption coefficients of materials depend on angle of incidence wave.

There is an empirical formula for calculation of random incidence sound absorption coefficient (Equation 2.75) from normal incidence results. However, results show that, empirical results have difference compared to experimental ones. Especially pyramid shaped sponge material, there is big difference because of its shape.

Also, a rotation apparatus has been developed for measurement of random incidence sound absorption coefficient and constant angled specimen holders are manufactured for verification of apparatus measurements. There are little differences between results because of the “space” inside of the apparatus. The “space” is a air gap in apparatus because of design. If effect of this space can be eliminated, rotation apparatus will be used in measurements and reverberation rooms can be simulated completely in impedance tubes.

#### 4.4 Transmission Loss Measurement Results of Materials

In this section; transmission losses of three different materials, petroleum based insulant material, foam material and pyramid shaped sponge material, are determined with the “new impedance tube set”. Low frequency transmission loss measurement set is used for low frequency measurements (200-1000 Hz) and high transmission loss measurement set is used for high frequency measurements (1000 Hz - 5 kHz). These tube sets are shown in Figures 3.64 and 3.65.

Transmission loss measurement result of petroleum based sponge material is shown in Figure 4.26.

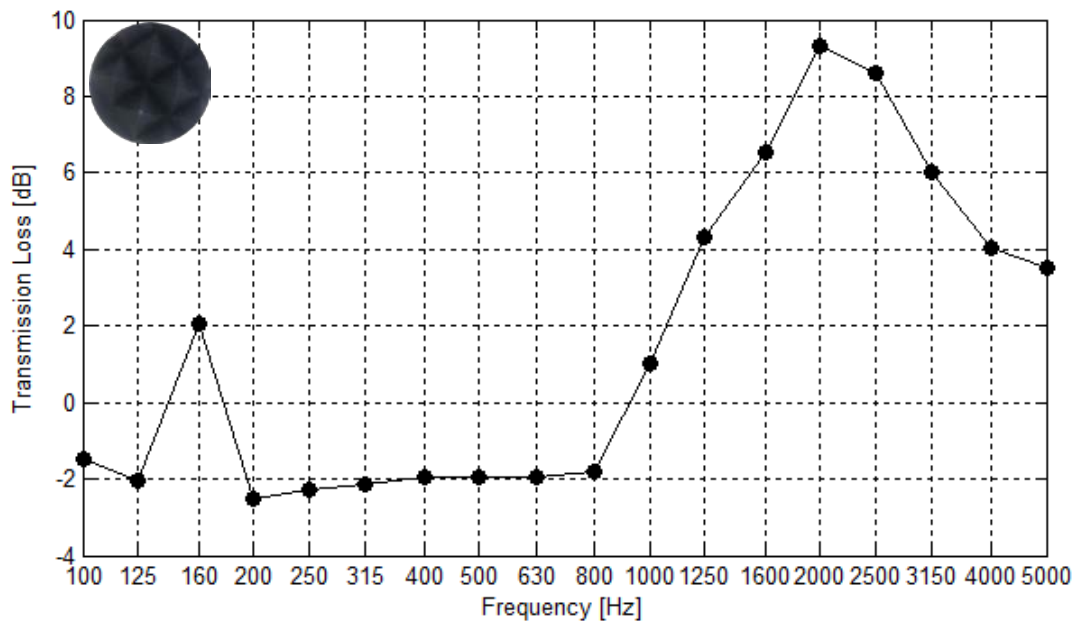


Figure 4.26 Transmission loss measurement result of pyramid shaped sponge material

Transmission loss measurement result of foam material is shown in Figure 4.27.

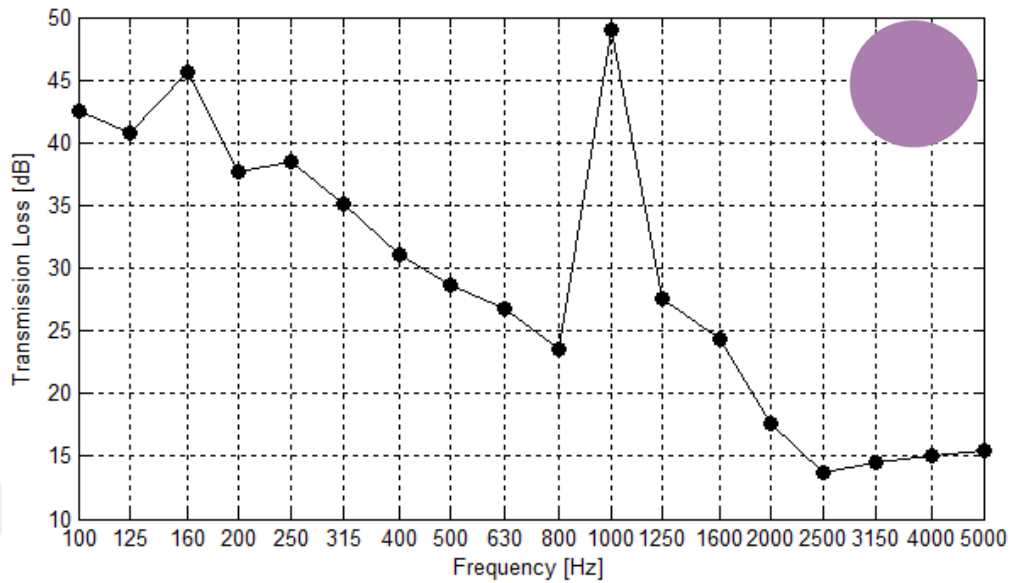


Figure 4.27 Transmission loss measurement result of foam material

Transmission loss measurement result of petroleum based insulant material is shown in Figure 4.28.

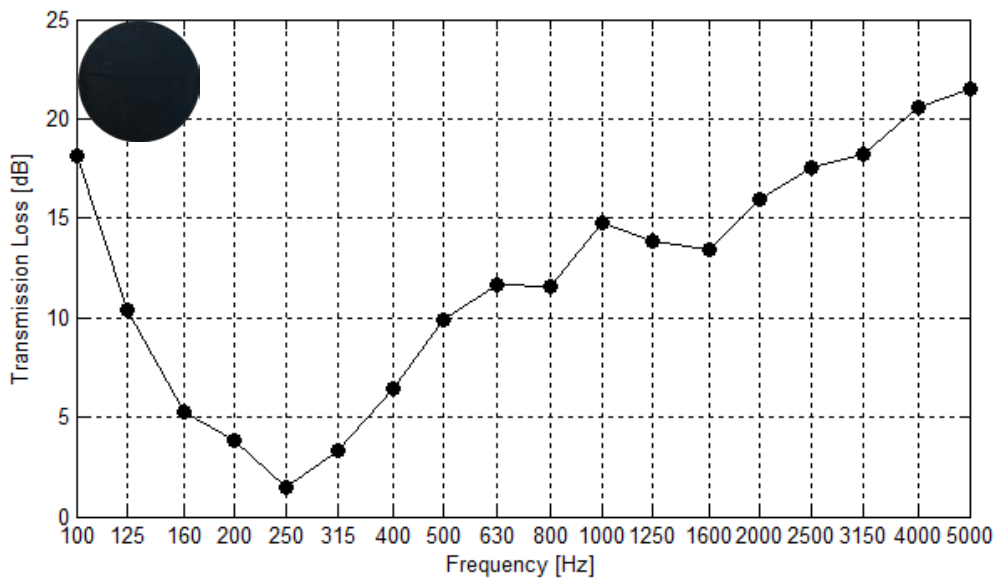


Figure 4.28 Transmission loss measurement result of petroleum based insulant material

Results show that, tough materials like foam have better performance for transmission loss than porous ones.

## **CHAPTER FIVE**

### **CONCLUSION**

The Importance of determination of acoustic performance parameters of materials is increasing day after day. Acoustic specialists who are working in automotive, aerospace and aeronautical industries, white goods and other several industries need to determine acoustical behaviors of insulation materials. Reverberation room technique is a very expensive and difficult method for determination of these parameters. On the other hand, impedance tubes can be used for measurements but they cannot simulate all conditions of real situations, especially for different angle of incidence of sound wave (random incidence) and temperature condition changes of materials and the medium.

In the study, a sandwich composite impedance tube kit has been designed and developed with respect to ASTM E1050-98 and E2611-6877 standards with autonomous measurement and calculation software. Structural and acoustical performances of this modern and light structure have been examined. Two-microphone and four-microphone techniques can be practicable with this modular tube set.

Acoustical performance parameters of several materials are measured via the “new impedance tube set”. In addition, results are compared with reliable ones for verification purpose. The results show that, designed impedance tube kit can be used for measurements of acoustical performance parameters of materials.

An air conditioning system has been designed and manufactured for determination of the effect of ambient temperature and relative humidity on the materials performance. Also, materials are conditioned to different temperatures. Results show that clearly, relative humidity of ambient are not effective so much on sound absorption coefficient of materials, but material temperature variations have significant effect on the results.

On the other section of the study, effect angle of incidence of sound wave has been investigated. A specimen rotation apparatus has been designed and manufactured for this aim. Also three different constant angled specimen holders have been manufactured for comparison and verification of results. The results show that, angle of incidence of the wave has significant effect on the sound absorption coefficients of materials.

As a conclusion, a new sandwich composite impedance tube kit has been successfully developed in this study and acoustic performance parameters of several materials have been tested via this tube. Effect of specimen temperature and incidence wave angle of sound has been investigated and validated via experimental results. The thesis has the following outcomes;

- 1) Secgin, A., İhtiyarođlu, Y., & Kara, M. (2015). Experimental vibro-acoustic modal analysis of a composite tube. *International Conference on Advances in Applied and Computational Mechanics, İzmir*, presented.
- 2) Secgin, A., İhtiyarođlu, Y., & Yapanmıř, B. E. (2015). Comparison of vibro-acoustic performances of composite and brass tubes under acoustic excitation. *International Conference on Advances in Applied and Computational Mechanics, İzmir*, presented.
- 3) Secgin, A., Kara, M., İhtiyarođlu, Y., Ozankan, A. (2017). Empedans Tüpü ile malzemelerin farklı geliş açılardaki ses yutma katsayılarının belirlenmesi. *18th National Machine Theory Symposium, Trabzon*, 308-316.
- 4) Secgin, A., İhtiyarođlu, Y., Kara, M., Ozankan, A. (2017). Akustik yalıtım malzemelerinin ses yutma katsayılarının farklı sıcaklık koşulları altındaki deđişiminin deneysel olarak incelenmesi. *18th National Machine Theory Symposium, Trabzon*, 317-324.

## REFERENCES

- Ahn, T. K., & Mote Jr, C. D. (1998). Mode identification of a rotating disk. *Experimental Mechanics*, 38(4), 250-254.
- Allemang, R. J. (1984). Experimental modal analysis bibliography. *Proceedings of the 2<sup>nd</sup> International Modal Analysis Conference, Florida*, 1085–1097.
- ASTM International. (2004). *ASTM C384-04: Standard test method for impedance and absorption of acoustical materials by impedance tube method*.
- ASTM International. (2009). *ASTM C423-09a: Standard test method for sound absorption and sound absorption coefficients by the reverberation room method*.
- ASTM International. (1998). *ASTM E1050-98: Standard test method for impedance and absorption of acoustical materials using a tube, two microphones and a digital frequency analysis system*.
- ASTM International. (2009). *ASTM E2611-09: Standard test method for measurement of normal incidence sound transmission of acoustical materials based on the transfer matrix method*.
- Ando, Y., & Kosaka, K. (1970). Effect of humidity on sound absorption of porous materials. *Applied Acoustics*, 3, 201-206.
- Batou, A., Soize, C., & Audebert, S. (2015). Model identification in computational stochastic dynamics using experimental modal data. *Mechanical Systems and Signal Processing*, 50-51, 307-322.
- Clemente, P., Marulo, F., Lecce, L., & Bifulco, A. (1998). Experimental modal analysis of the Garigliano Cable-Stayed bridge. *Soil Dynamics and Earthquake Engineering*, 17, 485-493.

- Cooley, J. W., & Tukey, J. W. (1965). An algorithm for the machine calculation of complex Fourier series. *Mathematics and Computations*, 19(90), 297–301.
- Couteau, B., Darmana, R., Brignola, J., C., & Arlaud, J., Y. (1998). Finite element modelling of the vibrational behaviour of the human femur using CT-based individualized geometrical and material properties. *Journal of Biomechanics*, 31, 383-386.
- Dunlop, J. I. (1985). An open tube technique for the measurement of acoustic parameters of porous absorbing materials. *The Journal of the Acoustical Society of America*, 77, 2173–2185.
- Everest, F. A., & Pohlman, K. (2009). *Master handbook of acoustics*. California: McGraw Hill Professional.
- Fahy, F. (2001). *Foundations of engineering acoustics*. London: Elsevier Academic Press.
- Gaul L., Willner K., Hurlebaus S. (1999). Determination of material properties of plates from modal ESPI measurement. *Proceedings of the 17th International Modal Analysis Conference, Florida*, 1756–1763.
- Hamilton, F. M., Yuri, A. I., & Zabolotskaya, E. A. (2003). Thermal effects on acoustic streaming in standing waves. *The Journal of the Acoustical Society of America*, 114, 3092-3101.
- Han, J., Herrin, D., & Seybert, A. F. (2007). Accurate measurement of small absorption coefficients. *Society of Automotive Engineers (SAE)*, 2007-01-2224. Retrieved May 15, 2007, from SAE database.
- Harris, C. M. (1966). Absorption of sound in air versus humidity and temperature. *The Journal of the Acoustical Society of America*, 40, 148-159.
- He, J., & Fu, Z. F. (2001). *Modal analysis*. Oxford: Butterworth Heinemann.

- Kennedy, C. C., & Pancu, C. D. P. (1947). Use of vectors in vibration measurement and analysis. *Journal of the Aeronautical Sciences*, 14(11), 603–625.
- Lung, T. Y., & Doige, A. G. (1983). A time-averaging transient testing method for acoustic properties of piping systems and mufflers. *The Journal of the Acoustical Society of America*, 73, 867-876.
- Mason, J. T. Mills, G. B., & Garrett, S. L. (1983). Comparison of impedance measurement techniques. *The Journal of the Acoustical Society of America*, 74, 63–78.
- Mikota, G., Manhartsgruber, B., Kogler, H., & Hammerle, F. (1994). Modal testing of hydraulic pipeline systems. *Journal of Sound and Vibration*, 409, 256-273.
- Munjaj, M. L. (1987). *Acoustics of ducts and mufflers with application to exhaust and ventilation system design*. New York: Wiley.
- Munjaj, M. L., & Doige, A. G. (1990). Theory of a two source-location method for direct experimental evaluation of the four-pole parameters of an aeroacoustic element. *Journal of Sound and Vibration*, 141, 323-333.
- Nieter, S., & Singh, R. (1982). Acoustical modal analysis experiment. *The Journal of the Acoustical Society of America*, 72, 319-326.
- Secgin, A., Kara, M., & Ozankan, A. (2013). Determination of acoustic performance parameters of a duct system with an expansion chamber. *16th National Machine Theory Symposium, Erzurum*, 7–15.
- Seybert, A. F. (1988). Two-sensor methods for the measurement of sound intensity and acoustic properties in ducts. *The Journal of the Acoustical Society of America*, 83, 2233-2239.



- Seybert, A. F., & Ross, D. F. (1976). Experimental determination of acoustic properties using a two-microphone random-excitation technique. *The Journal of the Acoustical Society of America*, 61, 1362-1370.
- Seybert, A. F., & Soenarko, B. (1980). In-duct measurement of acoustic properties using a two-microphone technique with random and pure tone excitation. *The Journal of the Acoustical Society of America*, 67, 873-887.
- Tao, Z., & Seybert, A. F. (2003). A review of current techniques for measuring muffler transmission loss. *Society of Automotive Engineers (SAE)*, 2003-01-1653. Retrieved May 05, 2003, from SAE database.
- To, C. W. S., & Doige, A. G. (1979a). A transient testing technique for the determination of matrix parameters of acoustic systems, 1: Theory and principles. *Journal of Sound and Vibration*, 62, 207-222.
- To, C. W. S., & Doige, A. G. (1979b). A transient testing technique for the determination of matrix parameters of acoustic systems, 2: Experimental procedures and results. *Journal of Sound and Vibration*, 62, 223-233.
- Ver, L. I., & Beranek, L. L. (2005). *Noise and vibration control engineering: principles and applications*. New York: Wiley.
- Whear, F. R., & Morrey, D. (1996). A Technique for Experimental Acoustic Modal Analysis. *Proceedings of the Institution of Mechanical Engineers, Part C*, 210(2), 143-151.
- Wong, G. S. K. (1986). Effects of humidity on the characteristic impedance in air. *The Journal of the Acoustical Society of America*, 79, 1920-1932.
- Xu, L., & M., Guo, N. (2003). Modal testing and finite element modeling of subsystem in hard disk drive, *Mechanical Systems and Signal Processing*, 17, 747- 764.